"STUDIES ON THE EFFECTIVENESS OF MAGNETOSTRICTIVE SENSOR FOR SENSING DELAMINATION IN COMPOSITE BEAMS"

By

Tarun Kumar Jain

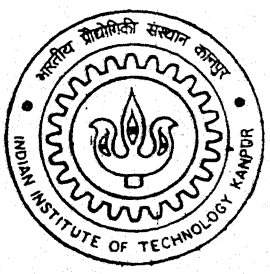

DEPARTMENT OF MECHANICAL ENGINEERING

Indian Institute of Technology Kanpur

DECEMBER, 2001

Certificate

This is to certify that the work contained in this thesis entitled "Studies on the Effectiveness of Magnetostrictive Sensor for Sensing Delamination in Composite Beams" by **Tarun Kumar Jain** has been carried out under our supervision and that this work has not been submitted elsewhere for a degree.

(Dr. Om Prakash)
Associate Professor
Department of Mechanical Engineering
Indian Institute of Technology,
Kanpur – 208016
India

(Dr. B. Bhattacharya)
Assistant Professor
Department of Mechanical Engineering
Indian Institute of Technology,
Kanpur - 208016
India

(December – 2001)

ACKNOWLEDGEMENT

I wish to express my sincere and heart full thanks to my supervisors Dr. Om Prakash and Dr. B. Bhattacharya whose excellent guidance, affectionate encouragement and inspiration with all-round cooperation has enabled me to bring the work to the present form. The care and freedom showed by them is greatly acknowledged. It is indeed a real pleasure and great privilege to have been associated with them.

I wish to express my special thanks to Pavan, for his help and the time he spent for me.

I am thankful to Mr. Anand Kumar (PhD scholar) for his valuable discussion with me about the thesis work.

I wish to express my special thanks to all my friends Avanindra, Gajju, Durgesh, Lalit, Kamal, Jeevan, Jeetu, Gaurav, Ashish, Pankaj and Datta for their endless love, encouragement and endurance which makes my life memorable in IIT Kanpur.

Finally I am grateful to the Almighty and my parents for what I am today.

Tarun Kumar Jain

Roll No. Y010556

Abstract

In recent years effort has been made at developing structure that can sense and control its own damage by using a distributed layer of smart sensors and actuators. Various types of smart patches have been used to sense/detect damage in composite beams. The present study is aimed at on the use of magentostrictive layers to detect the delamination in laminated composite beams. A classical laminated beam theory is used to study the electromagnetic response of a laminated beam with magnetostrictive layers during delamination. The delamination generated both by electrical and mechanical inputs are studied. Numerical simulations are carried out corresponding to different types of symmetric and asymmetric laminates. The effect of asymmetric bending and fracture toughness of different interface on delamination is brought out. It is observed that the presence of delamination and its growth in any interface of the laminate can be detected by change in the voltage in a coil surrounding the composite beam.

CONTENTS

List of Symbols:

a_r	area of magnetic domain i.e. cross-sectional area of beam
A	extensional stiffness matrix for laminate structure
A_1	extensional stiffness matrix for laminate, which is above the magnetostrictive layer
A_2	extensional stiffness matrix for laminate, which is below the magnetostrictive layer
a, b, c	distances
B	magnetic flux density vector
B	coupling matrix for extension and bending
B′	magnetic flux density vector after bending correction
c	crack length
d	piezoelectric constant
d	piezomagnetic coefficient matrix
D	dielectric charge density
D	bending Stiffness matrix
E	electric field strength
E_f	elastic modulus of fibre (carbon fibre)
E_L	Elastic Modulus in longitudinal direction
E_m	Elastic Modulus of matrix (epoxy resin)
E_T	Elastic Modulus in transverse direction
G	strain energy release rate
G_C	critical strain energy release rate
G_f	shear modulus of fibre
G_m	shear modulus for matrix
G_{LT}	shear modulus of composite
h_k	coordinate in thickness direction

h_m	thickness of magnetostrictive layer
H	magnetic field intensity vector
I_0	amplitude of the current
I_1	maximum carrier current vector passes through sensing coil
I_b	bias current vector
K_I	stress intensity factor
K_{IC}	critical stress intensity factor
l	length of the beam
M	moment in the composite laminate in Newton-metre per meter of width
n	number of turns of coil per meter length of beam
N	force vector in composite laminate Newton per metre of width
N_1	force vector for laminate, which is above magnetostrictive layer
N_2	force vector for laminate, which is below magnetostrictive layer
P	load applied
P_0	amplitude of applied load
Q	stiffness matrix
$\overline{Q}$	modified stiffness matrix
S_m^H	elastic compliance matrix measured at constant magnetic field intensity H
T	transformation matrix
V	voltage developed due to stress in the magnetostrictive layer
V'	voltage after bending correction
w	width of the beam
y_m	distance of magnetostrictive layer from mid-plane
ε^T	dielectric constant at constant stress
s^E	elasticity matrix at constant electric filed

ε_k	strain vector in different laminas where k denotes the lamina number from top if $k=m$ for magnetostrictive layer
$\varepsilon_m^{'}$	strain in the magnetostrictive layer after modification in mechanical strain.
σ_k	stress vector in different laminas where k denotes the lamina number from top
$\mu^{(H)}$	permeability matrix measured at constant stress σ,
ε_0	mid-plane strain vector in the composite laminate
λ	curvature of the composite beam
ν_f	poisson's ratio of fibre
ν_{LT}	poisson's ratio in transverse direction due to longitudinal load
ν_m	poisson's ratio of matrix
ν_{TL}	poisson's ration in longitudinal direction due to transverse load
Ω	carrier frequency
$\sigma_m^{'}$	stress vector after bending correction
$\varepsilon_m^{'}$	strain vector in the magnetostrictive layer after bending correction
υ_f	volume fraction of fibre in composite
υ_m	volume fraction of matrix in composite
θ	orientation of fibre with reference to principle axis.
β	Constant factor for fracture analysis.

List of Figures

CHAPTER-1

1.1 Introduction:

Delamination due to interlaminar stresses is one of the unique failure mechanisms in composite laminated structures. These stresses usually exist at the free edge of laminated material or around defect and discontinuities in the laminate. The presence of interlaminar stress in laminates implies that laminated composite can get delaminated near the edge of the laminate or near other defects. Though delamination initiation does not cause instantaneous failure of a laminate, it is usually the starting phase of failure in laminated composites. Delamination leads to reduced stiffness and degradation of the structural response of laminated composite structure and finally catastrophic failure. It is observed that most laminated composite fail due to the failure processes caused by delamination initiation much before the ultimate strength predicted by the classical laminate theory.

It is therefore of great importance to study the delamination characteristic of laminated composites and to attempt the detection and suppression of delamination in composite laminates. Shah, Chan and Joshi [1] has shown that the interlaminar stress is the main cause of the delamination in polymeric based smart composite. Their basis for this postulation was based on a combination of experimental and analytical stress analysis of laminates with different stacking sequences. It is found that the presence of tensile stress reduces the delamination strength of the laminate. Rybicki etal. [2] later demonstrated that delamination is a stable mode of crack propagation and their analysis was based on fracture mechanics quantification in terms of the strain energy release rate (SERR) analysis or fracture toughness analysis.

The character of fracture toughness coupled with the fact that it can be computed with a simple crack computation scheme which is explained in [2] makes it a useful tool for delamination analysis. The usefulness of the SERR approach to predict onset of delamination initiation is based on stress intensity factor which may reach to the critical stress intensity factor K_{IC} (frature toughness) because of interlaminar flaws of finite detectable size are present.

Over the years a number of non-destructive technique have been used to detect delamination initiation and growth in laminated composites. In recent years effort has been aimed at developing structure that can sense and control damage by using smart materials as sensors and actuators [1].

1.2 What is a Smart Material?

Smart or intelligent materials are materials, which respond to environmental changes at the most optimum condition, and manifest their function according to the changes in conditions. Most commonly these materials respond with a change in shape upon application of externally applied driving forces. Typically this shape change is reflected in elongation of the sample, thus allowing the use of it for e.g. in electromechanical devices.

In order to have better understanding of the smart materials it is appropriate to introduce an approach to classify different smart materials. Ideally the classification should be collectively exhaustive and mutually exclusive. The most common way of structuring is by finding out required electromechanical input and the response of a material sample as illustrated below in Fig. 1.

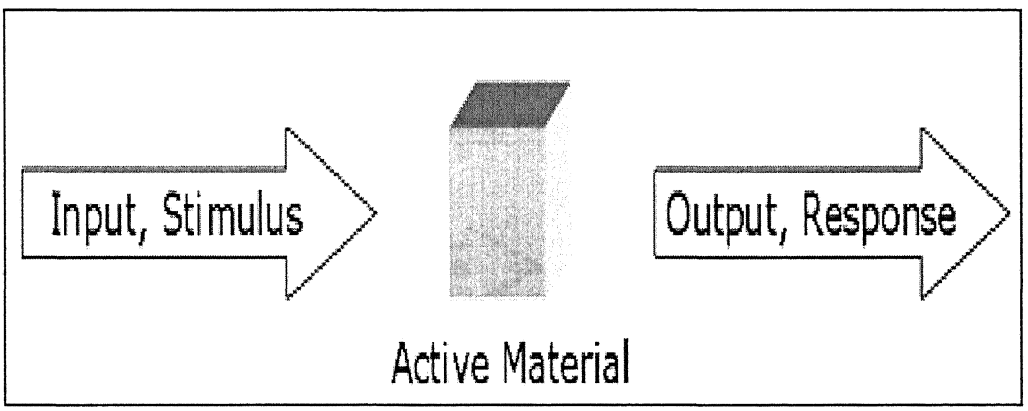

Fig.: 1

1.2.1 Classification of Smart Materials

The input or stimulus can be for example a change in temperature or magnetic field. The material then intrinsically responds with an output, which can be for example a change in length of the material, change in viscosity or change in electrical conductivity.

Smart materials can be divided into two groups. One group comprises of "classical" active materials and is characterized by the type of response these materials generate. Upon application of a stimulus the materials respond with a change in shape and/or in the length of the material. Devices based on materials that respond with a change in shape are often referred to as smart actuators.

Conversely smart materials can be also used as sensors where a strain applied on the material is transformed into a signal that allows estimation of the strain levels in the system. The Fig. below illustrates the basic principles of an actuator/sensor smart material system. Depending on the stimulus-response-direction some active materials can be used as both actuator and sensor.

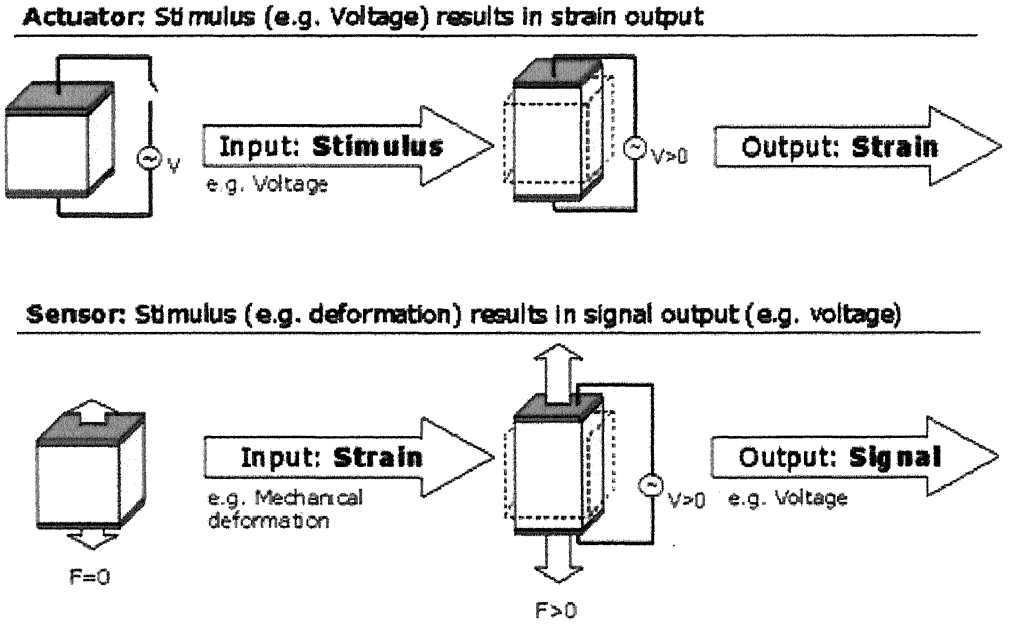

Fig. 2 Active material devices used as actuator (top) and sensor (bottom)

The second group consists of materials that can respond to a stimulus with a change in a key material property, for example electrical conductivity or viscosity. The materials in this group do not produce strain upon application of an external stimulus. Examples include the electro- and magnetorheological fluids, which respond with an increase in viscosity upon application of an external electrical or magnetic field. However these materials are less frequently integrated into mechanical structures.

1.2.2 Electrical field as driving force: -

There are several materials that exhibit an electromechanical coupling, which results in a expansion/compression of the material upon application of an electric field. The two main classes are piezoelectric and electrostrictive materials. Common examples of these materials are different piezoceramics with the exception of some polymers (like PVDF) that exhibit also piezoelectric behavior.

The difference between piezoceramics and electrostrictors lies in response upon reversing of the electric field. Piezoceramics can be both elongated and compressed by reversing the applied voltage, while electrostrictors only exhibit elongation independent of the direction of the applied electric field.

1.2.2.1 Piezoelectric Effect in piezoelectric material:

Piezoelectricity, discovered first in Rochelle salt by the brothers Jaques and Pierre Curie is defined as a change in electric polarization; with change in applied stress, which is usually referred to as the direct piezoelectric effect.

The converse piezoelectric effect is the change in strain for a free crystal (or stress for a clamped system) with change in applied field. Thus the converse piezoelectric effect is typically used when a material system is to be used as an actuator. For low fields, there is a linear relationship between strain and electrical field. Reversing the field also reverses the direction of the strain.

Historically, Rochelle salt and quartz are the most frequently used piezoelectric materials. However, only relatively new materials system like PZT offers properties that enable the development of active structural devices. The microscopic origin of the piezoelectric effect is the displacement of ionic charges within a crystal structure. In the absence of external strain, the charge distribution within the crystal is symmetric and the net electric dipole moment is zero. However when an external stress is applied, the charges are displaced and the charge distribution is no longer symmetric. The general idea of electromechanical coupling in a piezoceramic is illustrated below in Fig. 3.

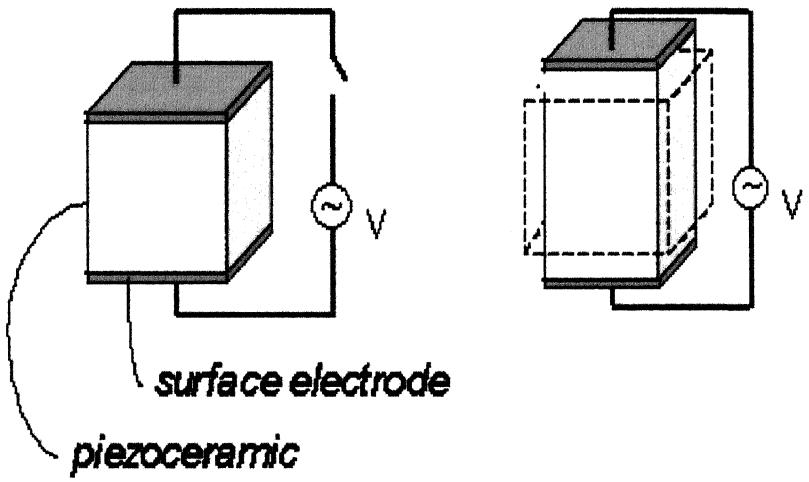

Fig. 3. Piezoelectric effect: Upon application of an electric field a sample changes shape

1.2.2.1.1 Constitutive Equation:

In the piezoelectric material, the dielectric charge density D and the mechanical strain ε are dependent on the mechanical stress σ and the field strength E. By considering the tensor of the mechanical parameters ε and σ at the surface of the crystal, the linear state equation can be written in vectorial form:

$$D = d\,\sigma + \varepsilon^{T} E \tag{1.1}$$

$$\varepsilon = s^{E}\,\sigma + d\,E \tag{1.2}$$

In this set of equations, the matrix of piezoelectric constant d indicates the strength of the piezoelectric effect. ε^{T} is the matrix of dielectric constants for constant σ and s^{E} the elasticity matrix for constant E.

Eq. (1.1) describes the direct piezoelectric effect or sensory effect. The converse piezoelectric effect is described by Eq. (1.2), which is used to define the actuation for piezoelectric material, a mechanical stress σ causes a strain ε (Hooke's law), which can be controlled by an electric field E. The actuation and sensory effect are coupled so that each piezoelectric transducer can be used either for actuation or for sensing, or both simultaneously [8].

1.2.2.2 Electrostriction:

Generally speaking electronic polarization leads to electrostrictive effect. Using a simple atomic core electron cloud particle model one can readily see why a sample cannot contract.

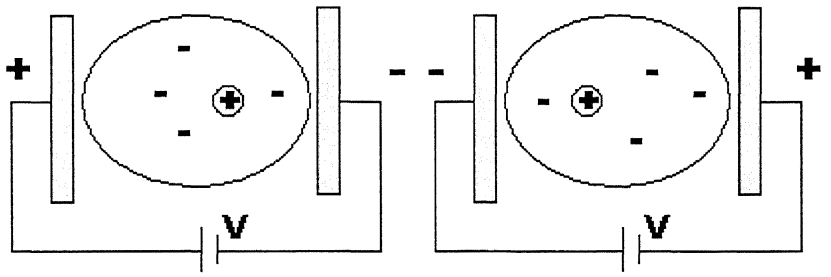

Fig. 4. Neutral atom (left) is elongated as it is polarized by the application of an electric field. Polarity of field does not affect strain direction (always strain>0). On a macroscopic scale sample is always elongated.

1.2.3 Thermal field as driving force:

1.2.3.1 Shape Memory Alloys (SMAs)

The most common group of materials that respond to a temperature changes with a shape change or elongation are Shape Memory Alloys (SMAs). These alloys undergo a phase transformation upon temperature change. The austenitic to martensitic transformation can directly lead to a volume and change of shape of the sample. Furthermore, if properly designed, the material (e.g. in wire or spring form) can be trained to transform fully reversibly in an exactly reproducible way [3].

1.2.4 Magnetic fields as driving forces –

1.2.4.1 Magnetostriction:

Magnetostriction is a property encountered in magnetic materials where the material changes its shape on the application of a magnetic field. A magnetostrictive material has a property, which convert magnetic energy into mechanical energy and vice versa. As the magnetostrictive material is magnetized, it strains, or exhibits a change in length accompanied by an invesrse change in other dimensions. Conversely, if an external force is applied causing a strain, the materials magnetic state changes. This coupling between magnetic and mechanical energies gives the transduction capability in such material and the magenetostrictive material to be used in both actuation and sensing devices.

1.2.4.2 The History of Magnetostriction:

The first positive identification of a magnetostrictive effect was in 1842 when James Joule observed that a sample of nickel changed in length when it was magnetised. Subsequently, cobalt, iron and alloys of these materials were found to show a significant magnetostrictive effect with strains of about 50 parts per million (ppm). The reciprocal effect, known as the Villari effect. An additional phenomenon known as the Wiedemann effect is defined by a twisting in a material when a helical magnetic field is applied. The inverse of this, called the Matteuci effect is the creation of a helical field when a magnetostrictive material is subject to a torque [4].

One of the first practical applications of magnetostriction was its use in sonar devices in echo location during the Second World War. The nickel based materials used in these devices had saturation magnetostriction values of 50 parts per million (ppm). These strains are quite low and so have limited applications.

In the 1960s the rare-earth elements terbium (Tb) and dysprosium (Dy) were found to have between 100 and 10,000 times the magnetostrictive strains found in nickel alloys. However because this property only occurs at low temperatures, applications at ambient temperature and above were not possible. It was found that the addition of iron to Tb and Dy to form the compounds $TbFe_2$ and $DyFe_2$ brought the magnetostrictive

properties to room temperature. These materials require very large magnetic fields to generate large strains. By alloying the two compounds it was found that the magnetic field required to produce saturated strains was considerably reduced. The resulting alloy is defined as $Tb_x Dy_{1-x} Fe_y$, where x = 0.27 to 0.3 and y = 1.92 to 2.0. Small changes in x and y can result in significant changes in the magnetic and a magnetostrictive property of the material, which is (commercially available as Terfenol-D) is at present the most widely used magnetostrictive material.

1.2.4.3 Magnetostricive Behavior:

As shown is Fig. 5 that the external stress is set to a constant compressive value ($\sigma = \sigma_0$) with the help of the mass resting on stiff spring on the top of the magnetostrictive core [5].

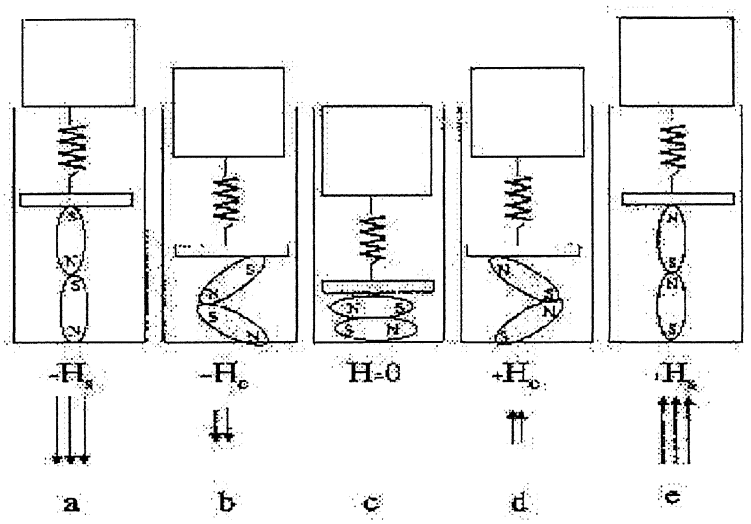

Fig. 5. Cartoon of changing strain, ε and magnetic induction, B, in a magnetostrictive element subjected to a constant compressive stress, The applied magnetic field, H, increases from (a) $-H_s$ through (c) $H = 0$ to (e) H_s.

Looking first at the case of no applied field (H = 0) the sample has an initial length (ε = 0) and no net axial magnetic induction (B = 0), as depicted in Fig. 5c. As the magnitude of the applied field H increases to its saturation limits, $\pm H_s$, the elliptical magnets rotate to align with the applied field; the axial strain increases to ε_s and magnetization of the element in the axial direction increases to $+B_s$ (Fig. 5e) or decreases to - B_s (Fig. 5a). At an applied field strength of H_s, the saturation magnitudes of strain and magnetic induction have been reached, that is the strain and magnetization of the sample will not change with further increases in the applied field. Thus, both the magnetically induced strain and the magnetic induction magnitudes increase moving from the center Fig. outward as the magnitude of the applied field increases to its saturation values [5].

Alternatively, in the same Fig. we can observe that if the applied field being set to a constant, like H_s, and then placing an increasing mass load or compressive force on the magnetostrictive element as you move from the outermost Fig. to the center Fig.. Both the axial strain and axial magnetization magnitude in the element will decrease with increasingly negative (compressive) stress.

1.2.4.4 Magnetistrictive Actuator Model:

The development of magnetostrictive material has led to the advent of actuator, which are advantageous in many structural applications. These actuators utilize the property that strain in the material are generated in response to an applied magnetic field. In Terfenol-D material the strain and generated forces are sufficiently large to drive system comprised of thick structure and heavy components. In such system the magnetostrictive actuator is often advantageous over other smart material transducer such as piezoceramic and electrostrictives. The difficulty associated with magnetostrictive actuator is its hysteresis behaiviour [6].

A magnetostrictive transducer detailed in [7] is shown in Fig. 6, the primary components of the transducer include a magnetostrictive rod, a wound wire solenoid, and a cylindrical permanent magnet. The sensor/actuator capabilities of the magnetostrictive

material are provided by magnetic moment, which rotate in the presence of an applied magnetic field. As depicted in Fig. 7a, the moments are primarily oriented perpendicular to the longitudinal rod axis in the absence of an applied field. Prestressing the rod with spring washer serves to increase the number of moments perpendicular to the axis as in Fig. 7b. When the field is applied in the direction of the rod axis, moments align in the sense depicted in Fig. 7c and significant strain and forces are generated.

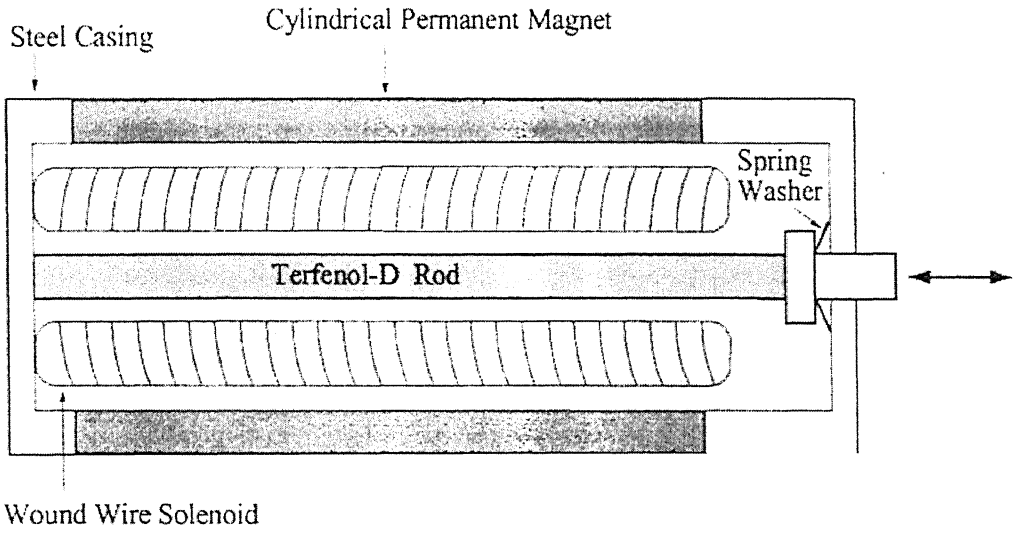

Fig. 6. Cross-section of a typical Terfenol-D magnetostrictive transducer.

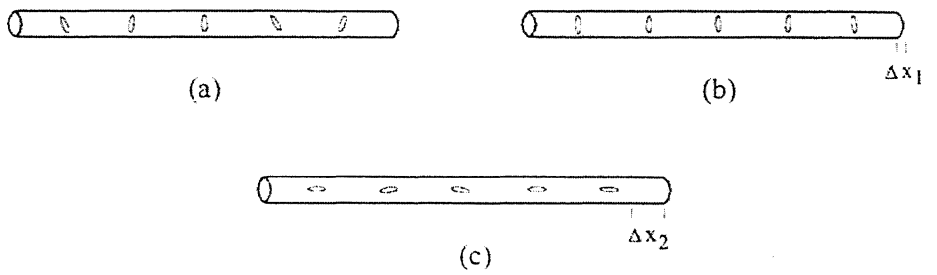

Fig. 7. Magnetic moments in the Terfenol-D rod;
(a) Orientation of moments in unstressed rod in absence of applied magnetic field;
(b) Orientation of moments in prestressed rod with no applied field;
(c) Orientation of moments in prestressed rod when field is applied in direction of longitudinal rod axis.

1.2.4.5 Constitutive Relation:

In most general way the behaviour of magnetostrictive material is nonlinear [9,10] and has to be described with nonlinear relation:

$$\begin{aligned} \varepsilon &= f(\sigma, H) \\ \mathrm{B} &= g(\sigma, H) \end{aligned} \tag{1.3}$$

Although the magnetostrictive material shows the nonlinear relation, the behaviour of the most of the magnetostrictive can be well described using a linear theory, because the active materials are biased. With this assumption the material behaves in quasi-linear manner and follows the piezomagnetic laws [11]:

$$\{\varepsilon\}_m = \lfloor S^H \rfloor_m \{\sigma\}_m + [d]\{H\} \tag{1.4}$$

$$\{\mathrm{B}\} = [d]\{\sigma\}_m + [\mu]\{H\} \tag{1.5}$$

CHAPTER-2

2.1 Introduction:

Magnetostrictive material, Terfenol-D, is now available in particle form, and can be embedded in laminated composites. Its suitability as actuator for smart structural application has been discussed in Chapter-1. Although, it is well known that magnetostrictive materials can be useful for sensing applications; systematic studies are not available to expose its use for sensing applications in composite beams. In this chapter we attempt to bring out this interesting possibility of sensing the delamination in any laminated composite with the help of magnetostrictive layer embedded on the laminate. Laminated composite with one of its layer made up of Terfenol-D particle embedded in a suitable resin is referred as a "Smart laminate beam". In such a laminate the Terfenol-D layer will experience a change in stress due to the onset of delamination, which can be sensed as an induced open circuit voltage in a coiled called "sensing coil" enclosing the beam. Adopting a linear approach in this chapter, we attempt to bring out the possibility of sensing delaminations [12].

A laminated beam with one of the layers made up of the Terfenol-D particle layer is shown in Fig.8. In this beam there is p_1 number of laminae above the magnetostrictive layer and p_2 number of laminae below the magnetostrictive layer.

The Terfenol-D composite carries an initial or bias mechanical stress and magnetic field intensity. There are two coils, one is called actuation coil, the other is the sensing coil enclosing the embedded delamination.

A carrier current of the form

$$\{I_1\} = \{I_b\} + \{I_0\} \sin \Omega t \tag{2.1}$$

is applied along with an appropriate bias field through the actuator coil resulting in stresses in the magnetostrictive layer in a localized portion only over a width equal to the width of the coil. Where I_b is the bias current, I_0 is the amplitude and Ω is the frequency of the applied current.

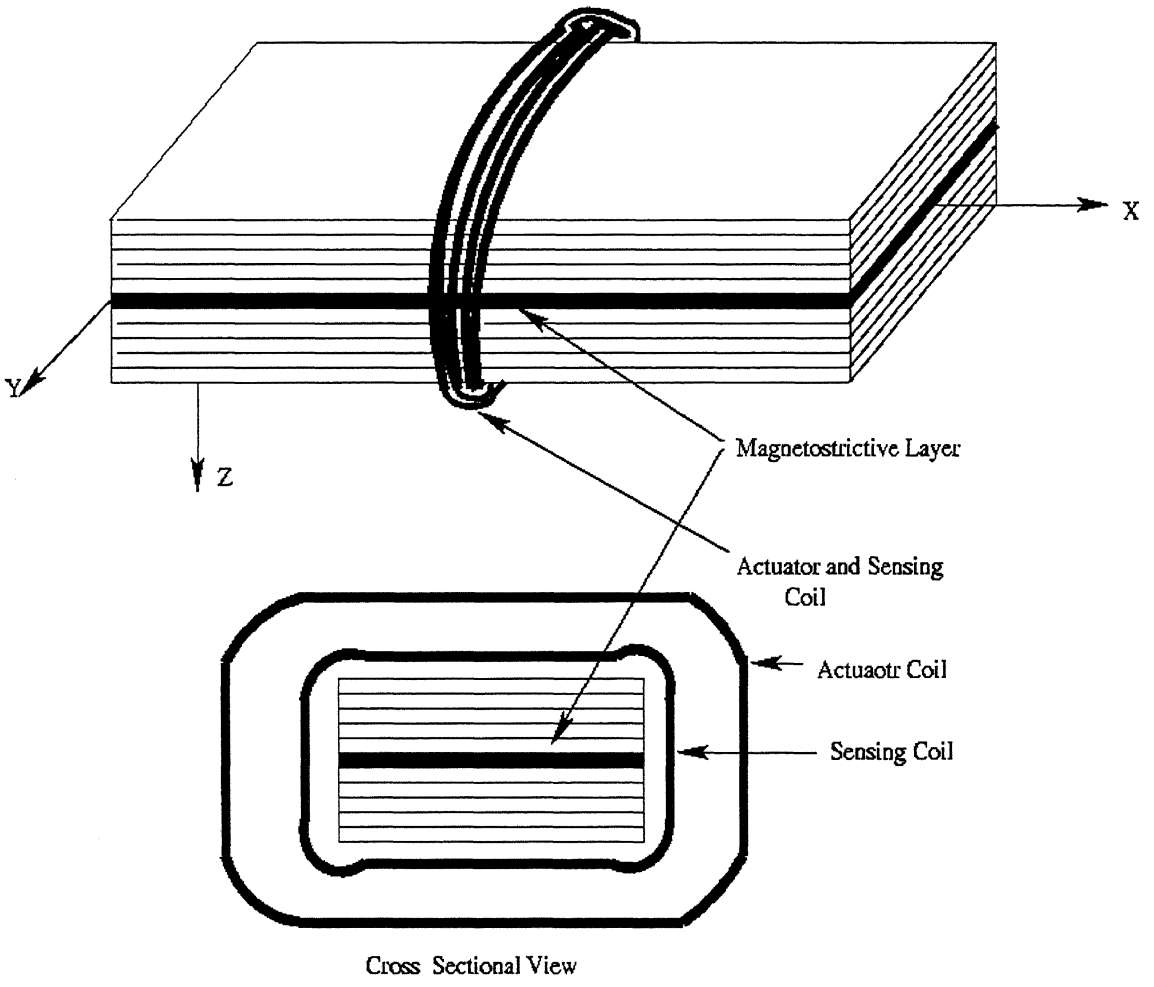

Fig. 8. Composite Beam with magnetostrictive layer with sensing and actuating coil

2.1.1 Analysis Without Bending Correction:

2.1.1.1 Theoretical Review

After the application of current of the form as in Eq. (2.1) the stress in the smart layer (magnetostrictive layer) is of compressive in nature generates and due to these stress is an equivalent mechanical load in the magnetostrictive layer as shown in Fig. (9). To balance the laminated composite beam statically there will be an equivalent and opposite forces above and below the magnetostrictive layer which will produce tensile force and correspondingly tensile stress in the upper and lower composite. For the simplification initially it is assumed that the smart layer is located in the middle in the over all laminate structure. With this assumption the curvature in the beam can be neglected.

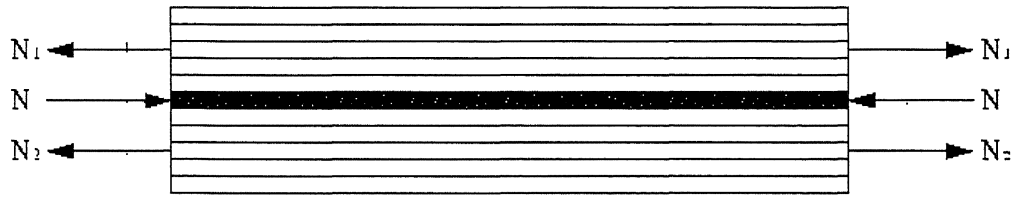

Fig. 9. Laminated beam without bending with forces

N is the equivalent force due to the stress in the smart layer and there is opposite and tensile load to balance is N_1 and N_2.

2.1.1.2 Pre Analysis:

The constitutive relationship for Terfenol-D material can be written as

$$\{\varepsilon\}_m = [S^H]_m \{\sigma\}_m + [d]\{H\} \tag{2.2}$$

$$\{B\} = [d]\{\sigma\}_m + [\mu]\{H\} \tag{2.3}$$

where

$$\{\varepsilon\}_m = \begin{Bmatrix} \varepsilon_x \\ \varepsilon_y \\ \varepsilon_{xy} \end{Bmatrix}; \qquad [S]_{m3\times3} = [Q]_{m3\times3}^{-1}$$

$$\{\sigma\}_m = \begin{Bmatrix} \sigma_x \\ \sigma_y \\ \sigma_{xy} \end{Bmatrix}; \qquad [d]_{3\times3} = d[I]_{3\times3};$$

$$\{B\} = \begin{Bmatrix} B_1 \\ B_2 \\ B_3 \end{Bmatrix}; \qquad \{H\} = n\{I_1\};$$

$$[\mu]_{3\times3} = \mu[I]_{3\times3}; \qquad [I]_{3\times3} = \begin{bmatrix} 1 & 0 & 0 \\ 0 & 1 & 0 \\ 0 & 0 & 1 \end{bmatrix};$$

The stress strain relation for composite layer is simply [13]

$$\begin{Bmatrix} \sigma_x \\ \sigma_y \\ \tau_{xy} \end{Bmatrix}_k = \left[\overline{Q}\right]_{k3\times3} \begin{Bmatrix} \varepsilon_x \\ \varepsilon_y \\ \varepsilon_{xy} \end{Bmatrix}_k ; \tag{2.4}$$

Where k is for k_{th} lamina, and when $k=m$ its for magnetostrictive layer.

Constitutive relations of smart material Eq. (2.2 and 2.3) are in general non-linear and detailed studies based on the non-linear constitutive behavior are given elsewhere [14,15]. But here for simplicity we have used linear relation as in given equation (2.2) and (2.3).

2.1.1.3 Composite Analysis:

The constitutive relation in terms of the stress resultants may be readily written as from classical laminate theory [13]

$$\begin{Bmatrix} N \\ M \end{Bmatrix} = \begin{bmatrix} A & B \\ B & D \end{bmatrix} \begin{Bmatrix} \varepsilon_0 \\ \lambda \end{Bmatrix}; \tag{2.5}$$

where $\{N\} = \begin{Bmatrix} N_x \\ N_y \\ N_{xy} \end{Bmatrix}$; $\{M\} = \begin{Bmatrix} M_x \\ M_y \\ M_{xy} \end{Bmatrix}$;

$$\{N\} = \int \{\sigma\} dz; \qquad \{M\} = \int \{\sigma\} z dz; \tag{2.6}$$

$$[A]_{3\times3} = \sum_{i=1}^{z} [\overline{Q}](h_i - h_{i-1});$$

$$[B]_{3\times3} = \frac{1}{2}\sum_{i=1}^{z} [\overline{Q}]\left(h_i^{\,2} - h_{i-1}^{\,2}\right);$$

$$[D]_{3\times3} = \frac{1}{3}\sum_{i=1}^{z} [\overline{Q}]\left(h_i^{\,3} - h_{i-1}^{\,3}\right); \tag{2.7}$$

Calculating the elastic properties of laminated composite using the rule of mixture as in [13]

$$E_L = E_f \upsilon_f + E_m \upsilon_m \tag{2.8}$$

$$\nu_{LT} = \nu_f \upsilon_f + \nu_m \upsilon_m \tag{2.9}$$

Assume that the fiber and matrix behave as isotropic material individually

The shear modulus of fiber and matrix may be written as

$$G_f = \frac{E_f}{2(1+\nu_f)} \tag{2.10}$$

$$G_m = \frac{E_m}{2(1+\nu_m)} \tag{2.11}$$

Since the volumes of each constituent are known the volume fraction may be calculated as

$$\upsilon_m = V_m / (V_m + V_f) \tag{2.12}$$

$$\upsilon_f = V_f / (V_m + V_f) \tag{2.13}$$

Transverse elastic modulus can be calculated using Halpin-Tsai Hill formula [13]

$$\frac{E_T}{E_m} = \frac{1-\xi\eta\upsilon_f}{1-\eta\upsilon_f} \tag{2.14}$$

where

$$\eta = \frac{\left(\frac{E_f}{E_m}\right)-1}{\left(\frac{E_f}{E_m}\right)+\xi}$$

$\xi = 2$ is the measure of reinforcement

we can also write it as

$$v_{TL} = v_{LT}\frac{E_T}{E_L} \tag{2.15}$$

and

$$G_{LT} = \frac{G_f G_m}{G_m \upsilon_f + G_f \upsilon_m} \tag{2.16}$$

As we have assumed that the curvature in the structure is zero, one can easily say that the strain in the composite beam will be equal to strain in the mid-plane of the composite.
So we can write as

$$\{\varepsilon\} = \{\varepsilon_0\} \tag{2.17}$$

$$[\overline{Q}] = [T]^{-1}[Q][T] \tag{2.18}$$

where

$$[T] = \begin{bmatrix} \cos^2\theta & \sin^2\theta & 2\sin\theta\cos\theta \\ \sin^2\theta & \cos^2\theta & -2\sin\theta\cos\theta \\ -\sin\theta\cos\theta & \sin\theta\cos\theta & \cos^2\theta - \sin^2\theta \end{bmatrix};$$

$$[Q] = \begin{bmatrix} Q_{11} & Q_{12} & 0 \\ Q_{12} & Q_{22} & 0 \\ 0 & 0 & Q_{66} \end{bmatrix};$$

Using Eqs. (2.7) to (2.15) we can calculate all elastic properties in the material axis of composite using Eqs. (2.17-2.19).
From above relation the elements of stiffness matrix may be written as

$$Q_{11} = \frac{E_L}{1 - v_{LT}v_{TL}};$$

$$Q_{22} = \frac{E_T}{1 - v_{LT}v_{TL}};$$

$$Q_{12} = \frac{v_{TL}E_T}{1 - v_{LT}v_{TL}} = \frac{v_{LT}E_L}{1 - v_{LT}v_{TL}}; \tag{2.19}$$

$$Q_{66} = G_{LT}$$

2.1.1.4 Post Analysis:

From the Fig. (9) it is clear that the curvatures is zero in the composite beam, and let's consider the laminate which is above the magnetostrictive layer separately and using Eq. (2.5) for this we can write as

$$\begin{Bmatrix} N_1 \\ M_1 \end{Bmatrix} = \begin{bmatrix} A_1 & B_1 \\ B_1 & D_1 \end{bmatrix} \begin{Bmatrix} \varepsilon_0 \\ \lambda \end{Bmatrix}; \tag{2.20}$$

Similarly we can express for laminate, which is below magnetostrictive layer and can be written in the form

$$\begin{Bmatrix} N_2 \\ M_2 \end{Bmatrix} = \begin{bmatrix} A_2 & B_2 \\ B_2 & D_2 \end{bmatrix} \begin{Bmatrix} \varepsilon_0 \\ \lambda \end{Bmatrix}; \tag{2.21}$$

Upper laminate with p_1 number of laminas with tensile force N_1 and lower part with p_2 number of laminas having N_2 as tensile force. From Eq. (2.20) and Eq. (2.21)

$$\{N_1\} = [A_1]\{\varepsilon\}; \qquad [A_1] = \sum_{i=1}^{p_1} [\overline{Q}](h_i - h_{i-1});$$

$$\{N_2\} = [A_2]\{\varepsilon\}; \qquad [A_2] = \sum_{i=1}^{p_2} [\overline{Q}](h_i - h_{i-1}); \tag{2.22}$$

The net force in the magnetostrictive layer

$$\{N\} = \{\sigma\}_m h_m \tag{2.23}$$

Since there is no applied external axial force, then for axial equilibrium we have from Fig. (9)

$$\{N\} = \{N_1\} + \{N_2\} \tag{2.24}$$

substituting Eq. (2.22) into Eq. (2.24), we get

$$\{N\} = [A_1]\{\varepsilon\} + [A_2]\{\varepsilon\}$$

$$\{\varepsilon\} = [[A_1] + [A_2]]^{-1}\{N\} \tag{2.25}$$

$\{\varepsilon\}$ is also equal to the strain in the magnetostrictive layer i.e. $\{\varepsilon\}_m$ which is obtained from Eq. (2.2) as

$$\{\varepsilon\}_m = [S]_m\{\sigma\}_m + [d]\{H\} = \{\varepsilon^{(e)}\}_m + \{\varepsilon^{(H)}\}_m$$

since the strain in the composite host and the magnetostrictive layer are equal, it can be written as

$$\{\varepsilon\} = \{\varepsilon\}_m = [[A_1] + [A_2]]^{-1}\{N\} = \{\varepsilon^{(e)}\}_m + \{\varepsilon^{(H)}\}_m \tag{2.26}$$

using Eq. (2.2) and recognizing

$$\{\varepsilon^{(e)}\}_m = [S]_{m3\times3}\{\sigma\}_m \text{ and } \{\varepsilon^{(H)}\}_m = [d]n\{I_1\}$$

We also have from Eq. (2.23)

$$\{N\} = \{\sigma\}_m h_m$$

From Eq. (2.26) we have

$$[[A_1] + [A_2]]^{-1}\{N\} = [S]_m\{\sigma\}_m + [d]\{H\}$$

As we know ([14]) that

$$\{H\} = n\{I_1\} \tag{2.27}$$

$$[[A_1] + [A_2]]^{-1}\{\sigma\}_m h_m = [S]_m\{\sigma\}_m + [d]n\{I_1\}$$

By simply inverting the relation we can write it

$$\left[[[A_1] + [A_2]]^{-1} h_m - [S]_m\right]\{\sigma\}_m = [d]n\{I_1\}$$

$$\{\sigma\}_m = \left[[[A_1] + [A_2]]^{-1} h_m - [S]_m\right]^{-1}[d]n\{I_1\} \tag{2.28}$$

Substituting Eq. (2.1) we get into Eq. (2.28) we get

$$\{\sigma\}_m = [\alpha_1]\{\{I_b\} + \{I_0\}\sin \Omega t\} \tag{2.29}$$

where

$$[\alpha_1] = \left[[[A_1] + [A_2]]^{-1} h_m - [S]_m\right]^{-1} [d] n$$

for strain in the magnetostrictive layer we can write it as using Eq. (2.26)

$$\{\varepsilon\}_m = [[A_1] + [A]_L]^{-1}\{N\}$$

Putting {N} from Eq. (2.23) into above Equation

$$\{N\} = \{\sigma\}_m h_m$$

$$\{\varepsilon\}_m = [[A_1] + [A_2]]^{-1}\{\sigma_m\} h_m$$

Finally from Eq. (2.28)

$$\{\varepsilon\}_m = [[A_1] + [A_2]]^{-1}[\alpha_1]\{I_1\} h_m \tag{2.30}$$

2.1.1.5 Voltage Analysis:

Using Eq. (2.3) we can write flux density B as

$$\{\mathrm{B}\} = [d]\{\sigma\}_m + [\mu]\{H\}$$

from Eq. (2.29) and Eq. (2.27)

$$\{\mathrm{B}\} = [d]\left[[[A_1] + [A_2]]^{-1} h_m - [S]_m\right]^{-1}[d]n\{I_1\} + [\mu]n[I_1]$$

$$\{\mathrm{B}\} = [d][\alpha_1]\{I_1\} + [\mu]n\{I_1\}$$

$$\{\mathrm{B}\} = [[d][\alpha_1] + [\mu]n]\{I_1\} \tag{2.31}$$

$$\{I_1\} = \{I_b\} + \{I_0\}\sin\Omega t$$

By differentiating Eq. (2.31) with respect to time we get

$$\left\{\frac{d\mathrm{B}}{dt}\right\} = [[d][\alpha_1] + [\mu]n]\{I_0\}\Omega\cos\Omega t \tag{2.32}$$

and the open circuit voltageis given by

$$\{V\} = -nl\,a_r\left\{\frac{d\mathrm{B}}{dt}\right\} \tag{2.33}$$

Using Eq. (2.32) in Eq. (2.33) we get

$$\{V\} = -nl\,a_r[[d][\alpha_1] + [\mu]n]\{I_0\}\Omega\cos\Omega t \tag{2.34}$$

2.1.2 Analysis With Bending Correction:

2.1.2.1 Theoretical Review

Similarly as in previous the same form of current is passed as in Eq. (2.1) the stress in the smart layer (magnetostrictive layer) is of compressive in nature generates. The only difference between these both analysis is that here the magnetostrictive layer is placed asymmetrically and because of the stress in the magnetostrictive layer their will be a bending which try to bend the laminate, and due to these stresses there is an equivalent mechanical load is of the same nature generates in the magnetostrictive layer as shown in Fig. (10). To balance the laminated composite beam statically there will be an equivalent and opposite forces above and below the magnetostrictive layer which will produce tensile force and a moment will also act. With this assumption the curvature in the beam cannot be neglected. So in the above analysis we are considering the bending effect also.

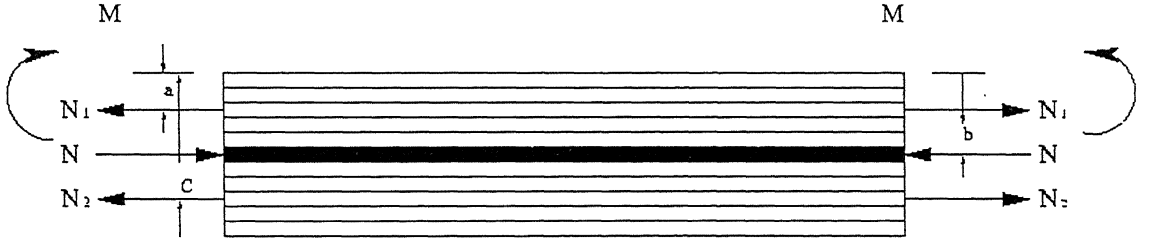

Fig. 10 The laminate striucture with moment acting on it.

2.1.2.2 Pre Analysis:

When the magnetostrictive layer is located asymmetrically, it induces a moment, which is chosen above in Fig. (10)

Taking the moment about upper edge of the composite beam we get

$$\{M\}=\{N_1\}a+\{N_2\}c-\{N\}b \tag{2.35}$$

Here Moment is represented as a vector because of two-dimensional forces, but this is purely a beam problem so we will have axial loading only so other two component of moment is zero.

As already explained that there is no external applied force present in the beam, so to reformulate for strain and curvature and for final voltage response we are starting from the same expression as in Eq. (2.2)

So on the basis of previous assumption

$$\{N_1\}=[A_1]\{\varepsilon\}$$

$$\{N_2\}=[A_2]\{\varepsilon\};$$

From Eq. (2.25) we have

$$\{\varepsilon\}=[[A_1]+[A_2]]^{-1}\{N\}$$

Also from Eq. (2.23)

$$\{N\}=\{\sigma\}_m h_m$$

from Eq. (2.28)

$$\{\sigma\}_m=[\alpha_1]\{\{I_b\}+\{I_0\}\sin\Omega t\}$$

where

$$[\alpha_1]=\left[[[A_1]+[A_2]]^{-1}h_m-[S]_m\right]^{-1}[d]n$$

From Eq. (2.35)

$$\{M\}=[A_1]\{\varepsilon\}a+[A_2]\{\varepsilon\}c-\{N\}b$$

Hence by combining all equations into one equation we get

$$\{M\} = [A_1][[A_1] + [A_2]]^{-1}\{N\}a + [A_2][[A_1] + [A_2]]^{-1}\{N\}c - \{\sigma\}_m h_m b$$

$$\{M\} = [A_1][[A_1] + [A_2]]^{-1}\{\sigma\}_m h_m a + [A_2][[A_1] + [A_2]]^{-1}\{\sigma\}_m h_m c - \{\sigma\}_m h_m b$$

$$\{M\} = [A_1][[A_1] + [A_2]]^{-1}[\alpha_1]\{I_1\}h_m a + [A_2][[A_1] + [A_2]]^{-1}[\alpha_1]\{I_1\}h_m c - [\alpha_1]\{I_1\}h_m b$$

$$\{M\} = \left[[A_1][[A_1] + [A_2]]^{-1} a + [A_2][[A_1] + [A_2]]^{-1} c - [I]b\right][\alpha_1]\{I_1\}h_m$$

$$\{M\} = [\alpha_2][\alpha_1]\{I_1\}h_m \qquad (2.36)$$

where

$$[\alpha_2] = \left[[A_1][[A_1] + [A_2]]^{-1} a + [A_2][[A_1] + [A_2]]^{-1} c - [I]b\right]$$

$$[\alpha_2] = \left[[[A_1]a + [A_2]c][[A_1] + [A_2]]^{-1} - [I]b\right] \qquad (2.37)$$

2.1.2.3 Composite Analysis:

We can write from the basic equation Eq, (2.5) i.e.

$$\begin{Bmatrix} N \\ M \end{Bmatrix} = \begin{bmatrix} A & B \\ B & D \end{bmatrix} \begin{Bmatrix} \varepsilon_0 \\ \lambda \end{Bmatrix};$$

After inverting the same relation we get

$$\{\lambda\} = [D]^{-1}\{\{M\} - [B]\{\varepsilon_0\}\} \tag{2.38}$$

Using Eq, (2.36) in Eq. (2.38) we can write

$$\{\lambda\} = [D]^{-1}\left\{[\alpha_2][\alpha_1]\{I_1\}h_m - [B][[A_1] + [A_2]]^{-1}[\alpha_1]\{I_1\}h_m\right\}$$

$$\{\lambda\} = [D]^{-1}\left[[\alpha_2] - [B][[A_1] + [A_2]]^{-1}[\alpha_1]\right]\{I_1\}h_m$$

$$\{\lambda\} = [\alpha_3]\{I_1\} \tag{2.39}$$

where

$$[\alpha_3] = [D]^{-1}\left[[\alpha_2] - [B][[A_1] + [A_2]]^{-1}[\alpha_1]\right]h_m$$

The axial strain in the magnetostrictive layer will be affected by the curvature because of asymmetry introduced on it. Let $\varepsilon_m^{'}$ is the axial strain in the magnetostrictive layer, which can be written as

$$\{\varepsilon\}_m = \{\varepsilon_0\} + y_m\{\lambda\} \tag{2.40}$$

where y_m is the distance of the magnetostrictive layer from the mid-plane of the over all beam structure in z direction

Similarly we can write strain for all lay-up of composite with relation having

$$\{\varepsilon\}_k = \{\varepsilon_0\} + h_k \{\lambda\} \tag{2.41}$$

Where k denotes the lamina number in composite from top when $k=m$ then its for magnetostrictive layer

From composite analysis we can find out stress in each layer

$$\{\sigma'\}_k = [\overline{Q}]_k \{\varepsilon\}_k \tag{2.42}$$

From the constitutive relation Eq. (2.3) we can write equate strain in magnetostrictive

From composite analysis and from constitutive relation

$$\{\varepsilon\}_m = [S]_m \{\sigma'\}_m + [d]\{H\}$$

where from Eq. (2.27) $\{H\} = n\{I_1\}$

By inverting above strain-stress constitutive relation we get

$$\{\sigma'\}_m = [S]_m^{-1} \{\{\varepsilon\}_m - [d] n \{I_1\}\}$$

From Eq. (2.40) we can write it as

$$\{\sigma'\}_m = [S]_m^{-1} \{\{\varepsilon_0\} + y_m \{\lambda\} - [d] n \{I_1\}\}$$

Using Eq. (2.30), and Eq. (2.39) we can write as

$$\{\sigma'\}_m = [S]_m^{-1} \{[[A_1] + [A_2]][\alpha_1]\{I_1\} h_m + y_m [\alpha_3]\{I_1\} - [d] n \{I_1\}\}$$

$$\{\sigma'\} = [S]^{-1} \left[[[A_1] + [A_2]][\alpha_1] h_m + y_m [\alpha_3] - [d] n\right] \{I_1\}$$

Here we have

$$[S]_m^{-1} = [Q]_m$$

$$\{\sigma'\}_m = [\alpha_4]\{I_1\} \tag{2.43}$$

where

$$[\alpha_4] = [Q]\left[[[A_1] + [A_2]][\alpha_1] h_m + y_m [\alpha_3] - [d] n\right]$$

2.1.2.4 Delamination Analysis:

In Composite mainly delamination at the interfaces start due to internal flaws present in the interface or due to lower fracture toughness value at the interfaces. As we have done the analysis for the stresses in all the interfaces, because of these stresses in the interfaces the delamination starts when the acting stresses exceed the critical stress value according to the strength property.

As we have stress in each layer of laminate given by Eq. (2.43)

$$\{\sigma\}_k = \left[\overline{Q}\right]_k \{\varepsilon\}_k$$

There are various Failure criteria if any of this is satisfied by laminate structure then delamination may start:

2.1.2.4.1 Failure Criteria:

Stress Intensity factor ≥ fracture toughness

$$K_I \geq \beta K_{IC}$$

Since $$G = \frac{K_I^2}{E}$$

$$K_I = \sigma\sqrt{\pi c} \geq \beta\sqrt{E G_C} = \beta K_{IC}$$

Loading and geometry material properties

β is the constant, which depends on mode of failure, geometries we have taken and also on some other fracture parameter. The detailed study is needed to get exact value of this factor. In our case this factor is taken unity.

2.1.2.5 Voltage Analysis:

As we have the stress distribution on overall structure of the laminate, our aim here is to get the signal in the form of open circuit voltage at which delamination started. So when Delamination started we will have the stress in the magnetostrictive layer which is able to give us electrical signal as explained in the following analysis.

using $\{\sigma'\}_m$ from Eq. (2.43) in place of $\{\sigma\}_m$ in Eq. (2.4) to get the modified flux density vector

$$\{B'\} = [d]\{\sigma'\}_m + [\mu]\{H\}$$

$$\{B'\} = [d][\alpha_4]\{I_1\} + [\mu]n\{I_1\}$$

$$\{B'\} = [[d][\alpha_4] + [\mu]n]\{I_1\} \tag{2.44}$$

We have from Eq. (2.1)

$$\{I_1\} = \{I_b\} + \{I_0\}\sin\Omega t$$

After differentiating Eq. (2.44) we get

$$\left\{\frac{dB'}{dt}\right\} = [[d][\alpha_4] + [\mu]n]\{I_0\}\Omega\cos\Omega t$$

We have from Eq. (2.33) by using

$$\{V'\} = -nl\,a_r\left\{\frac{dB'}{dt}\right\} \tag{2.45}$$

$$\{V'\} = -nl\,a_r[[d][\alpha_4] + [\mu]n]\{I_0\}\Omega\cos\Omega t \tag{2.46}$$

CHAPTER-3

3.1 Introduction:

As in the previous Chapter we have concerned with application of stresses due to electrical loading only, there is no applied external loading. To extend similar type of approach using the constitutive relation on the cantilever beam with sinusoidal loading at the cantilever end and a constant current is supplied. As we increase the external loading i.e. mechanical in nature we will get increment in stress at each interface, which becomes the cause of delamination. The Failure criteria used in this analysis is same as in previous analysis. In this approach due to mechanical load there will be the stresses in each layer can be calculated using classical laminate theory [13]. As one layer is of the magnetostrictive material Terfenol-D as shown in Fig. 11.

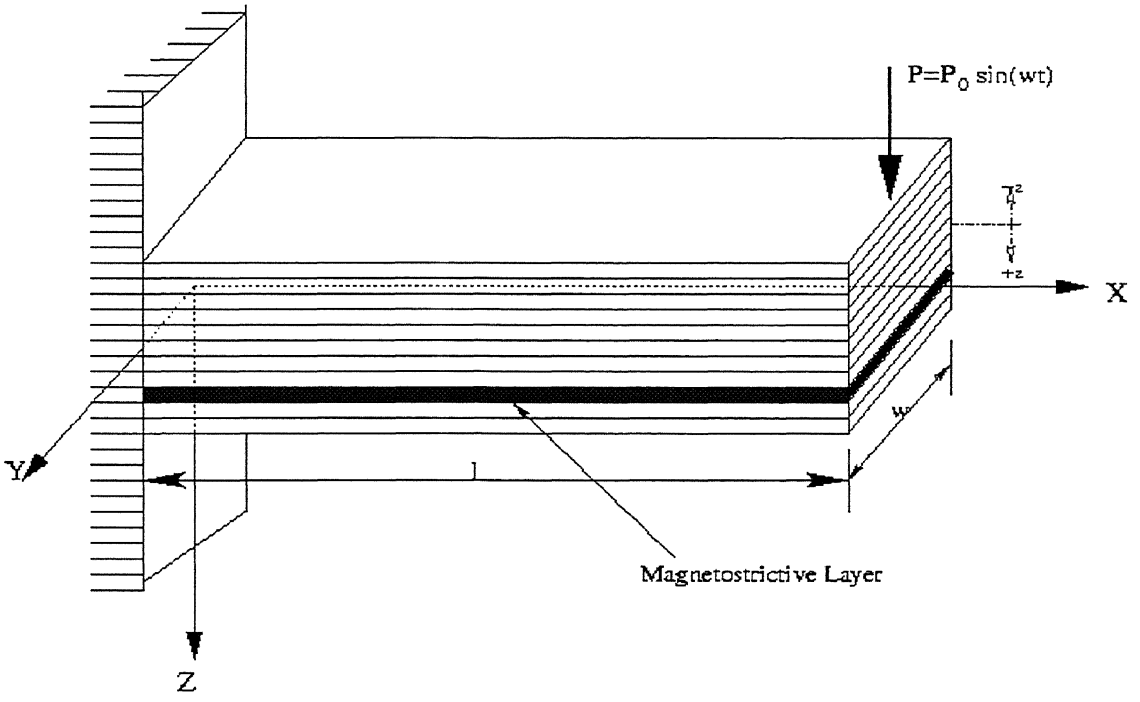

Fig. 11 Cantilever Beam with magnetostrictive layer shown in black

Due to theses stresses the magnetostrictive property of the smart layer will change which can be sensed in the form of open circuit voltage, when the delamination is just about to start at any of the interface based upon the failure criteria.

3.2 Analysis:

3.2.1 Composite Analysis:

From Eq. (2.5) we can write as

$$\begin{Bmatrix} N \\ M \end{Bmatrix} = \begin{bmatrix} A & B \\ B & D \end{bmatrix} \begin{Bmatrix} \varepsilon_0 \\ \lambda \end{Bmatrix}; \tag{3.1}$$

where $$\{N\} = \begin{Bmatrix} N_x \\ N_y \\ N_{xy} \end{Bmatrix}; \qquad \{M\} = \begin{Bmatrix} M_x \\ M_y \\ M_{xy} \end{Bmatrix};$$

Similarly from Eq. (2.7) we can write

$$[A]_{3\times3} = \sum_{i=1}^{z} [\overline{Q}]_i (h_i - h_{i-1});$$

$$[B]_{3\times3} = \frac{1}{2} \sum_{i=1}^{z} [\overline{Q}]_i \left(h_i^2 - h_{i-1}^2\right);$$

$$[D]_{3\times3} = \frac{1}{3} \sum_{i=1}^{z} [\overline{Q}]_i \left(h_i^3 - h_{i-1}^3\right);$$

As we can see from Fig.11 that there is no load on the xy plane from this N_X, N_Y and N_{XY} will be zero. But moment about Y-axis will be the only external applied loading due to the end load in the cantilever as shown in Fig. 11. All applied external loading is per unit meter width. So the moment about Y-axis can be calculated using general beam theory

$$M_x = \frac{P_0 \sin \Omega t \times l}{w} = P_1 \sin \Omega t \quad \text{in Nm per meter width} \tag{3.2}$$

where $$P_1 = \frac{P_0 \times l}{w}$$

where $P_1 = \dfrac{P_0 \times l}{w}$

Eq. 3.1 can be expanded and its inverted form can be represented with external applied loading

$$\begin{Bmatrix} \varepsilon_{0x} \\ \varepsilon_{0y} \\ \varepsilon_{0xy} \\ \lambda_x \\ \lambda_y \\ \lambda_{xy} \end{Bmatrix} = \begin{bmatrix} [A]_{3\times3} & [B]_{3\times3} \\ [B]_{3\times3} & [D]_{3\times3} \end{bmatrix}^{-1}_{6\times6} \begin{Bmatrix} 0 \\ 0 \\ 0 \\ P_1 \\ 0 \\ 0 \end{Bmatrix} \sin \Omega t \; ; \tag{3.3}$$

Hence from Eq. (2) we can write

$$\begin{aligned} \{\varepsilon_0\} &= \{\varepsilon_0\}' (\sin \Omega t); \\ \{\lambda\} &= \{\lambda\}' (\sin \Omega t); \end{aligned} \tag{3.4}$$

From Simple composite theory as in [13]. We can calculate the strain and stresses in all the layers as follows

$$\{\varepsilon\}_k = \{\varepsilon_0\} + z_k \{\lambda\} = \{\varepsilon_0\}' \sin \Omega t + z_k \{\lambda\}' \sin \Omega t \quad ; \tag{3.5}$$

Where z_k is the height of each layer from mid-plane axis in z direction as in Fig. 11.

$k=m$ is for magnetostrictive layer

Similarly the stress in each layer from Eq. (2.4) will be

$$\{\sigma\}_k = [\bar{Q}]_k \{\varepsilon\}_k = [\bar{Q}]_k \left(\{\varepsilon_0\}' + z_k \{\lambda\}' \right) \sin \Omega t \; ; \tag{3.6}$$

3.2.2 Delamination Analysis:

Here also the same delamination criterion is chosen as in electrical loading case. In Composite mainly delamination at the interfaces start due to internal flaws present in the interface or due to lower fracture toughness value at the interfaces. As we have done the analysis for the stresses in all the interfaces, because of these stresses in the interfaces the delamination starts when the acting stresses exceed the critical stress value according to the strength property.

As we have stress in each layer of laminate given by Eq. (3.6)

$$\{\sigma\}_k = \left[\overline{Q}\right]_k \{\varepsilon\}_k$$

There are various Failure criteria if any of this is satisfied by laminate structure then delamination may start:

3.2.2.1 Failure Criteria:

Stress Intensity factor ≥ fracture toughness

$$K \geq \beta K_{IC}$$

Since $$G = \frac{K_I^2}{E}$$

$$K_I = \sigma\sqrt{\pi c} \geq \beta\sqrt{E G_C} = \beta K_{IC}$$

Loading and geometry material properties

β is the constant, which depends on mode of failure, geometries we have taken and also on some other fracture parameter. The detailed study is needed to get exact value of this factor. In our case this factor is taken unity.

3.2.2 Voltage Analysis:

The constitutive relationship for Terfenol-D material is from Eq. (2.2) and (2.3) can be written as

$$\{\varepsilon'\}_m = [S]_m\{\sigma\}_m + [d]\{H\} \tag{3.7}$$

$$\{B\} = [d]\{\sigma\}_m + [\mu]\{H\} \tag{3.8}$$

As in this case the varying input is mechanical load with constant (amplitude) electrical loading, so we get modified strain on the smart layer from Eq. (3.7). Here the current input is also of sinusoidal nature but of constant amplitude.

Th e current form can be written as

$$\{I_1\} = \{I_0\}\sin\Omega t \tag{3.9}$$

The Eq. (3.7) can be written as

$$\{\varepsilon'\}_m = [S]_m[\overline{Q}]_m\left\{\{\varepsilon_0\}' + z_m\{\lambda'\}\right\}\sin\Omega t + [d]_n\{I_0\}\sin\Omega t$$

$$[S]_m = [\overline{Q}]_m^{-1} = [Q]_m^{-1}$$

$$[S]_m[\overline{Q}]_m^{-1} = [\mathrm{I}] \qquad \text{identity matrix}$$

After simplification we can write it in this form

$$\{\varepsilon'\}_m = \left\{\{\varepsilon_0\}' + z_m\{\lambda\}'\right\} + [d]_n\{I_0\}\sin\Omega t \tag{3.10}$$

Using Eq. (3.8) the flux density can be written as

$$\{B\} = [d]\{\sigma\}_m + [\mu]\{H\}$$

$$\{B\} = [d]\{\sigma\}_m + [\mu]_n\{I_1\}$$

From Eq. (3.6) the above can be modified as

$$\{\mathrm{B}\} = [d][\bar{Q}]_m \{\varepsilon\}_m + [\mu]n\{I_1\}$$

Using Eq. (3.6) and Eq. (3.9) we can write it as

$$\{\mathrm{B}\} = [d][\bar{Q}]_m \left\{\{\varepsilon_0\}' + z_m\{\lambda\}'\right\}\sin\Omega t + [\mu]n\{I_0\}\sin\Omega t\,; \tag{3.11}$$

By differentiating Eq. (3.11) we can get

$$\left\{\frac{d\mathrm{B}}{dt}\right\} = [d][\bar{Q}]_m \left\{\{\varepsilon_0\}' + z_m\{\lambda\}'\right\}\Omega\cos\Omega t + [\mu]n\{I_0\}\Omega\cos\Omega t \tag{3.12}$$

From Eq. (2.33) the voltage response

$$\{V\} = -nl\,a_r\left\{\frac{d\mathrm{B}}{dt}\right\};$$

Final Voltage Response using Eq. (3.12) can be written as

$$\{V\} = -n\,l\,a_r[d][\bar{Q}]\left\{\{\varepsilon_0\}' + z_m\{\lambda\}'\right\}\Omega\cos\Omega t + [\mu]n\{I_0\}\Omega\cos\Omega t$$

$$\{V\} = -nl\,a_r\left\{[d][\bar{Q}]_m\left\{\{\varepsilon_0\}' + z_m\{\lambda\}'\right\} + [\mu]n\{I_0\}\right\}\Omega\cos\Omega t \tag{3.13}$$

3.3 Input Parameters:

The Laminate we have taken above and below the magnetostrictive layer is CFRP (carbon fiber reinforced plastic) consisting p_1 number of laminae (CFRP) above magnetostrictive layer and p_2 number of lamina (CFRP) below magnetostrictive layer.

Geometrical Properties:

- Height of laminate configuration, which is above and below the magnetostrictive layer.
- Thickness of magntostrictive layer.
- Width of beam.
- Length of the beam.

Material Properties:

- Elastic properties of fiber and matrix that include modulus of elasticity and poissons ratio.
- Elastic properties of magnetostrcitive layer.
- Magnetostrictive properties of the Terfenol-D layer, which include piezomagnetic coefficients and permeability constant.
- Strength property of laimnae.

Lay-Up properties:

- Angle of fiber orientation with respect to reference axis system.

Other Properties:

- No. of turns per meter length
- Frequency in hertz.
- Initial carrier current.

3.4 Lay-Up Detail:

Table No. 3.1 Stacking sequences for asymmetric laminates

Lay-Up identification	Stacking Sequence
TA-I-E/TA-I-M	$\pm 45/0_2/90_2/0_2/m/\pm 45$
TA-II-E/TA-II-M	$\pm 45/0_2/90_2/0_2/-45/m/+45$
TA-III-E/TA-II-M	$\pm 45/0_2/90_2/0_2/\mp 45/m/+45$
TA-IV-E/TA-IV-M	$[90/0]_5/m$
TA-V-E/TA-V-M	$0_{10}/m$

Table No. 3.2 Stacking Sequences for Symmetric Laminates

Lay-Up identification	Stacking Sequence
TS-I-E/TS-I-M	$\pm 45/0_2/90/m/90/0_2/\mp 45$
TS-II-E/TS-II-M	$\mp 45/90_2/0/m/0/90_2/\pm 45$
TS-III-E/TS-III-M	$90_2/0_2/45/m/45/0_2/90_2$
TS-IV-E/TS-IV-M	90/0/90/0/90/m/90/0/90/0/90
TS-V-E/TS-V-M	0/45/90/0/−45/m/−45/0/90/45/0

Table No. 3.3. Numerical Detail used in the analysis

S. No.	Property	Constant Used
1.	Number of Laminae above and below magnetostrictive layer, which is indicated in Table No. (3.1) and (3.2) with angular details.	
2.	Composite Used	CFRP
3.	Thickness of Composite Laminae	0.4 mm
4.	Thickness of magnetostrictive Layer	0.4 mm
5.	Elastic modulus in Carbon fiber	350 GPa
6.	Elastic modulus for epoxy resin	3.5 GPa
7.	Poisson's Ratio of carbon fiber	0.3
8.	Poisson's ratio of epoxy resin used	0.4
8.	Elastic modulus for magnetostrictive material i.e. Terfenol-D	30 GPa
9.	Poisson's ratio for magnetostrictive material	.25
10.	Number of turns in the coil per meter length of beam	150
11.	Carrier Frequency	1000 Hz
12.	Carrier Current	0.4 amp
13.	Piezomagnetic coefficient	1.5e-08 m/amp
14.	Permeability	14.13e-07
15.	Width of over all beam structure	10 mm
16.	Length of the beam	100 mm
17.	Fracture strength of composite interface	3 Mpa-$m^{1/2}$

CHAPTER-4

Results and Discussion

The objective of this work is find out the electrical signal generated by magnetostrictive sensor when the crack in any of the interface of laminated beam is about to start. As the crack begins at any of the interface of the composite beam which leads to decrease in overall stiffness of the structure that becomes the cause of failure of the composite beam. This analysis is helpful in predicting the voltage signal when the delamination in the beam starts.

Various plots (Plot Nos. 4.1 to 4.104) has been shown for symmetric and asymmetric arrangement of laminae with different orientation of fiber. Especially the analysis includes first only the electrical loading, which leads to the increase in stress in the magnetostrictive layers, and finally balanced by composite beam. Secondly the analysis is also carried out for both electrical and mechanical loading together in which the mechanical load is varied while keeping the electrical load constant. Effect of frequency on peak voltage is also studied at the end.

4.1 Electrical Loading:

Various plots have been shown for electrical loading. The beam configuration shown in figure Fig. 8 (Chapter 2). In Plot No. 4.1 the black line shows the variation of the peak stress in the delaminating interface with respect to the peak voltage. Star shown in red colour denotes the point at which the delamination starts. (in the 7^{th} interface for that particular case of laminae configuration)

It may be noted that the interface, which are above and below the magnetostrictive layer, are of greater fracture toughness as compared to the fracture toughness of composite interfaces. So even if the stresses are higher in the magnetostrictive (smart) layer the interface is not expected to fail easily. In the same plot we are able to predict the

stresses in x, y and xy direction in the magnetostrictive layer, which are already shown by red, green and blue colors respectively. The Peak Voltage signal is generated only due to the stress in the magnetostrictive layer.

In the symmetric case (Plot No. 4.26), it can be noted that more than one interface have delaminated at the same stress value. This is because of symmetric orientation of the fiber, about the reference axis. This can be seen in the stress variation plot over all interfaces in Plot No. 4.28.

Plot No. 4.2 shows the variation of the peak voltage plot vs. time for two diffferent cases. The black line is for without bending consideration and the red one shows the plot when bending is taken into account. The peak voltage corresponding to the voltage at which the delamination has started. In this plot one can see that the peak voltage is greater if the bending effect is not considered as compared to the analysis with bending consideration. Here the beam with bending will get failure earlier as compared to compared to without bending because the stress will get higher in the delaminating interface after bending consideration for the same stress in the magnetostrictive layer. The voltage response is dependent on the stress in magnetostrictive layer. So if we reverse the situation then for the same failure stress the stress in smart layer without bending correction will be higher as compared to stress with bending correction. However the similar plot for symmetric case is plotted in Plot No. 4.27. Here since the beam is symmetric there will not be any bending effect. Because of this both the curve is overlapping each other.

Variation for strain across the interface of laminate is shown in Plot No. 4.3. for asymmetric case with TA-I-E configuration. Where in TA, A signifies the asymmetric case; I denote the first stacking sequence from table no.3.1, and E if for electrical loading. For symmetric case it is shown in Plot No. 4.28. Variation of the stresses is plotted across the laminate for asymmetric case in Plot No. 4.4. where one can easily find that the effect of orientation is much more effective as compared to the effect of bending. This is due to a large difference in the property of the carbon fiber and epoxy resin, which is

having the ratio of about 100. So the transverse property will be very low as compared to the longitudinal property because transverse property is dependent on the matrix property. When we will have the orientation changes from 0^0 angle to 90^0 angles the stress will get reduced by many times as shown in Plot No. 4.4. and Plot No. 4.29. From Plot No. 4.29 it is clear that the failure is started in more that one interface because teh stresses are same for all interface. This is because the orientation of the fiber in the layers just above and/or below the delaminating interface is same which gives the same stress there.

Plot No. 4.5 shows the variation of the peak stress at each interface with respect to time when any of the interfaces is going to delaminate. This plot shows that the stress in teh interface 8 and 9 is higher, but these interfaces are just above and below the magnetostrictive layer that cannot fail due to its higher strength properties (as we have discussed earlier). The next higher stress, which is shown in Plot No. 4.5 by yellow color, is the delaminating interface, which is 7^{th} interface.

Similar plot for 10 different cases of ply sequence are given in table no. 3.1-3.2 from Plot No. 4.6 to Plot No. 4.50. corresponding to the electrical loading.

4.2 Mechanical Loading:

In the case of mechanical loading, the laminate configuration is shown in Fig. (11) in Chapter 3. Similar to electrical loading in this case also various plots have been shown from Plot No. 4.51 to Plot No. 4.100 for symmetric and asymmetric cases with different fiber orientation. Here also the effect of bending is not much effective as the effect of orientation. Effect of bending can be seen in Plot No. 101 and Plot No. 102 for different Composite, having $E_f/E_m < 4$ having same volume fraction as in teh last case.

Probability of failure of more than one interface is higher in symmetric case. Plot No. 4.76 shows the symmetric laminate with stacking sequence TS-I-M where S in TS denotes for symmetric laminate, I is for first stacking sequence which is given in table no.

3.2 in detail, and M is for mechanical loading. Here two interfaces 2^{nd} and 9^{th} is delaminating because just below 2^{nd} and above 9^{th} interface laminae has fiber orientation of 0^0. Added bending is also predominant at the outermost and innermost fiber. The upper interface (i.e. the 2^{nd}) has tensile stress and the 9^{th} interface, which is the lowest one, is of compressive stress. Accordingly we will have two stresses in the middle (smart) layer one will be tensile and the other will be compressive with similar magnitude. Voltage response is dependent on stress in smart layer so in the plot absolute value of peak voltage is plotted.

It is also evident from analytical relation that tensile stress in the smart layer will give the negative voltage signal and similarly compressive stress jn smart layer will give us positive voltage signal. For varying mechanical loading and constant electrical loading similar plot is shown from Plot No. 4.51 to Plot No. 4.100.

The effect of carrier frequency plays an important role in the peak voltage response, which can be seen in Plot No.103 and Plot No.104 for asymmetric and symmetric cases.

4.1 Electrical loading:

Beam Configuration:

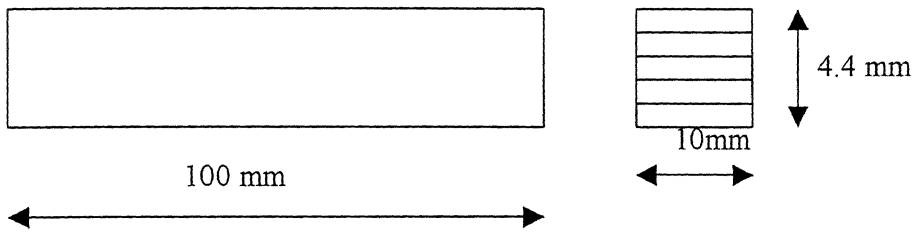

Laminate Detail: **CFRP**

Mechanical Properties:

Elastic modulus of carbon fiber E_f = 350 GPa, Poisson's ratio ν_f =0.35

Elastic modulus of epoxy resin E_m = 3.50 GPa, Poisson's ratio ν_m =0.4

Magnetostrictive Material: **Terfenol-D**

Properties: E_L =30Gpa, E_T =30Gpa, ν_{LT} =0.25

Type of Laminate: Asymmetric Laminate (TA-I-E)

Number of Laminas: 11

Number of Laminate above magnetostrictive Layer: 8

Ply Thickness: 0.4 mm

Stacking Sequence: $[\pm 45/0_2/90_2/0_2/m/\pm 45]$

Number of Turns per meter: 150

Carrier Frequency: 1000 Hz

Delamination Detail:

Delaminating Interface number from top: 7th

Peak Voltage: +431.401993 mV

Failure Stress: 22.331014 (Tensile in nature) in the delaminating interface

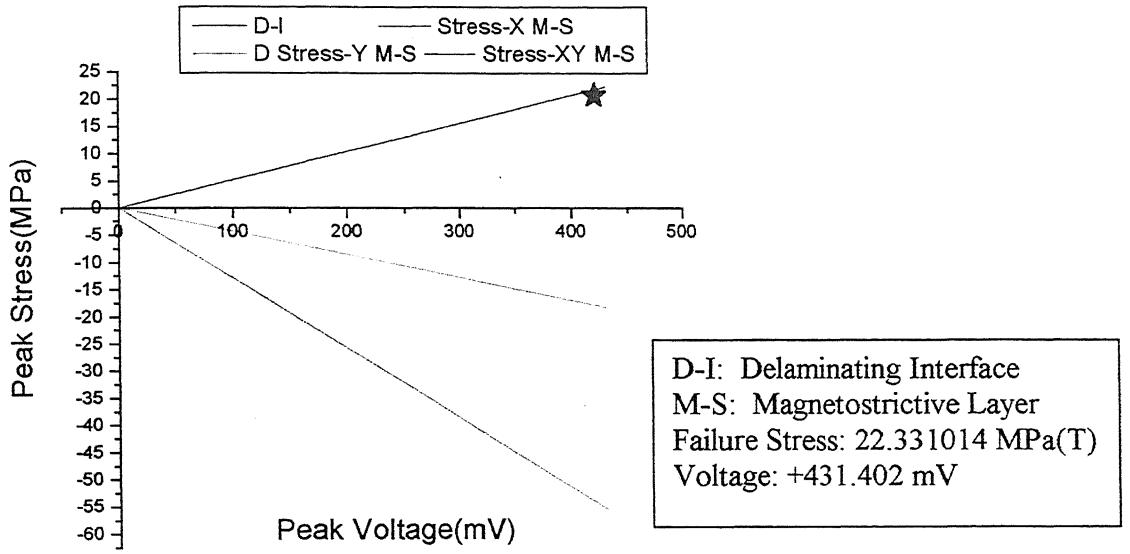

Plot No.4.1. This plots shows the variation of the peak stress in D-I interface and M-S Layer with respect to peak voltage, and star denotes the delamination start point i.e. 7th interface from top.

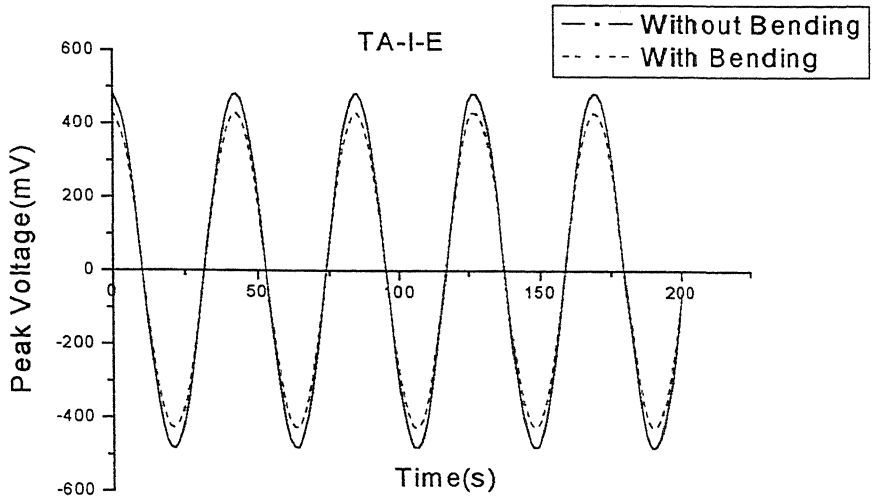

Plot. No.4.2. This shows the variation of the peak voltage with time for without bending and with bending correction when the delamination is just starting

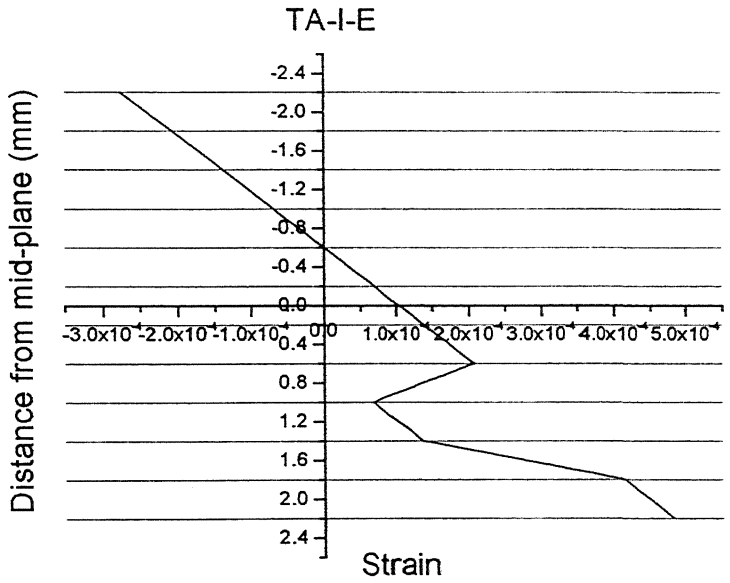

Plot. No. 4.3. This Plot shows the variation of the strain across all the interfaces in the laminate when the delamination starts

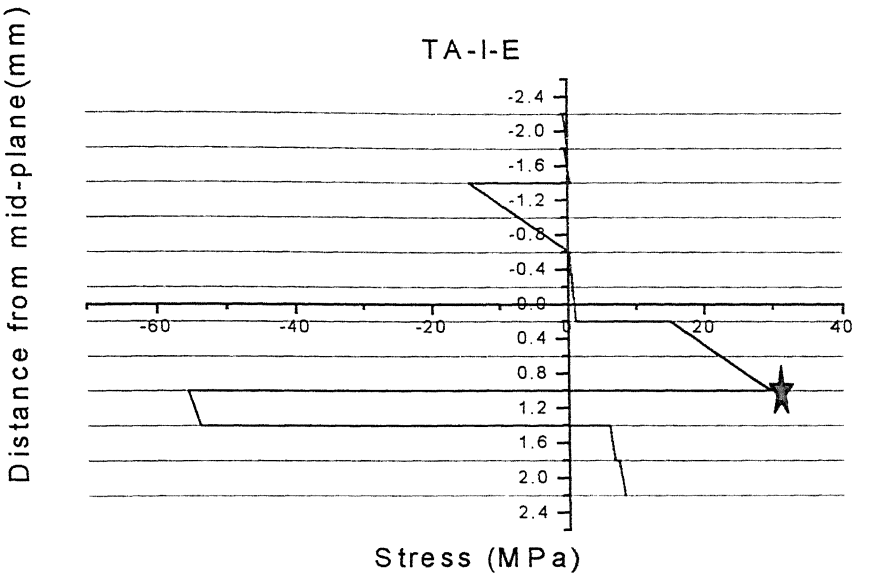

Plot. No. 4.4. This is the variation of the stresses across all the interfaces in the laminate when the delamination starts

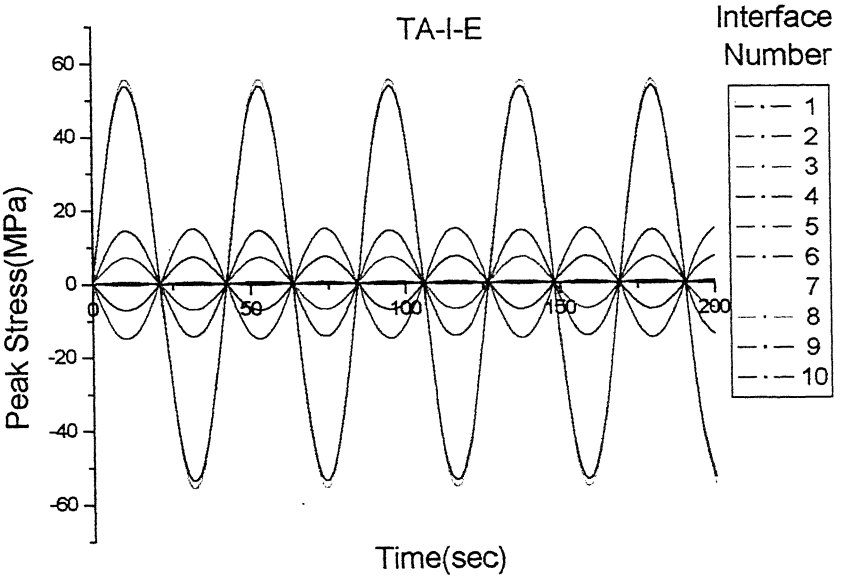

Plot. No. 4.5. The above plot shows the variation of the stresses at each interface when at the delamination has started at 7^{th} interface.

Type of Laminate: Asymmetric Laminate (TA-II-E)

Number of Laminate above magnetostrictive Layer: 9

Stacking Sequence: $[\pm 45/0_2/90_2/0_2/-45/m/+45]$

Delamination Detail:

Delaminating Interface number from top: 8^{th}

Peak Voltage: +285.736533 mV

Failure Stress: 22.324212 MPa (Tensile in nature) in the delaminating interface

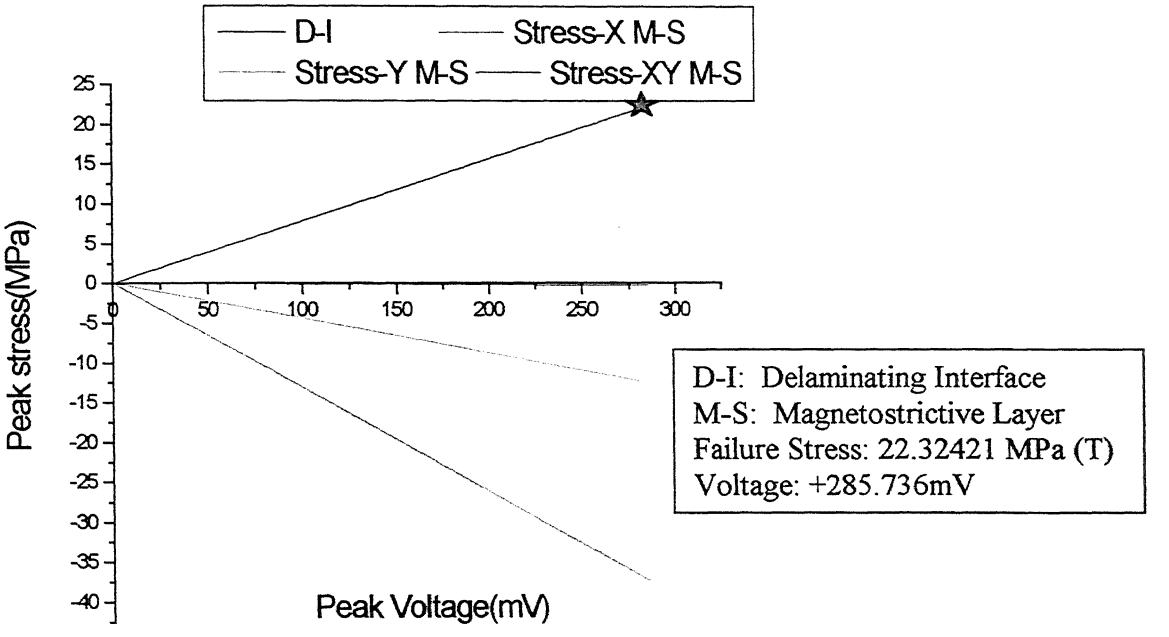

Plot No.4.6. This plots shows the variation of peak stress in D-I interface and M-S Layer with respect to peak voltage, and star denotes the delamination start point i.e. 8^{th} interface from top.

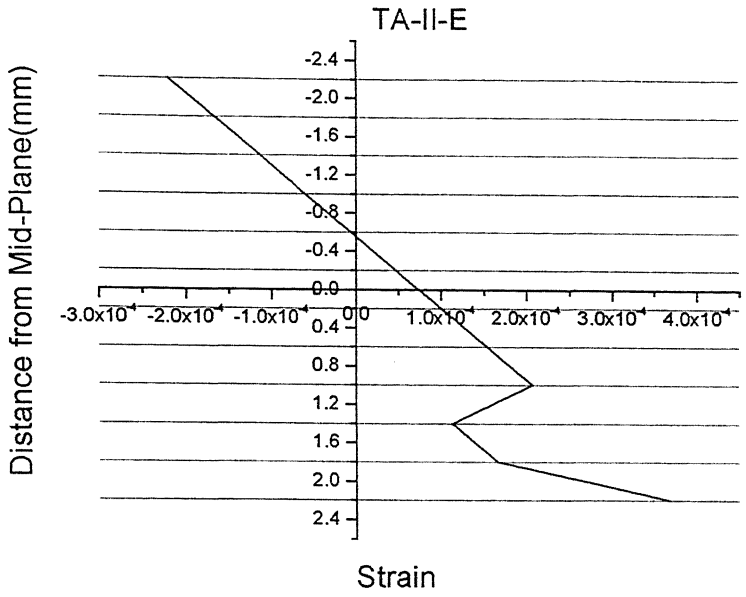

Plot. No. 4.7. This Plot shows the variation of strain across all interfaces in the laminate when the delamination starts

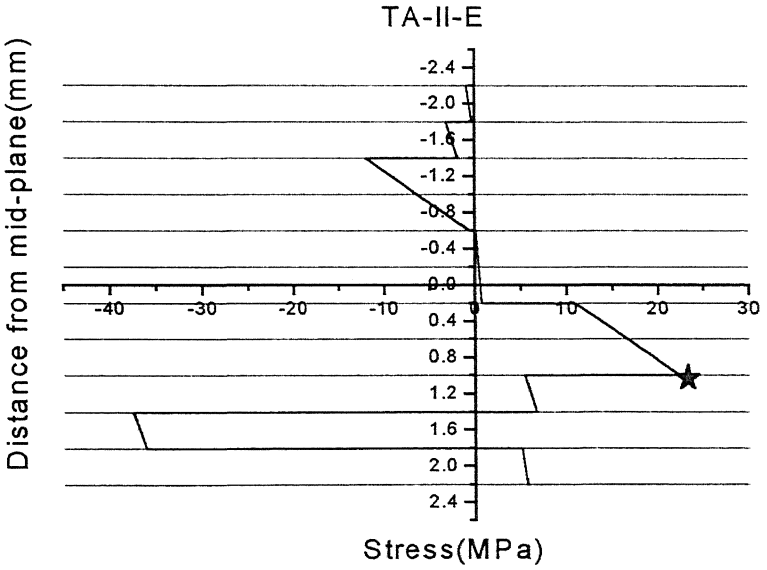

Plot. No. 4.8. This is the variation of the stress across all interfaces in the laminate when the delamination starts

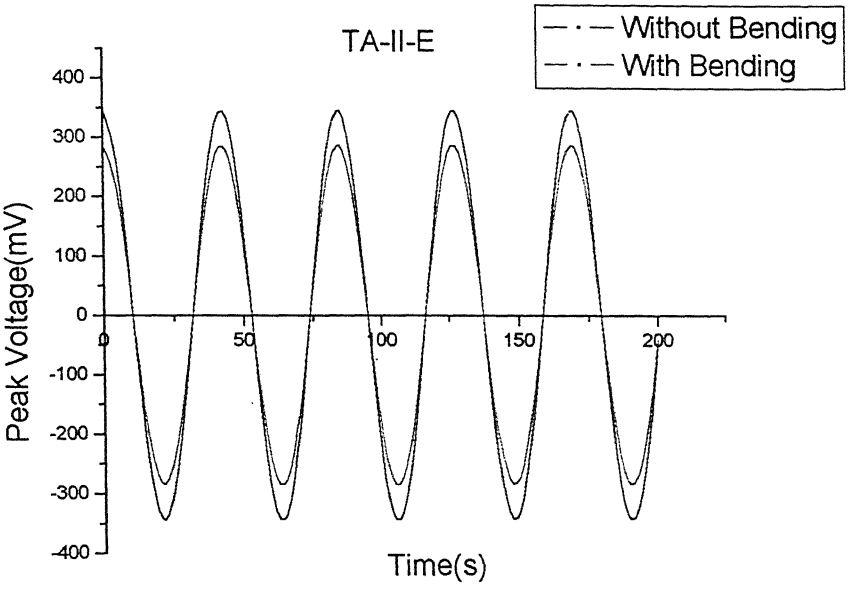

Plot. No. 4.9. This shows the variation of peak voltage with time for without bending and with bending correction when the delamination is just starting.

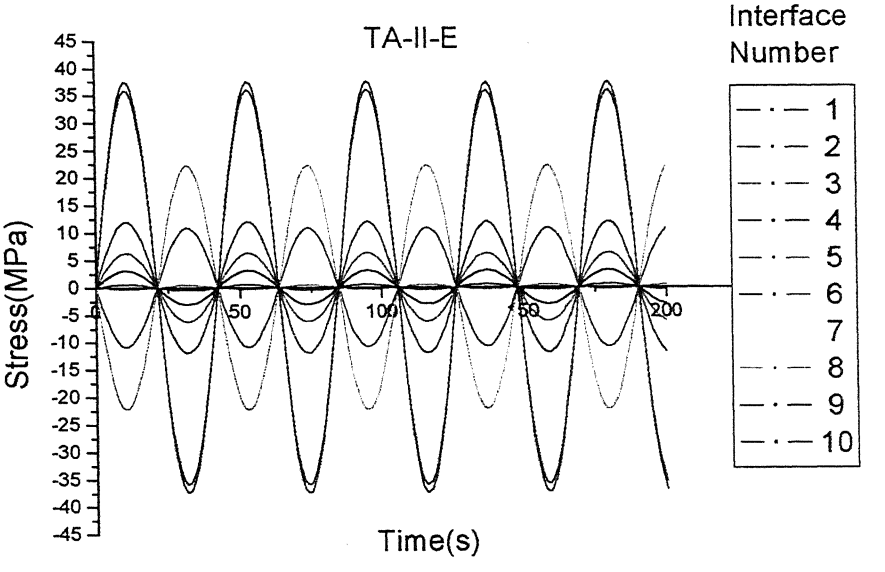

Plot. No. 4.10. The above plot shows the variation of the stresses at each interface when the delamination has started at 8th interface.

Type of Laminate: Asymmetric Laminate (TA-III-E)

Number of Laminate above magnetostrictive Layer: 10

Stacking Sequence: $[\pm 45/0_2/90_2/0_2/\mp 45/m]$

Delamination Detail:

Delaminating Interface number from top: 8th

Peak Voltage: +255.736533 mV

Failure Stress: 22.344733 MPa (Tensile in nature) in the delaminating interface i.e. 8th interface from top

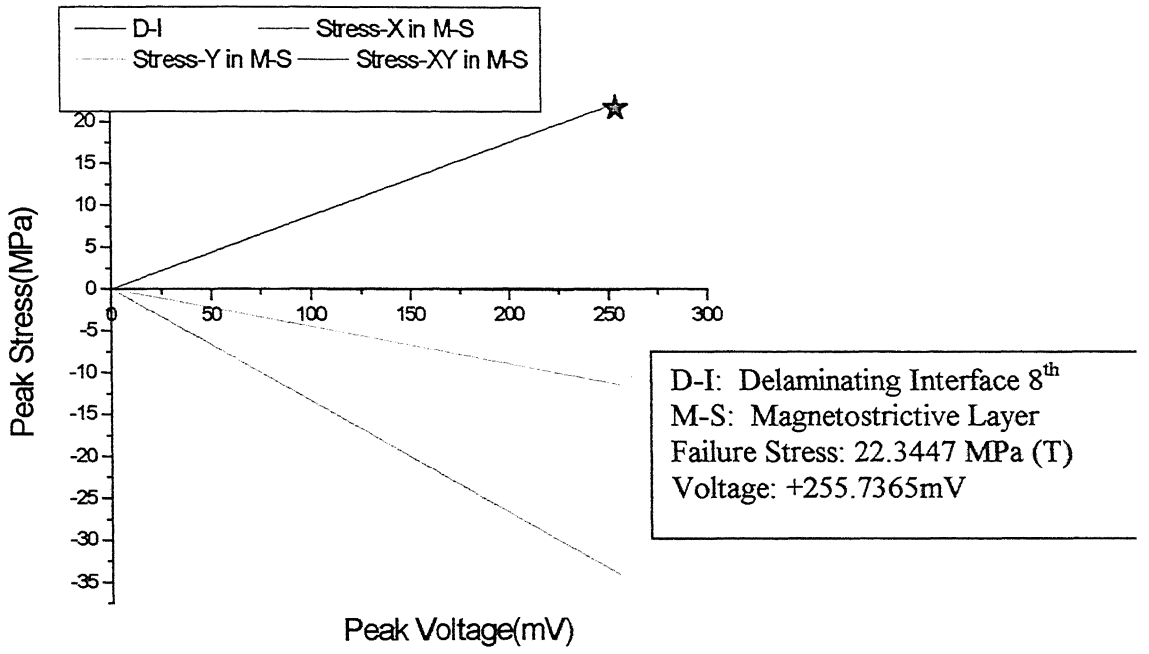

Plot No. 4.11. This plots shows the variation of peak stress in D-I interface and M-S Layer with respect to peak voltage, and star denotes the delamination start point i.e. 8th interface from top.

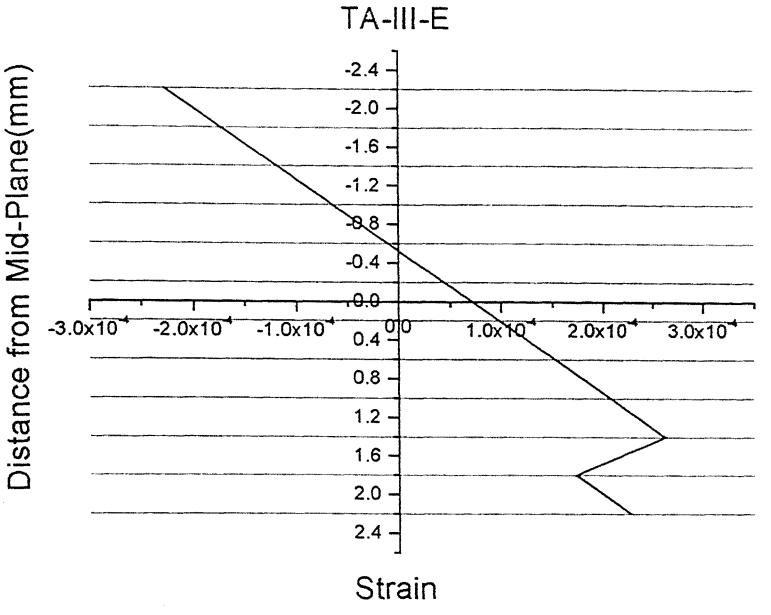

Plot. No. 4.12. This Plot shows the variation of strain across all interfaces in the laminate when the delamination starts.

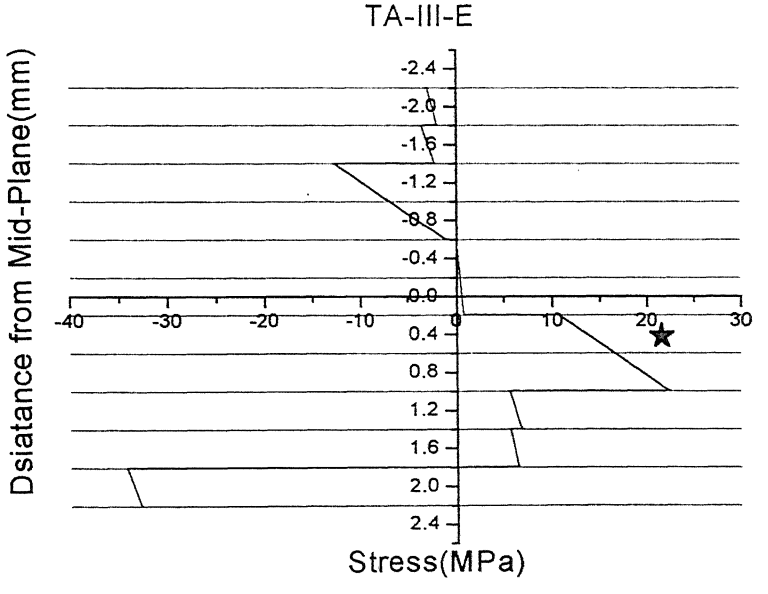

Plot. No. 4.13. This is the variation of the stresses across all interfaces in the laminate when the delamination starts at 8th interface from top as shown by star.

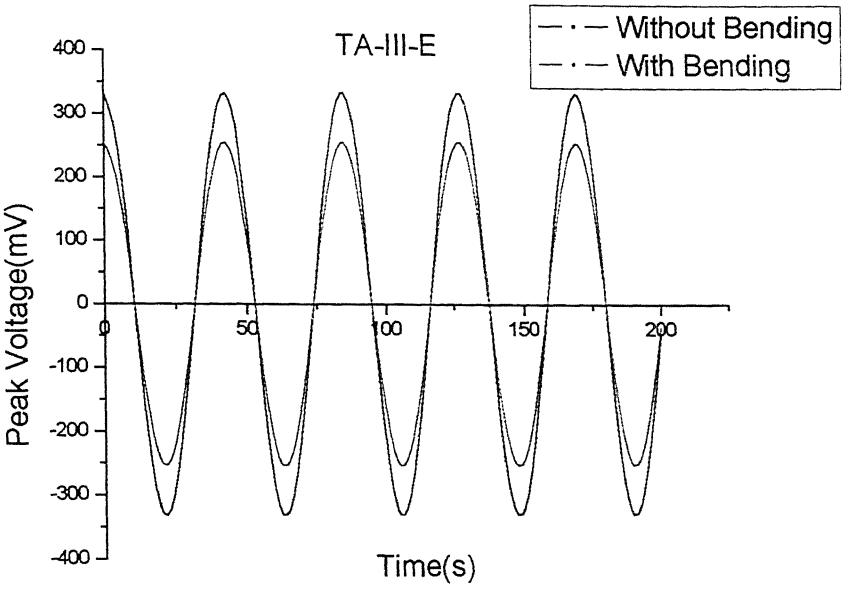

Plot. No. 4.14. This shows the variation of peak voltage with time for without bending and with bending correction when the delamination is just starting.

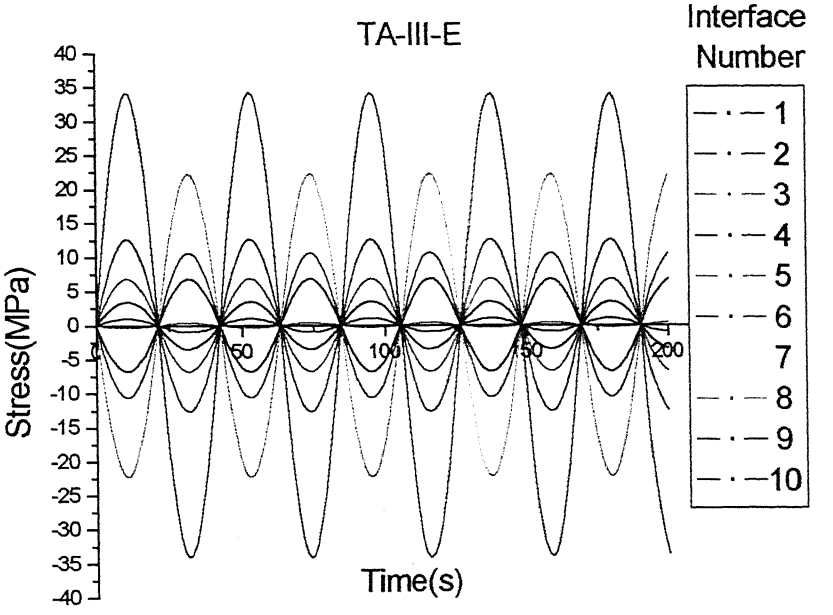

Plot. No. 4.15. The above plot shows the variation of the stress at each interface, when the delamination has started at 8th interface.

Type of Laminate: Asymmetric Laminate (TA-IV-E)

Number of Laminate above magnetostrictive Layer: 10

Stacking Sequence: $[[90/0]_5/m]$

Delamination Detail:

Delaminating Interface number from top: 9^{th}

Peak Voltage: +248.855951 mV

Failure Stress: 22.338577 MPa (Tensile in nature) in the delaminating interface 9^{th}

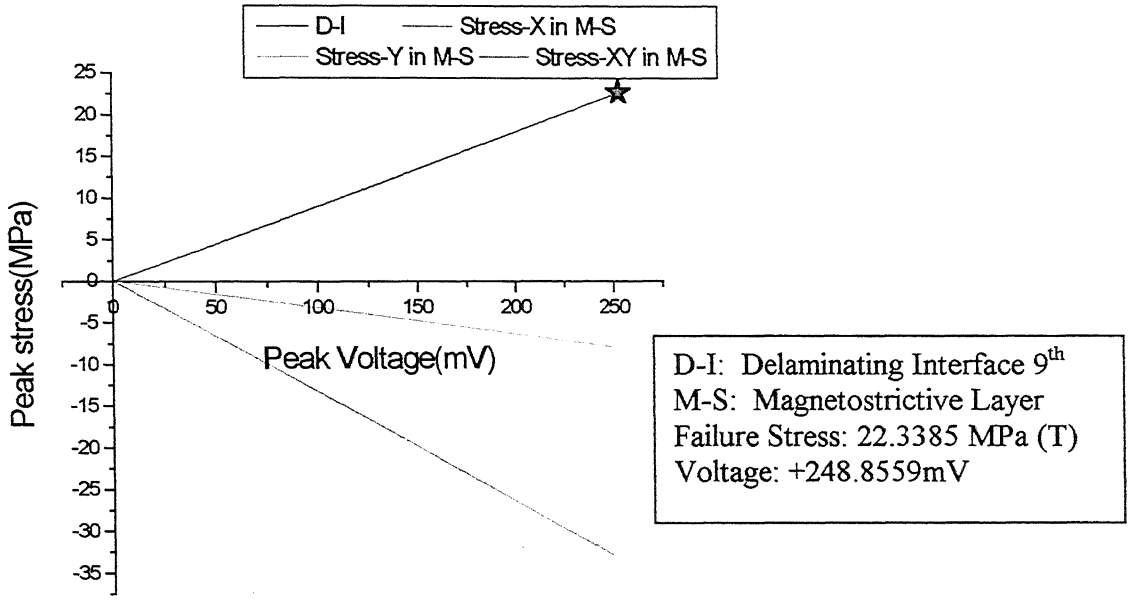

Plot No. 4.16. This plots shows the variation of peak stress in D-I interface and M-S Layer with respect to peak voltage, and star denotes the delamination start point i.e. 9^{th} interface from top.

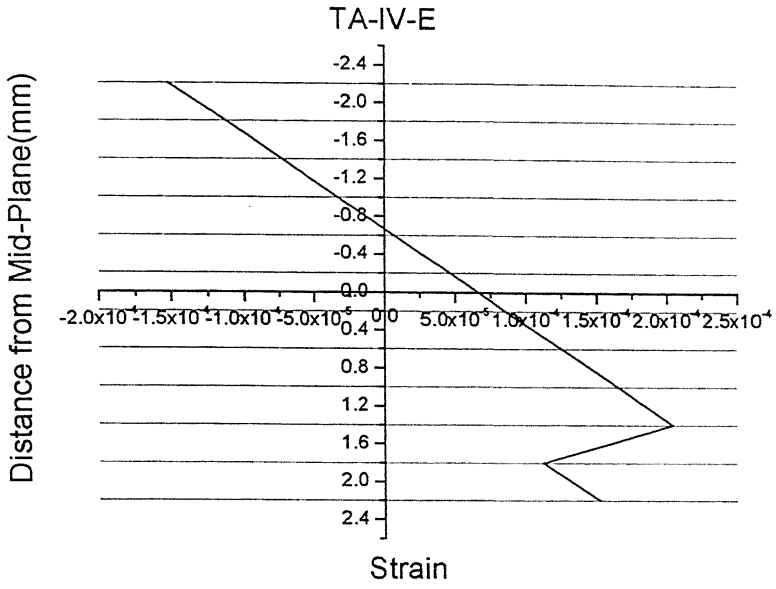

Plot. No. 4.17. This plot shows the variation of strain across all interfaces in the laminate when the delamination starts

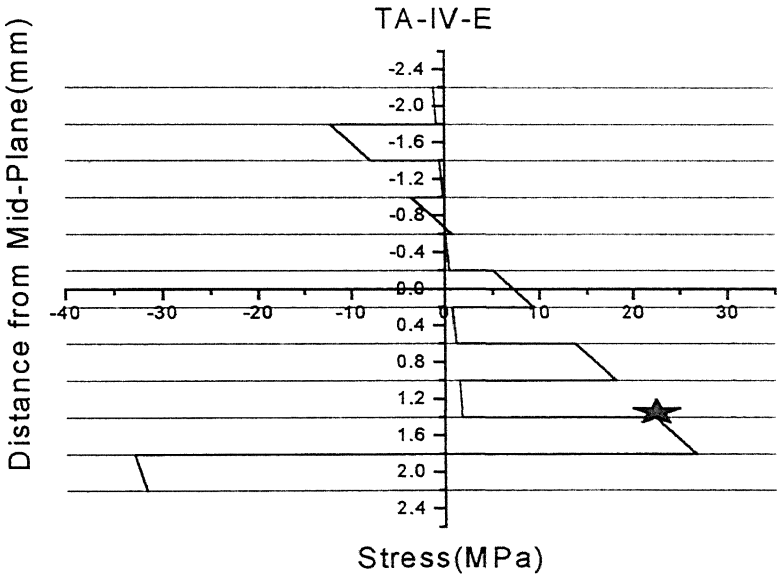

Plot. No. 4.18. This is the variation of the stresses across all interfaces in the laminate when the delamination starts at 9th interface from top as shown by star.

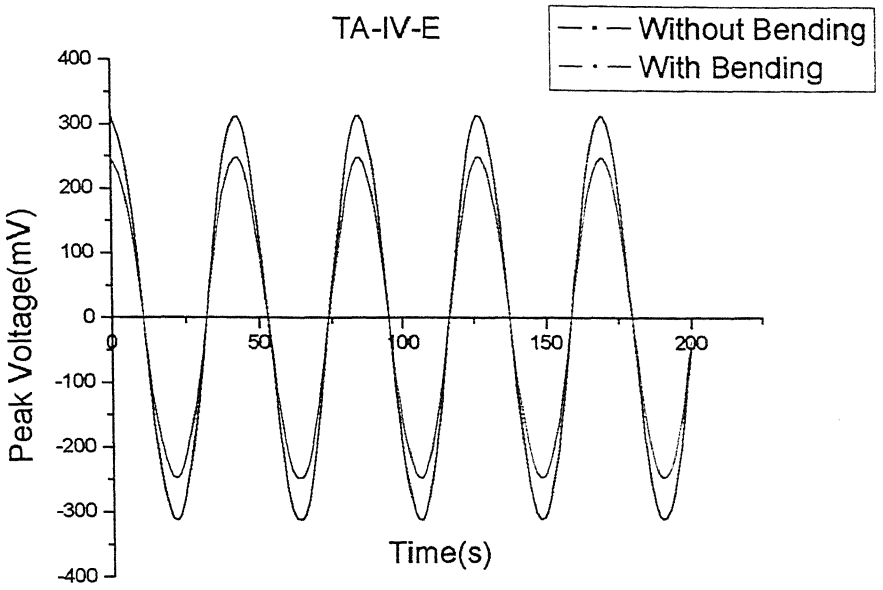

Plot. No. 4.19. This shows the variation of peak voltage with time for without bending and with bending correction when the delamination is just starting.

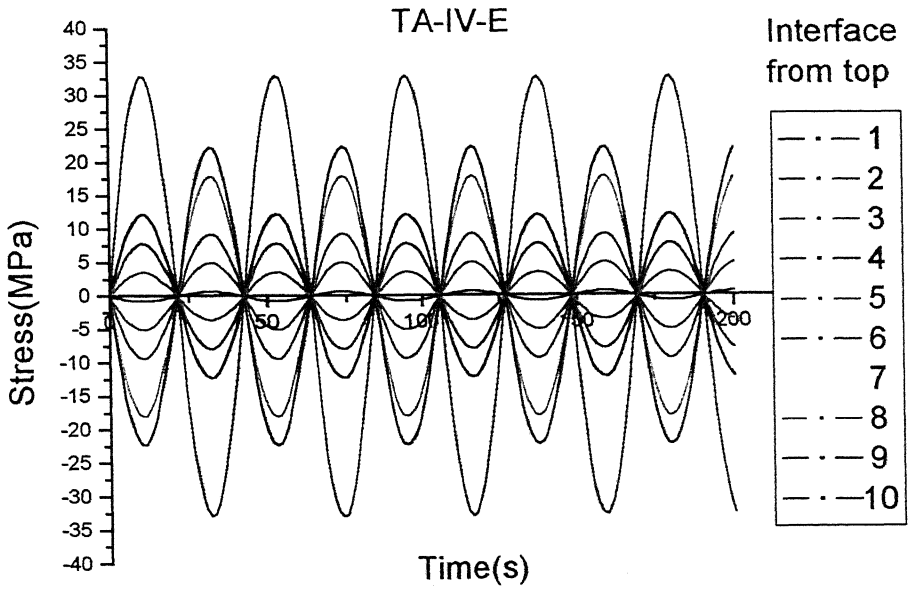

4.20. The above plot shows the variation of the stresses at each interface when the delamination has started at 9th interface.

Type of Laminate: Asymmetric Laminate (TA-V-E)

Number of Laminate above magnetostrictive Layer: 10

Stacking Sequence: $[0_{10}/m]$

Delamination Detail:

Delaminating Interface number from top: 9th

Peak Voltage: +518.343806 mV

Failure Stress: 22.322661 MPa (Tensile in nature) in the delaminating interface

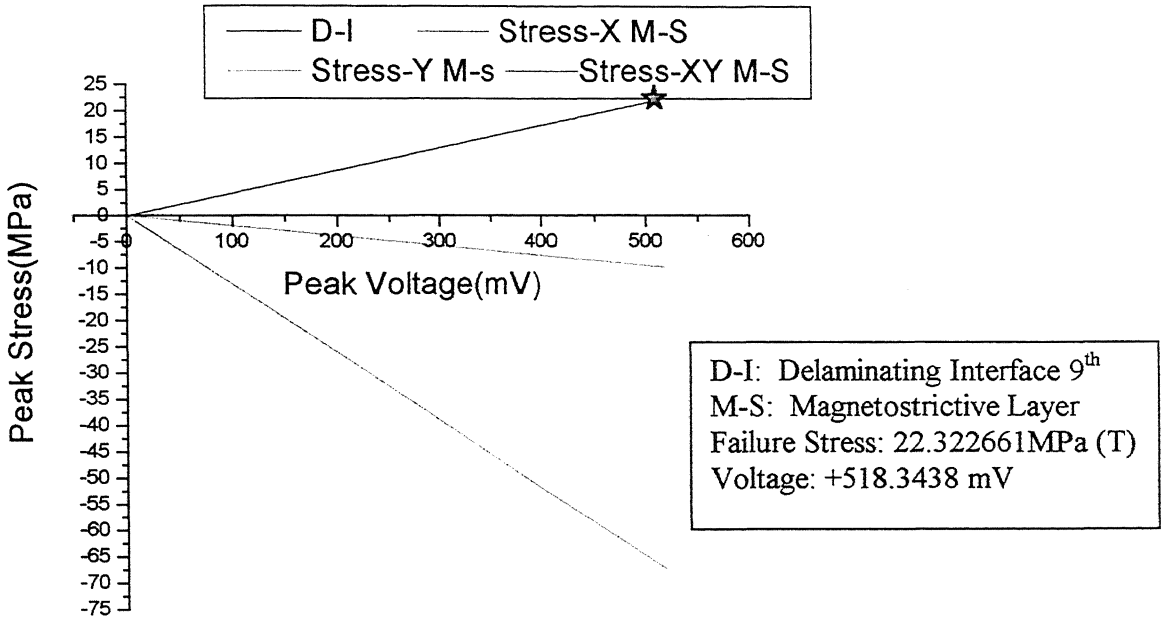

Plot No.4.21. This plots shows the variation of the peak stress in D-I interface and M-S Layer with respect to the peak voltage, and star denotes the delamination start point i.e. 9th interface from top.

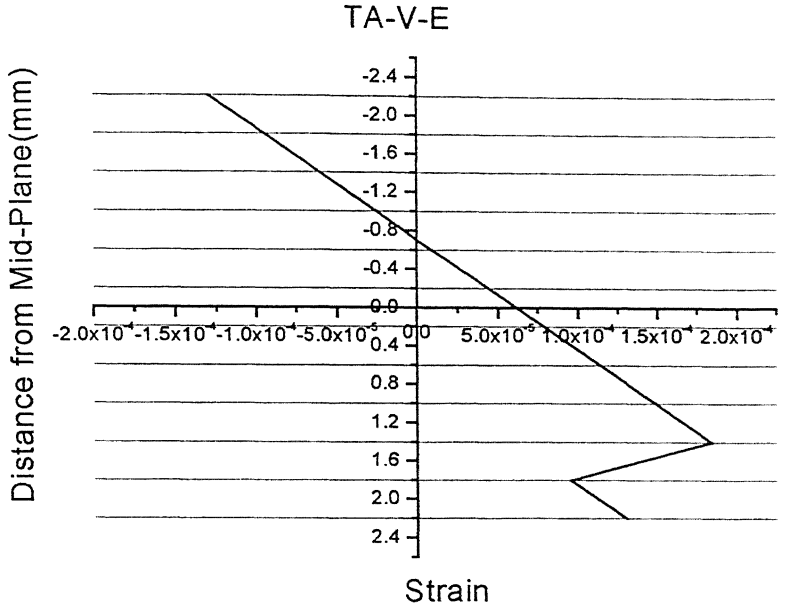

Plot. No. 4.22. This Plot shows the variation of strain across all the interfaces in the laminate when the delamination starts

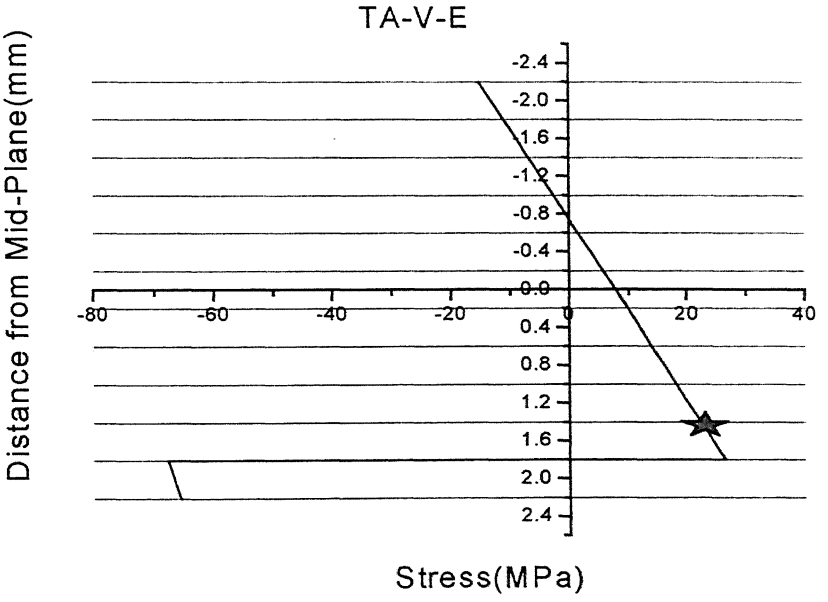

Plot. No. 4.23 This is the variation of the stresses across all the interfaces in the laminate when the delamination starts at 9th interface from top as shown by star.

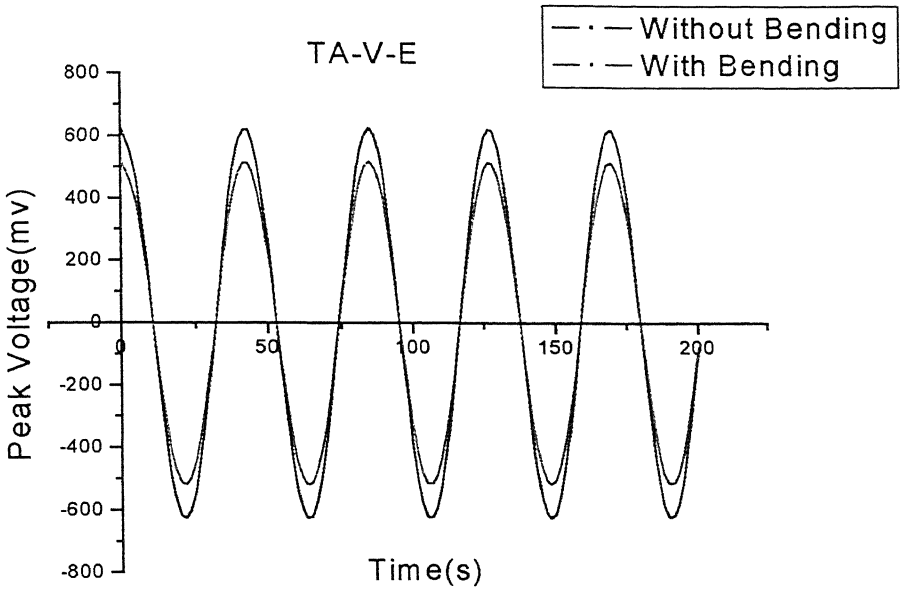

Plot. No. 4.24. This shows the variation of peak voltage with time, for without bending and with bending correction when the delamination is just starting.

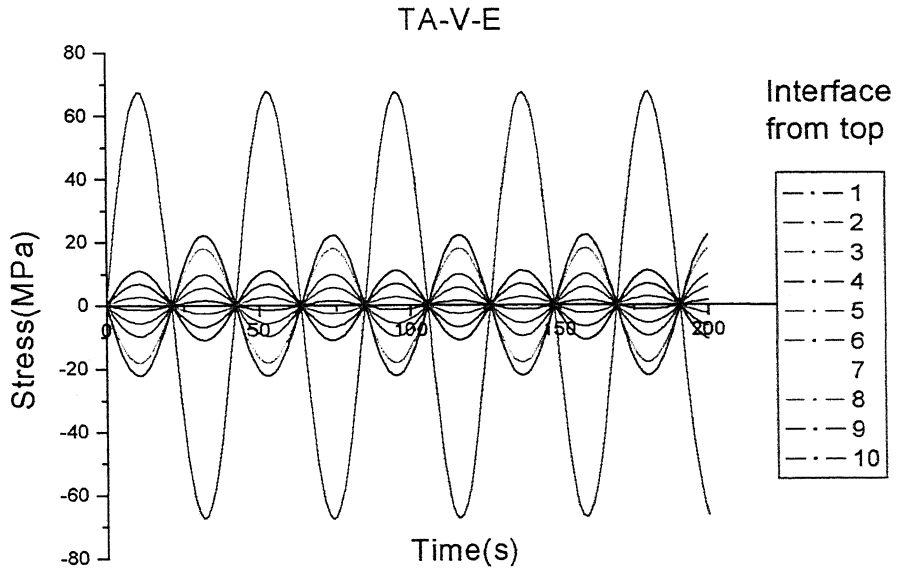

Plot. No. 4.25. The above plot shows the variation of the stresses at each interface when the delamination has started at 9th interface.

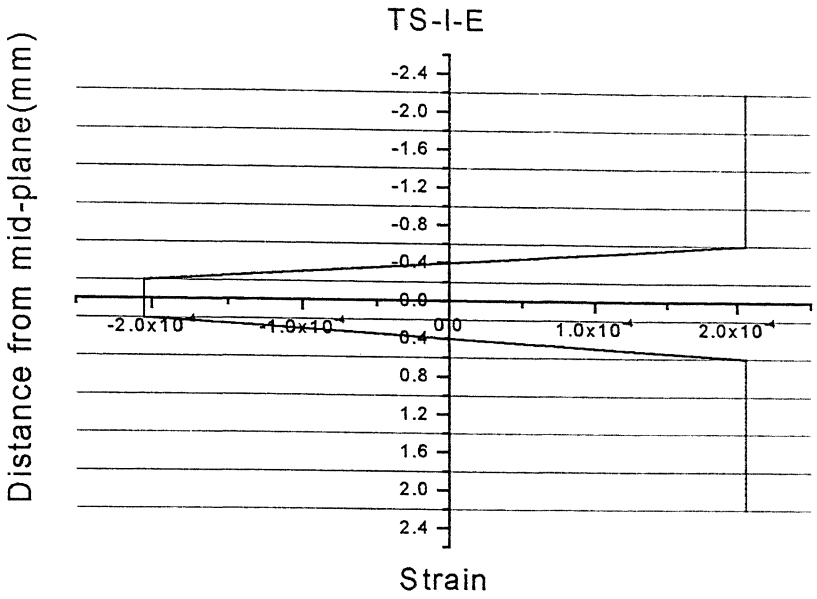

Plot. No. 4.27. This plot shows the variation of strain across all interfaces in the laminate when the delamination starts.

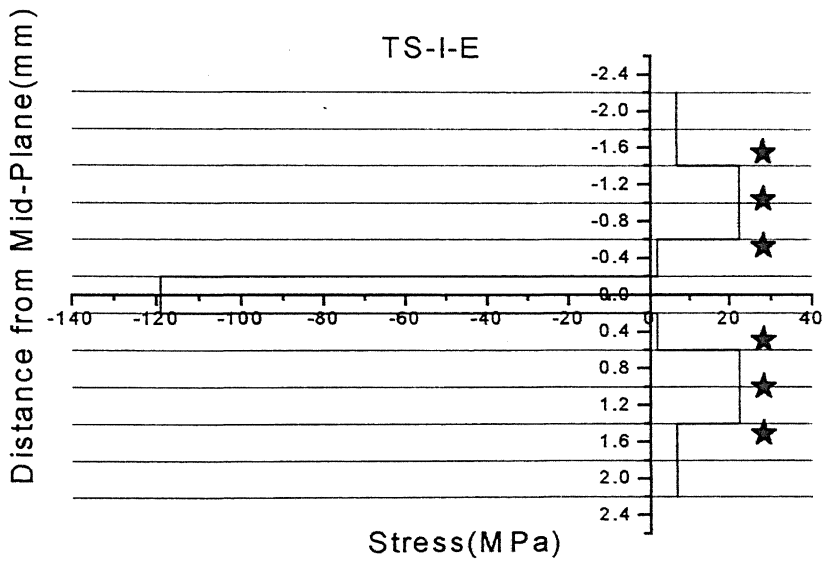

Plot. No. 4.28. This is the variation of the stress across all interfaces in the laminate when the delamination starts at: 2^{nd}, 3^{rd}, 4^{th}, 7^{th}, 8^{th} and 9^{th} interface from top as shown by star.

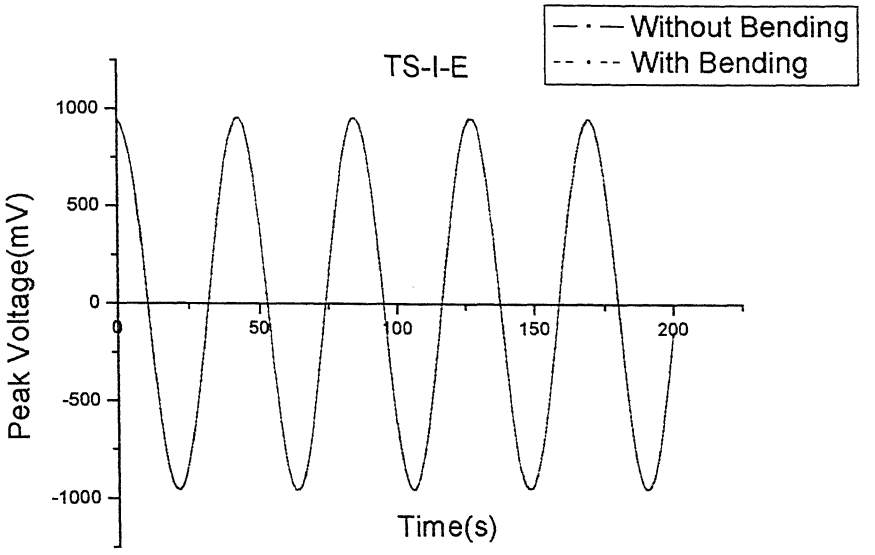

Plot. No. 4.29. This shows the variation of the peak voltage with time for without bending and with bending correction when the delamination is just starting.

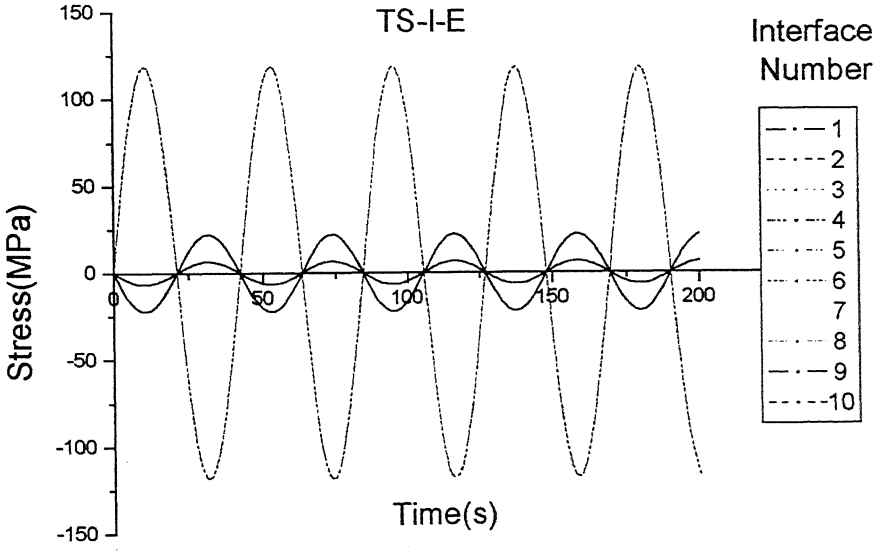

Plot. No. 4.30. The above plot shows the variation of the stresses at each interface when the delamination has started at 2nd, 3rd, 4th, 7th, 8th and 9th interface.

Type of Laminate: Symmetric Laminate (TS-II-E)

Number of Laminate above magnetostrictive Layer: 5

Stacking Sequence: $[\mp 45/90_2/0/m/0/90_2/\pm 45]$

Delamination Detail:

Delaminating Interface number from top: 4th and 7th

Peak Voltage: +608.446163 mV

Peak Stress: 22.323524 MPa (Tensile in nature) i.e. the delaminating interface

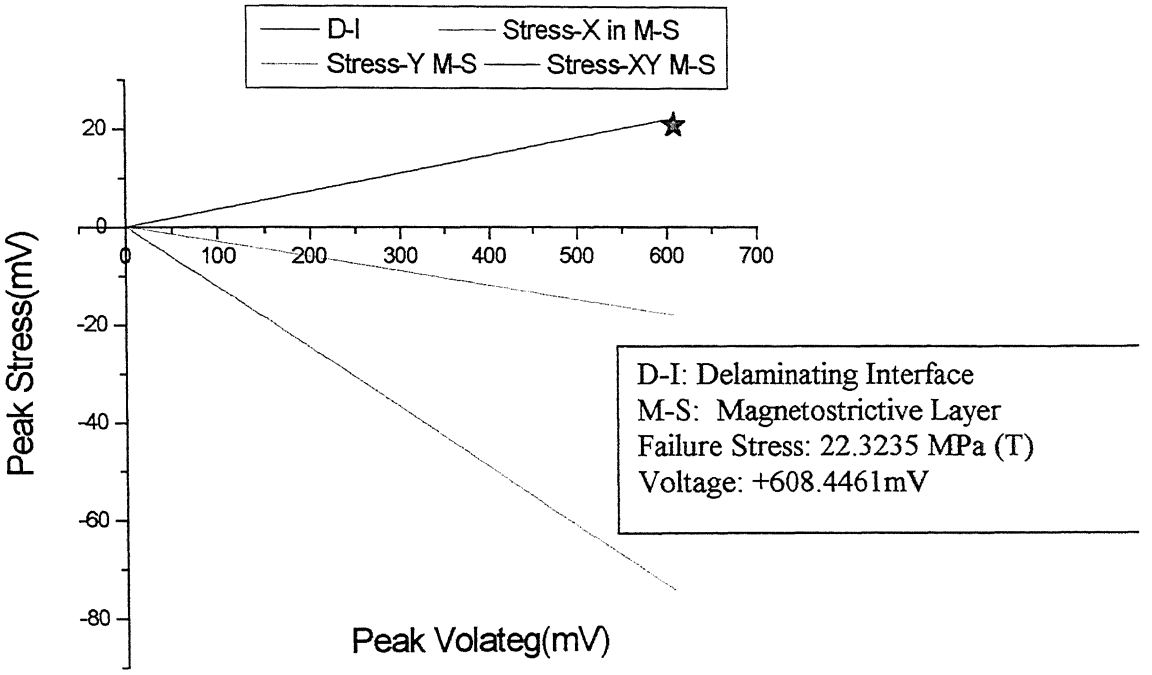

Plot No. 4.31. This plots shows the variation of peak stress in D-I interface and M-S Layer with respect to peak voltage, and star denotes the delamination start point i.e. 4th and 7th interface from top.

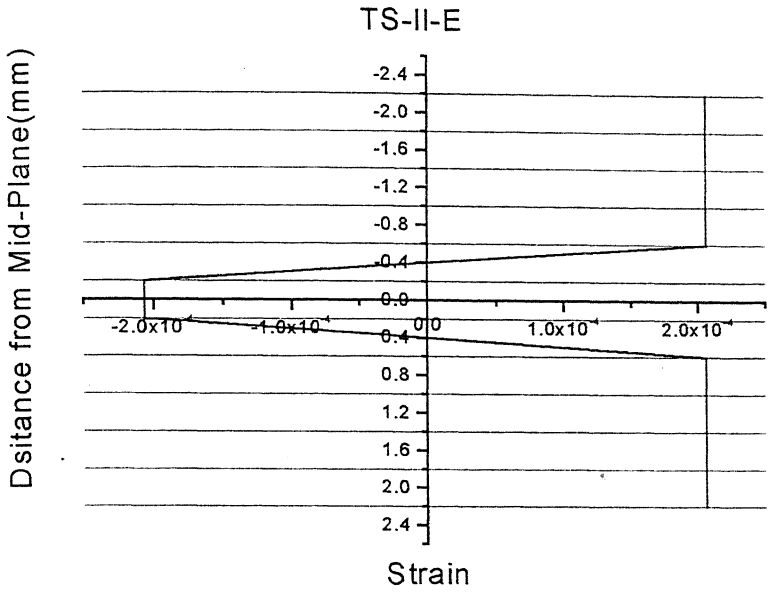

Plot. No. 4.32. This plot shows the variation of strain across all interfaces in the laminate when the delamination starts

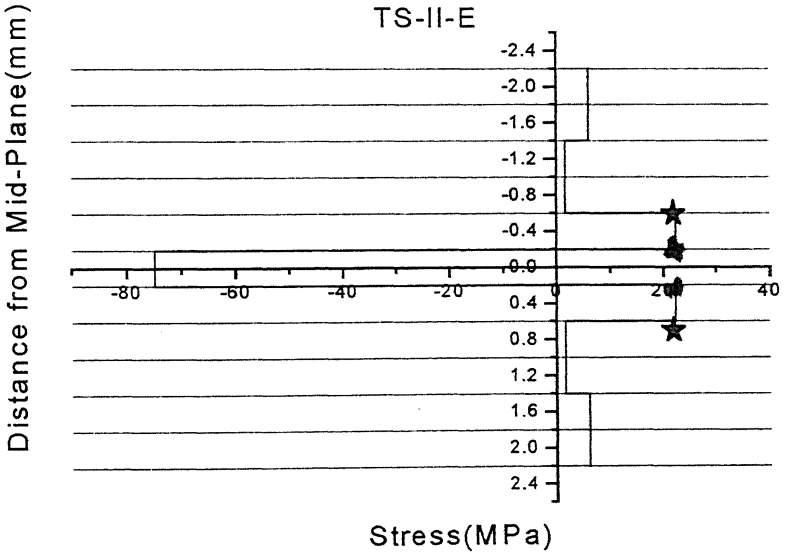

Plot. No. 4.33. This is the variation of the stresses across all interfaces in the laminate when the delamination starts at 4^{th} and 7^{th} interface from top as shown by star

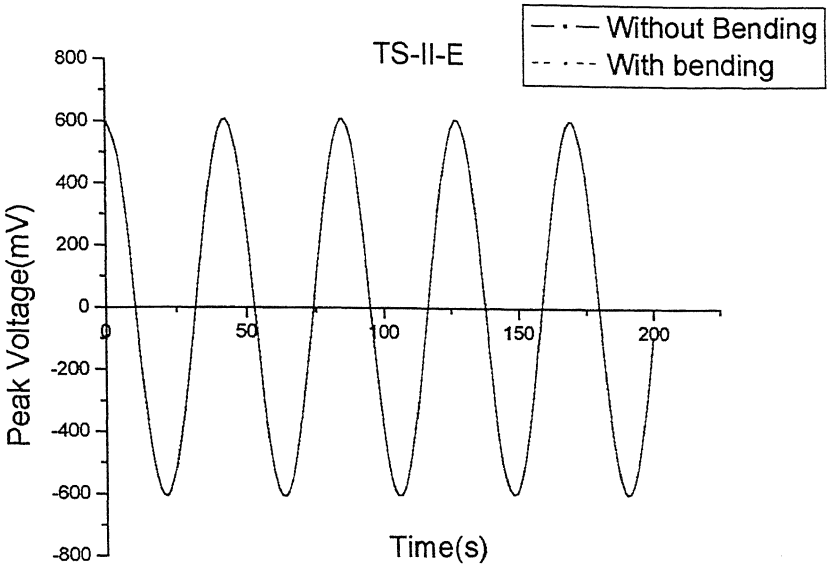

Plot. No. 4.34. This shows the variation of the peak voltage with time for without bending and with bending correction when the delamination is just starting

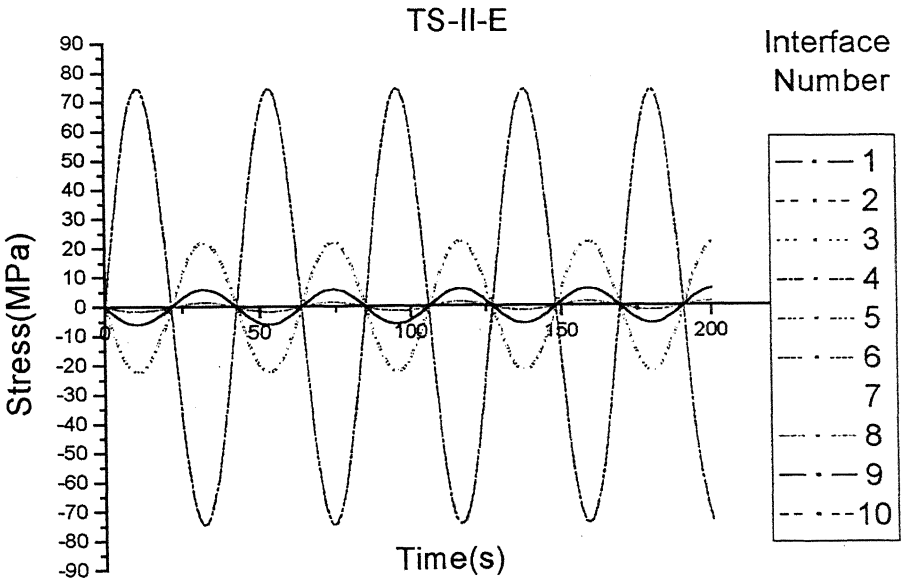

Plot. No. 4.35. The above plot shows the variation of the stresses at each interface when the delamination has started at 4^{th} and 7^{th} interface.

Type of Laminate: Symmetric Laminate (TS-III-E)

Number of Laminate above magnetostrictive Layer: 5

Stacking Sequence: $[90_2 / 0_2 / 45 / m / 45 / 0_2 / 90_2]$

Delamination Detail:

Delaminating Interface number from top: 2^{nd}, 3^{rd}, 4^{th}, 7^{th}, 8^{th} and 9^{th}

Peak Voltage: 812.303561 mV

Failure Stress: 22.316823 MPa (Tensile in nature) in the delaminating interface.

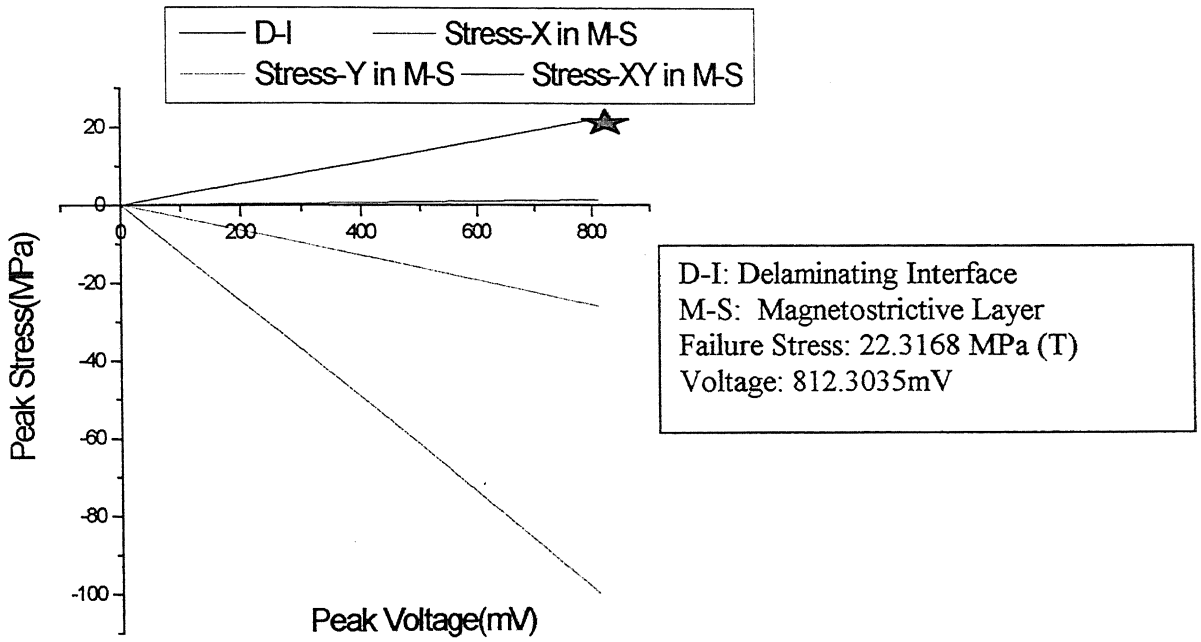

Plot No. 4.36. This plots shows the variation of the peak stress in D-I interface and M-S Layer with respect to peak voltage, and star denotes the delamination start point in the 2^{nd}, 3^{rd}, 4^{th}, 7^{th}, 8^{th} and 9^{th} interfaces from top

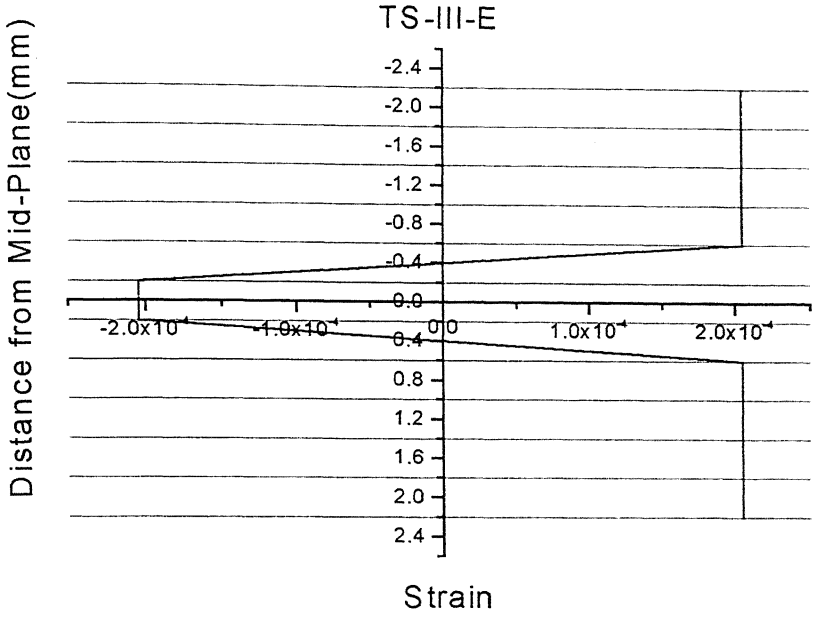

Plot. No.4.37. This Plot shows the variation of the strain across all interfaces in the laminate when the delamination starts in the 2^{nd}, 3^{rd}, 4^{th}, 7^{th}, 8^{th} and 9^{th} interfaces.

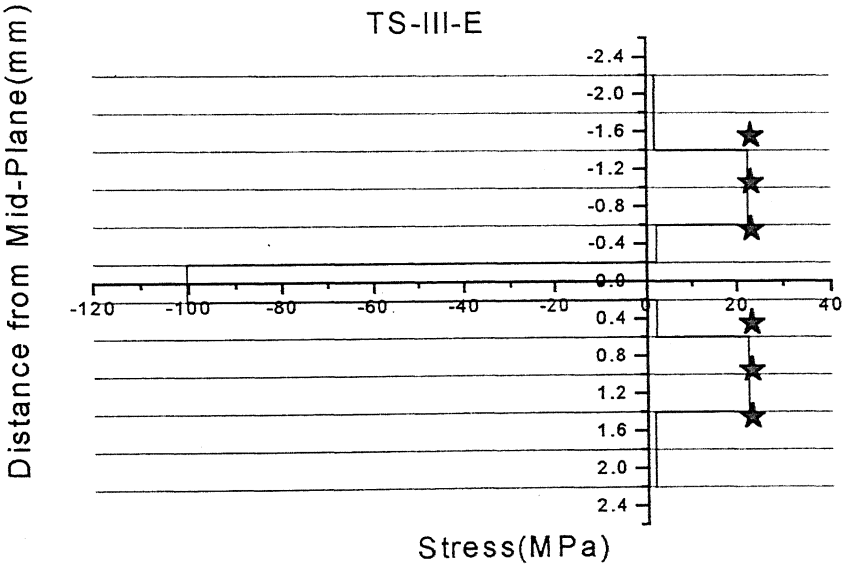

Plot. No. 4.38. This is the variation of the stresses across all interfaces in the laminate when the delamination starts in 2^{nd}, 3^{rd}, 4^{th}, 7^{th}, 8^{th} and 9^{th} interfaces.

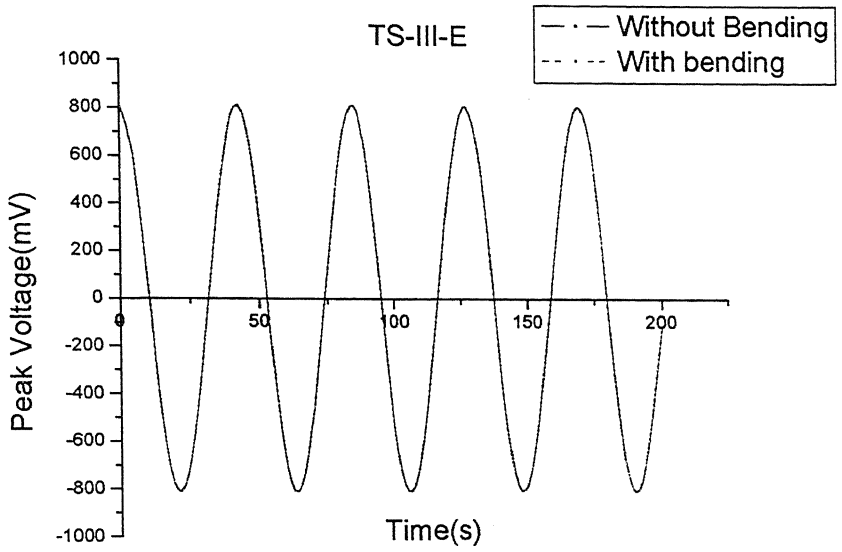

Plot. No. 4.39. This is the variation of the peak voltage induced with time, when the delamination just starts.

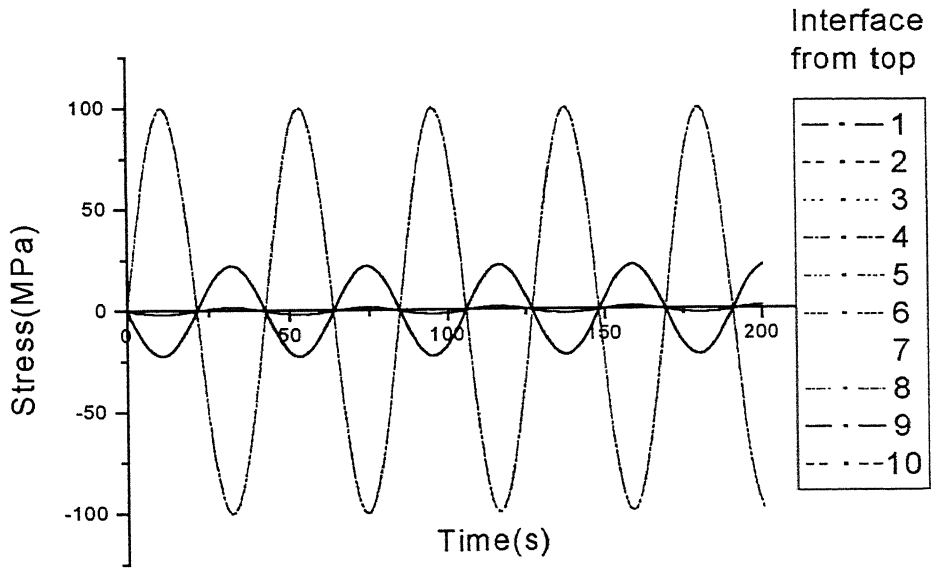

Plot. No. 4.40. The above plot shows the variation of the stresses at each interface when the delamination has started at 2nd, 3rd, 4th, 7th, 8th and 9th interface from the top.

Type of Laminate: **Symmetric** Laminate

Number of Laminate above magnetostrictive Layer: 5

Stacking Sequence: $[90/0/90/0/90/m/90/0/90/0/90]$

Delamination Detail:

Delaminating Interface number from top: 1^{st}, 2^{nd}, 3^{rd}, 4^{th}, 7^{th}, 8^{th}, 9^{th}, and 10^{th} interface

Voltage: 804.760008 mV

Failure Stress: 22.318104 MPa (Tensile in nature) i.e. in the delaminating interface.

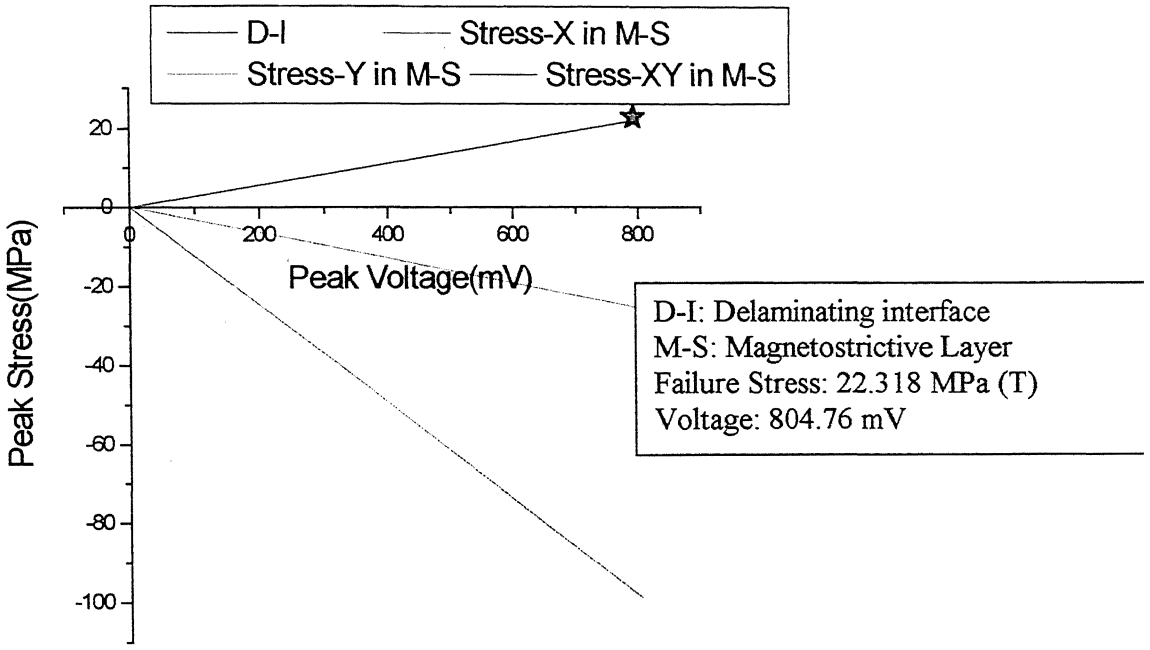

Plot No. 4.41. This plots shows the variation of the peak stress in D-I interface and M-S Layer with respect to peak voltage, and star denotes the delamination start point.

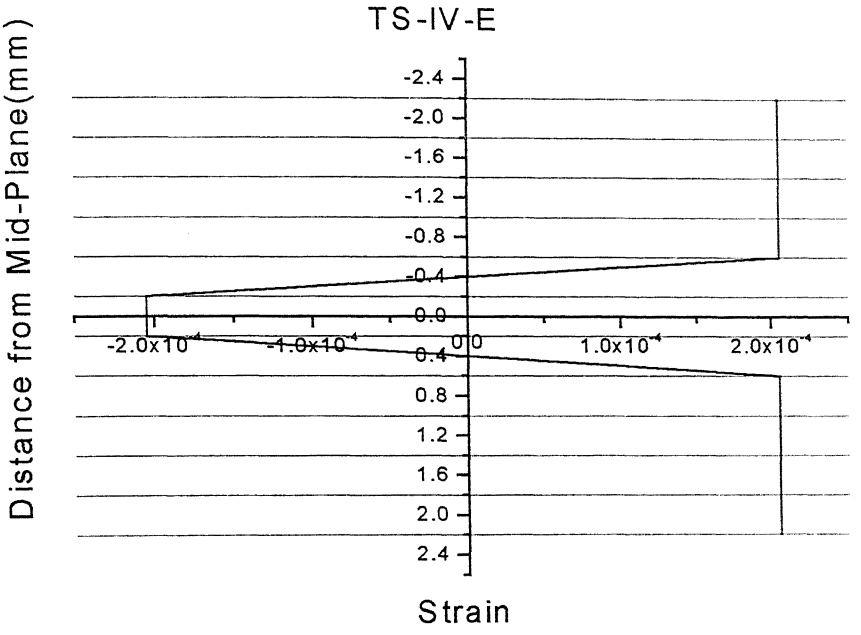

Plot. No. 4.42. This Plot shows the variation of the strain across all interfaces in the laminate when the delamination starts.

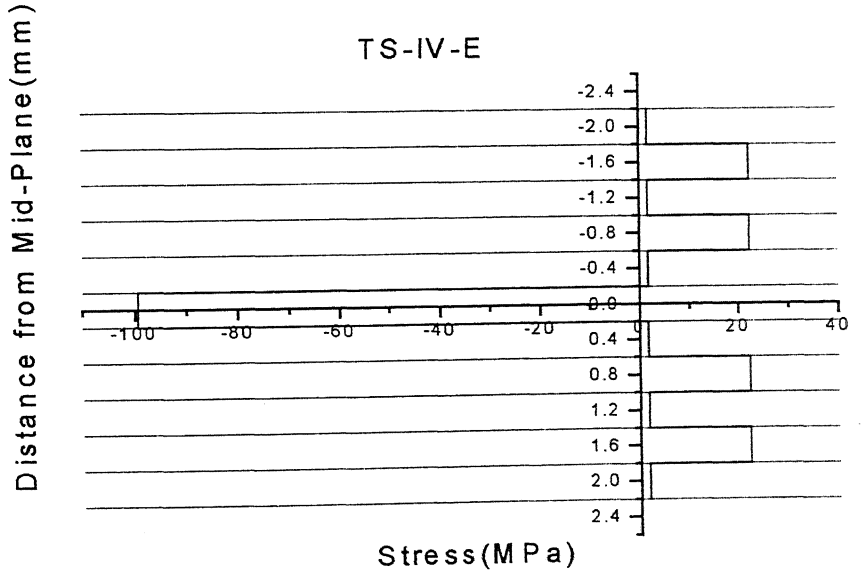

Plot. No. 4.43. This is the variation of the stresses across all interfaces in the laminate when the delamination starts.

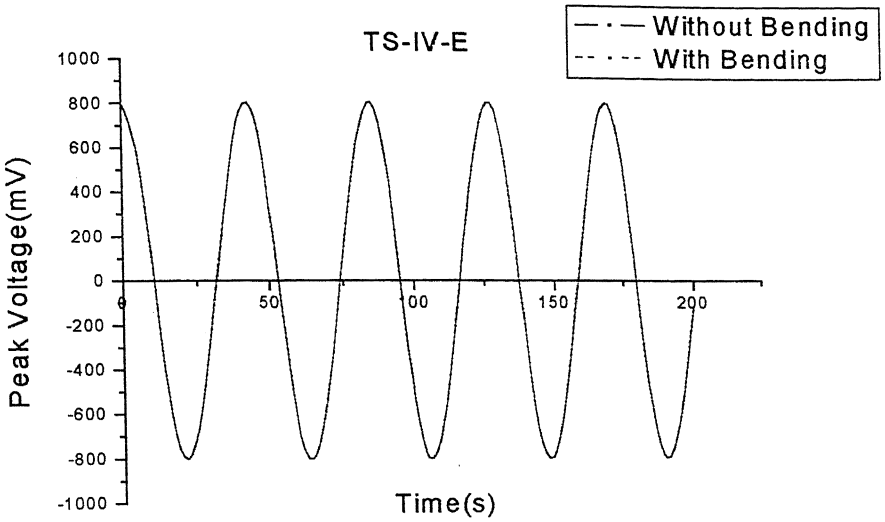

Plot. No. 4.44. This is the variation of the peak voltage induced with time, when the delamination begins.

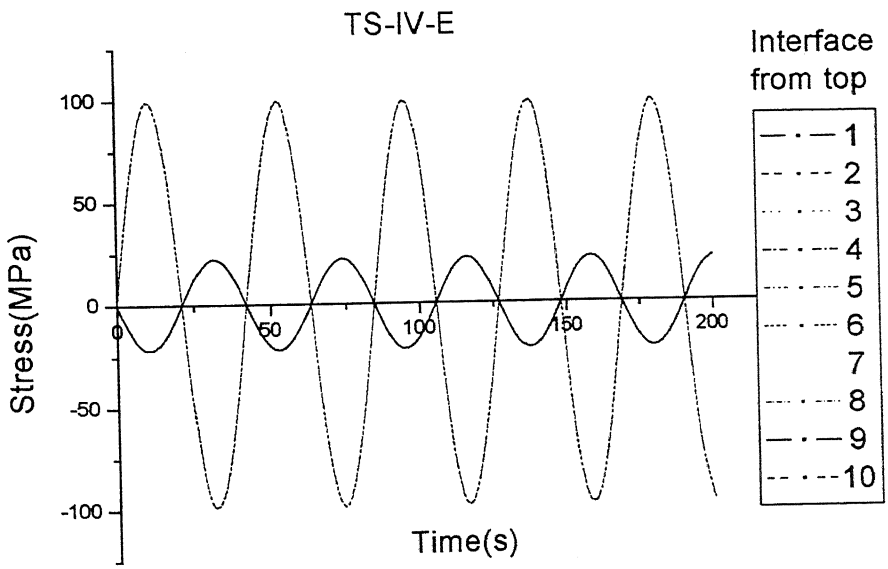

Plot. No. 4.45 The above plot shows the variation of the stresses at each interface when the delamination has started at 1st, 2nd, 3rd, 4th, 7th, 8th, 9th, and 10th interface from the top.

Type of Laminate: Symmetric Laminate

Number of Laminate above magnetostrictive Layer: 5

Stacking Sequence: $[0/45/90/0/-45/m/-45/0/90/45/0]$

Delamination Detail:

Delaminating Interface number from top: 1st, 3rd, 4th, 7th, 8th, and 10th

Peak Voltage: 960.051929 mV

Failure Stress: 22.316880 MPa (Tensile in nature) i.e. in the delaminating interface.

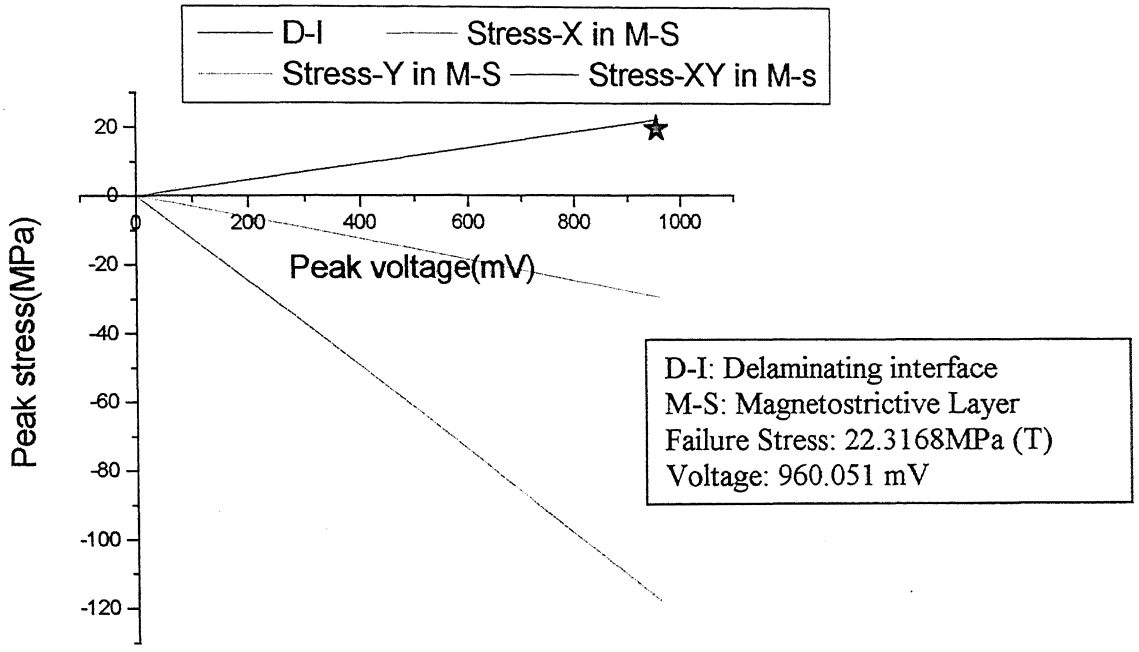

Plot No. 4.46. This plots shows the variation of the peak stress in D-I interface and M-S Layer with respect to peak Voltage, and star denotes the delamination start point in 1st, 3rd, 4th, 7th, 8th, and 10th interface from top

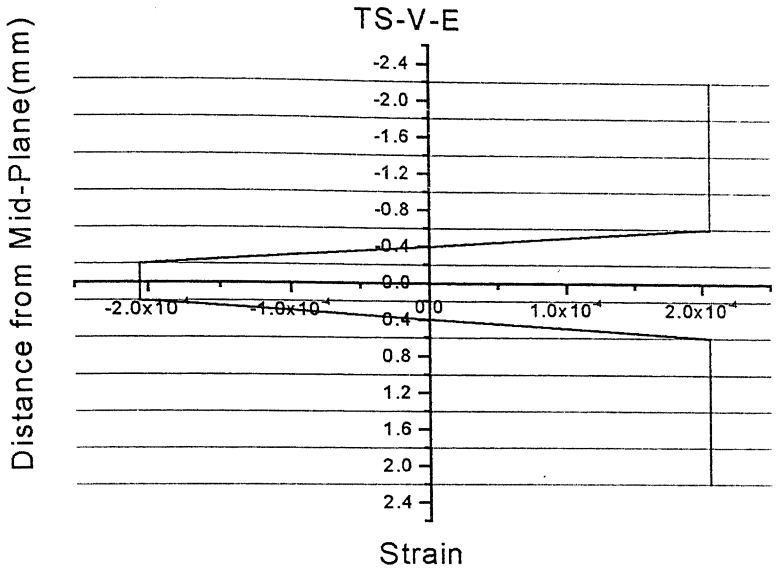

Plot. No. 4.47. This Plot shows the variation of the strain across all interfaces in the laminate when the delamination starts.

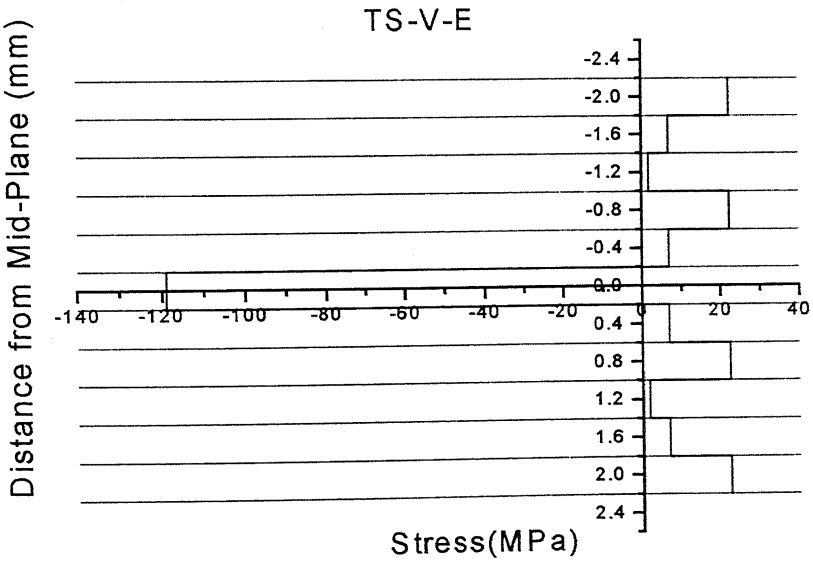

Plot. No. 4.48. This is the variation of the stresses across all interfaces in the laminate when the delamination starts.

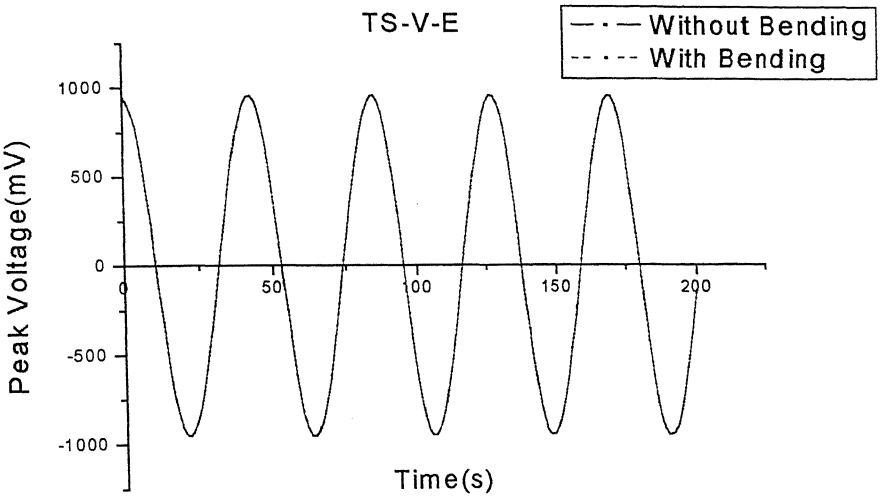

Plot. No. 4.49. This is the variation of the peak voltage induced with time, when the delamination begins.

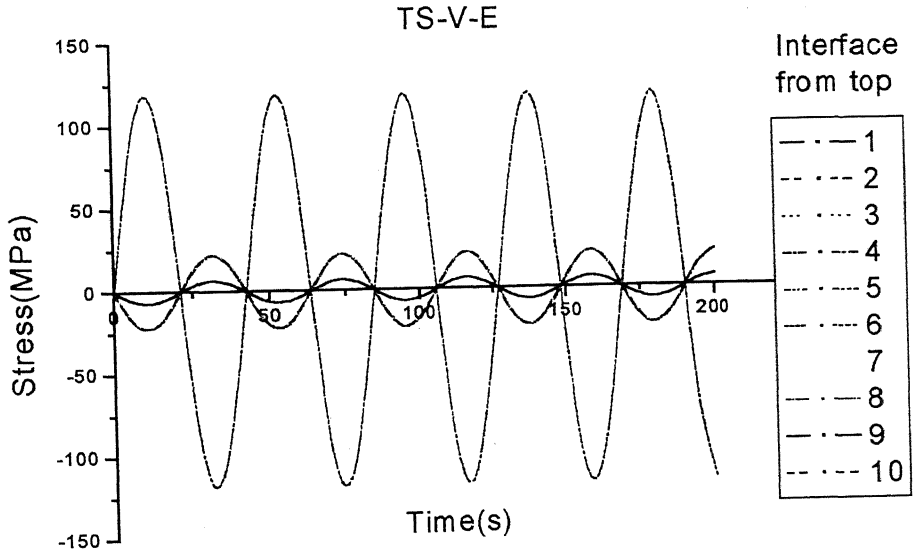

Plot. No. 4.50 The above plot shows the variation of the stresses at each interface when the delamination has started at1st, 3rd, 4th, 7th, 8th, and 10th interface from the top.

4.2 Mechanical Loading:

Beam Configuration:

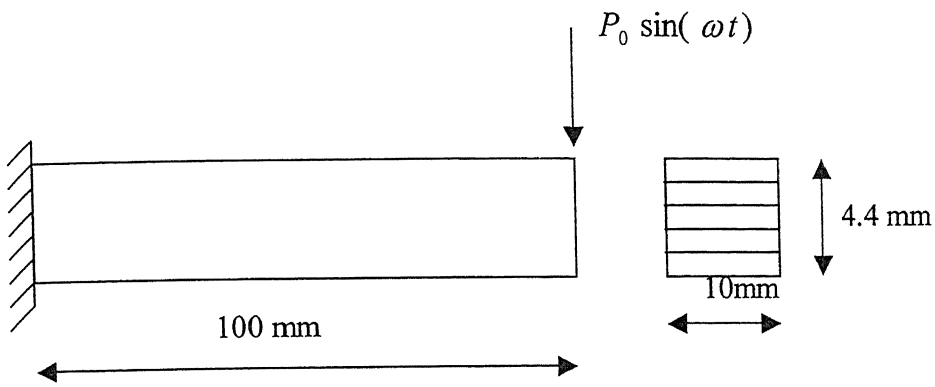

Laminate Detail: CFRP

Mechanical Properties:

Elastic modulus of carbon fiber E_f = 350 GPa, Poisson's ratio ν_f =0.35

Elastic modulus of epoxy resin E_m = 3.50 GPa, Poisson's ratio ν_m =0.4

Magnetostrictive Material: Terfenol-D

Properties: E_L =30Gpa, E_T =30Gpa, ν_{LT} =0.25

Type of Laminate: Asymmetric Laminate (TA-I-M)

Number of Laminas: 11

Number of Laminate above magnetostrictive Layer: 8

Ply Thickness: 0.4 mm

Stacking Sequence: $[\pm 45 / 0_2 / 90_2 / 0_2 / m / \pm 45]$

Number of Turns per meter: 150

Carrier Frequency: 1000 Hz

Delamination Detail:

Delaminating Interface number from top: 2^{nd}

Peak Voltage: +46.638451 mV

Failure Stress: 22.704831 MPa (Tensile in nature) in the delaminating interface

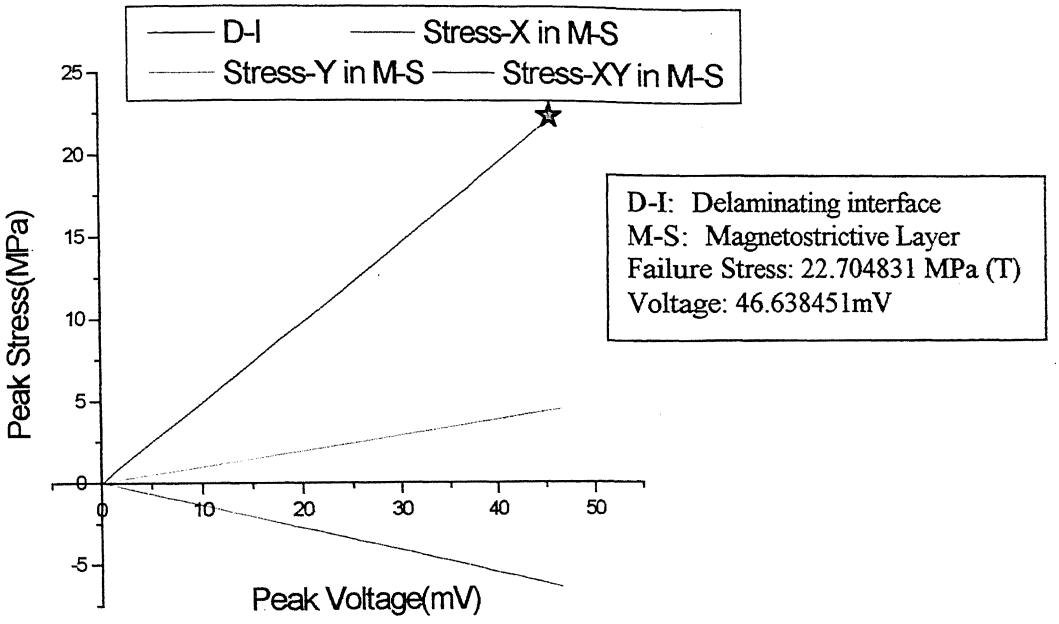

Plot No. 4.51. This plots shows the variation of the peak stress in D-I interface and M-S Layer with respect to peak voltage, and star denotes the delamination start point i.e. in 2^{nd} interface from top.

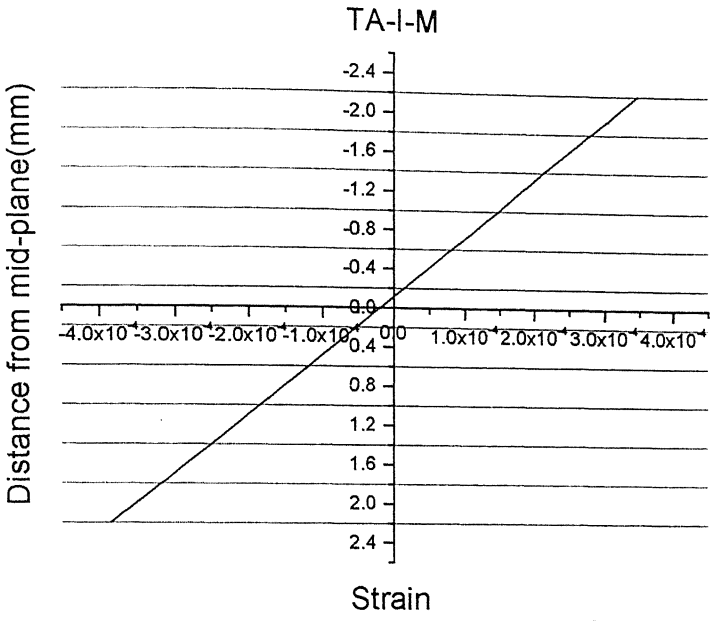

Plot. No. 4.52. This Plot shows the variation of the strain across all interfaces in the laminate when the delamination starts on 2nd interface

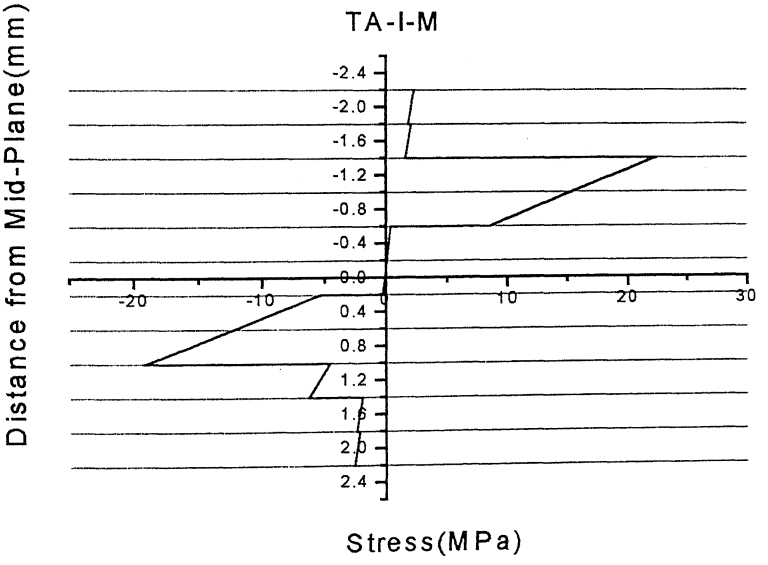

Plot. No. 4.53. This is the variation of the stresses across all interfaces in the laminate when the delamination starts on 2nd interface

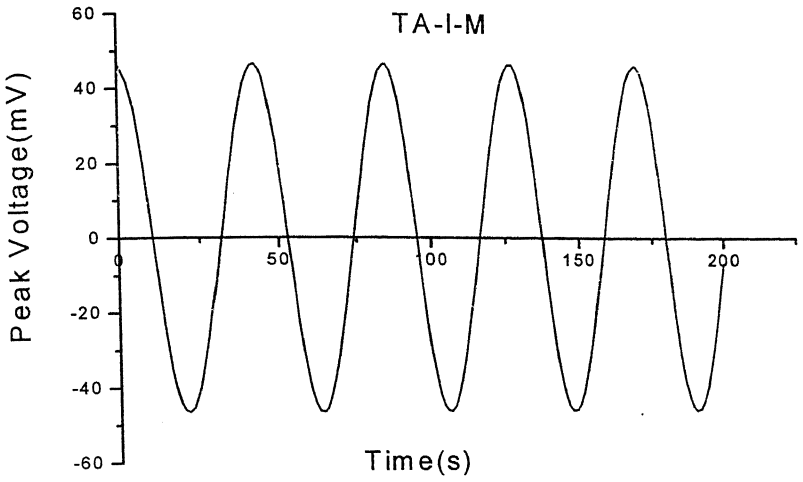

Plot. No.4.54. This is the variation of the peak voltage induced with time when the delamination begins at 2nd interface from top.

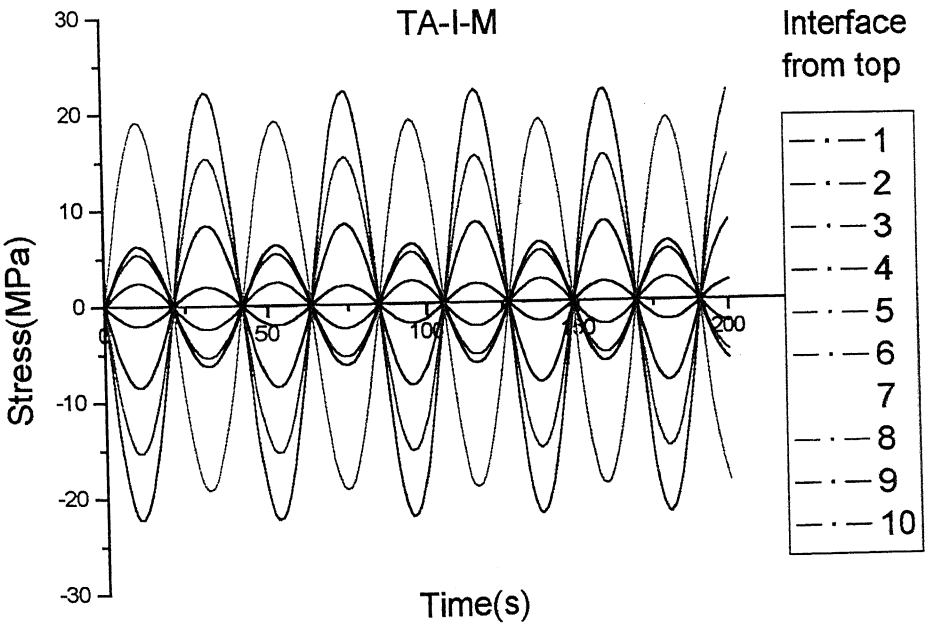

Plot No. 4.55. The above plot shows the variation of the stresses at each interface when the delamination has started at 2nd interface.

Type of Laminate: Asymmetric Laminate (TA-II-M)

Number of Laminate above magnetostrictive Layer: 9

Stacking Sequence: $[\pm 45/0_2/90_2/0_2/-45/m/+45]$

Delamination Detail:

Delaminating Interface number from top: 2^{nd}

Peak Voltage: +62.662352 mV

Failure Stress: 22.564042 MPa (Tensile in nature) in the delaminating interface

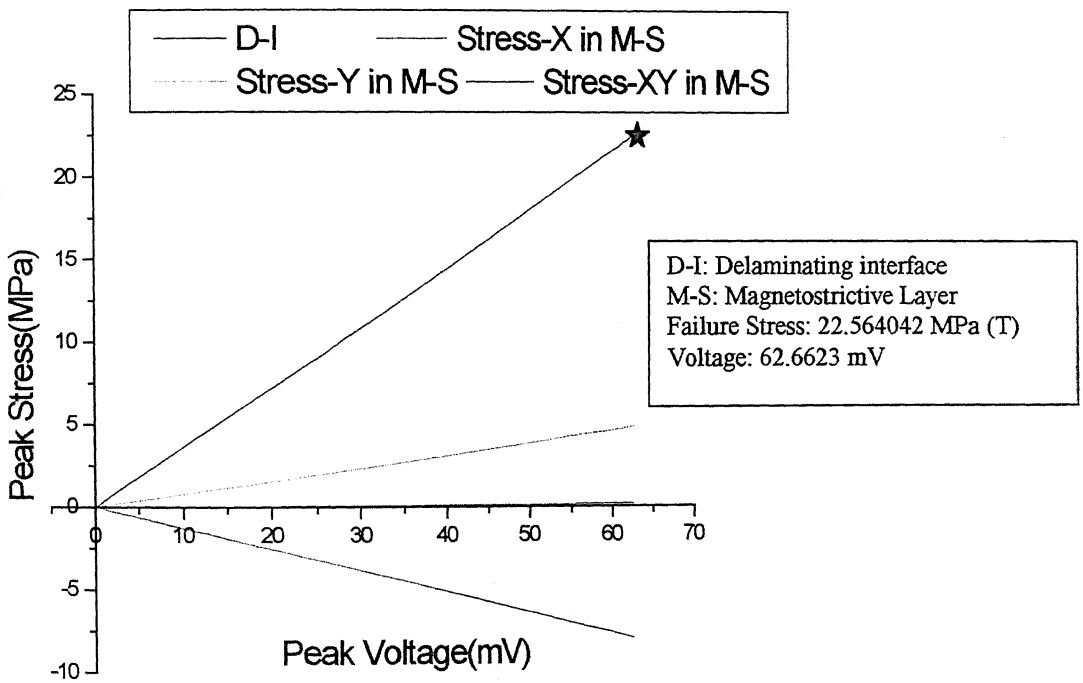

Plot No.4.56. This plots shows the variation of the peak stress in D-I interface and M-S Layer with respect to peak voltage, and star denotes the delamination start point i.e. 2^{nd} interface from top.

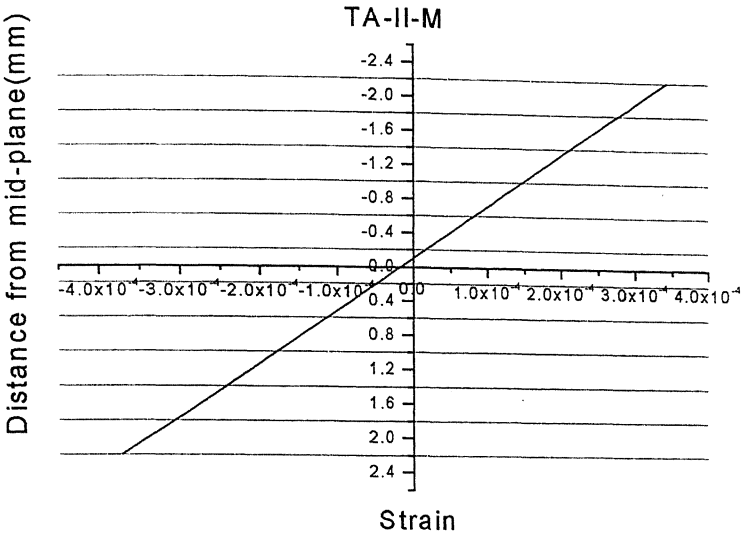

Plot. No.4.57. This Plot shows the variation of the strain across all interfaces in the laminate when the delamination starts on 2nd interface

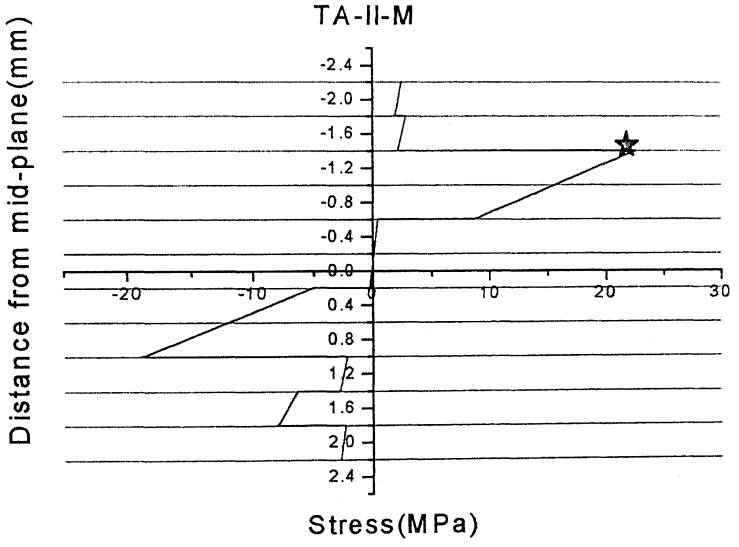

Plot. No. 4.58. This is the variation of the stresses across all interfaces in the laminate when the delamination starts on 2nd interface

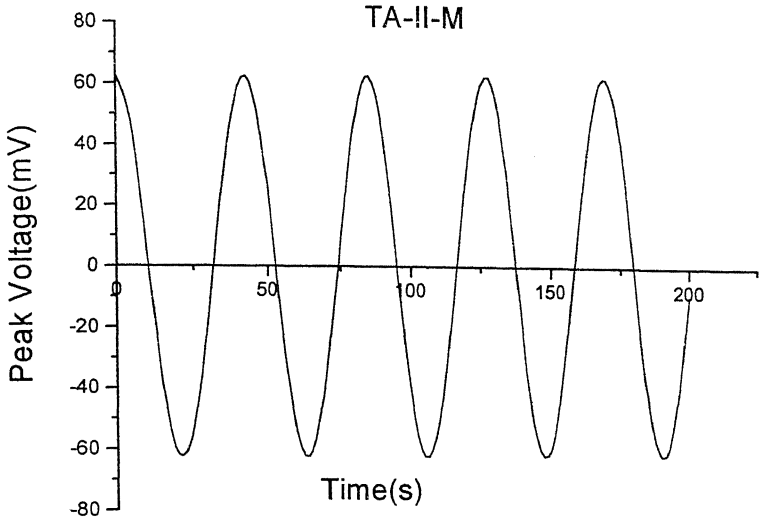

Plot. No. 4.59. This is the variation of the peak voltage induced with time, when the delamination begins at 2nd interface from top.

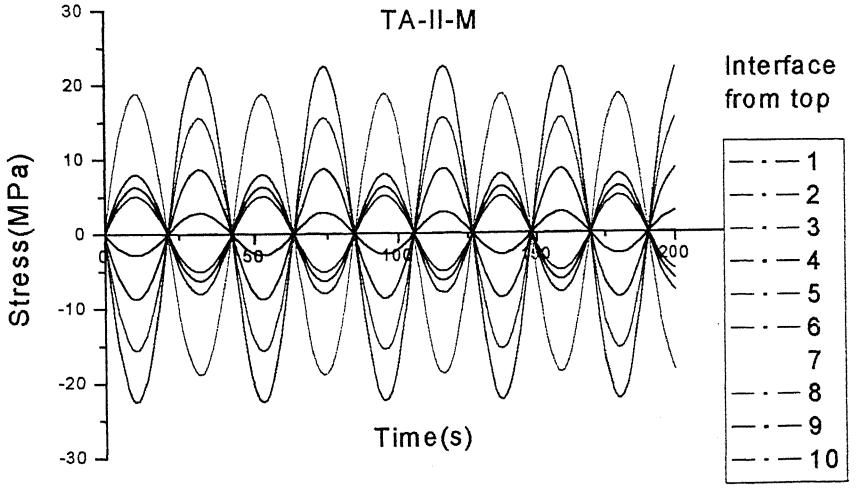

Plot No. 4.60. The above plot shows the variation of the stresses at each interface when the delamination has started at 2nd interface.

Type of Laminate: Asymmetric Laminate (TA-III-M)

Number of Laminate above magnetostrictive Layer: 10

Ply Thickness: 0.4 mm

Stacking Sequence: $[\pm 45/0_2/90_2/0_2/\mp 45/m]$

Delamination Detail:

Delaminating Interface number from top: 2^{nd}

Peak Voltage: +79.667458 mV

Failure Stress: 22.764706 MPa (tensile in nature) in delaminating interface

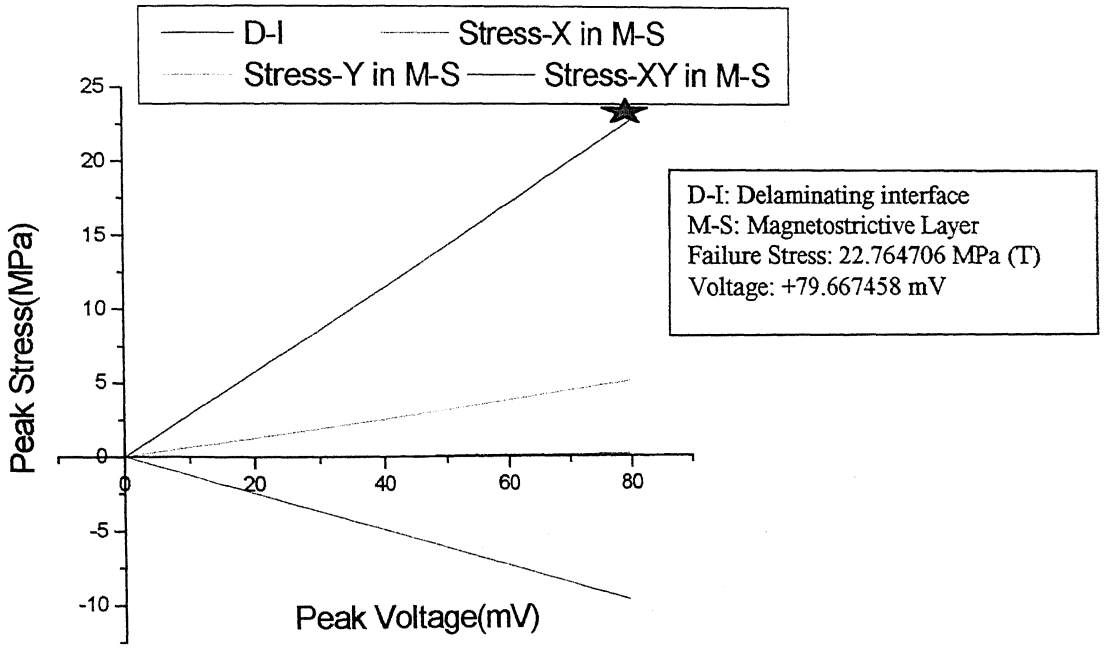

Plot No.4.61. This plots shows the variation of the peak stress in D-I interface and M-S Layer with respect to peak voltage, and star denotes the delamination start point i.e. 2^{nd} interface from top.

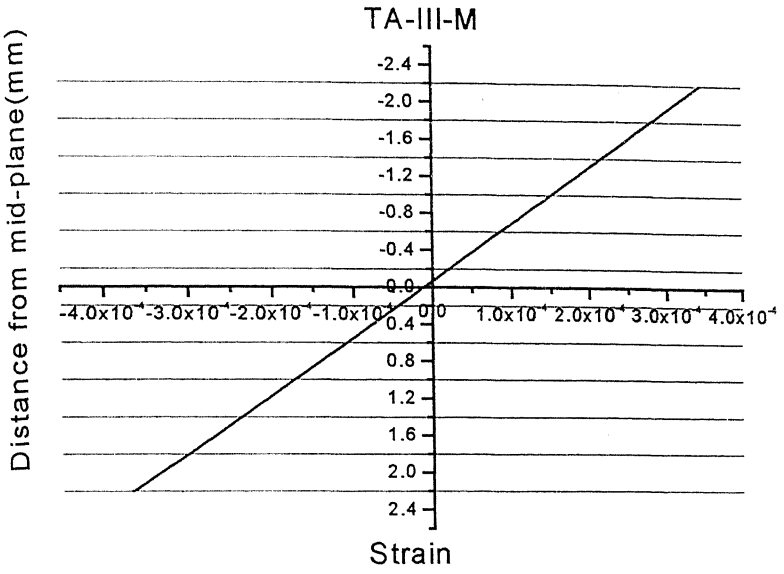

Plot. No. 4.62. This Plot shows the variation of the strain across all interfaces in the laminate when the delamination starts on 2nd interface

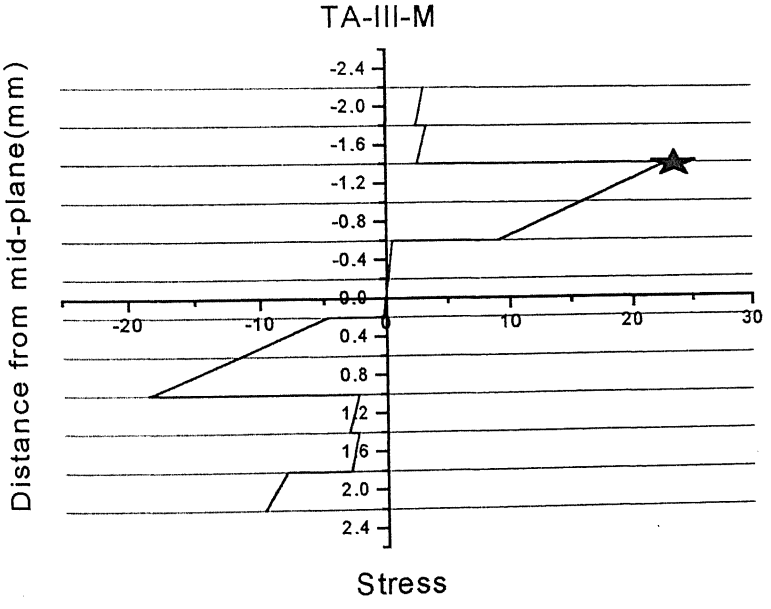

Plot. No. 4.63. This is the variation of the stresses across all interfaces in the laminate when the delamination starts on 2nd interface

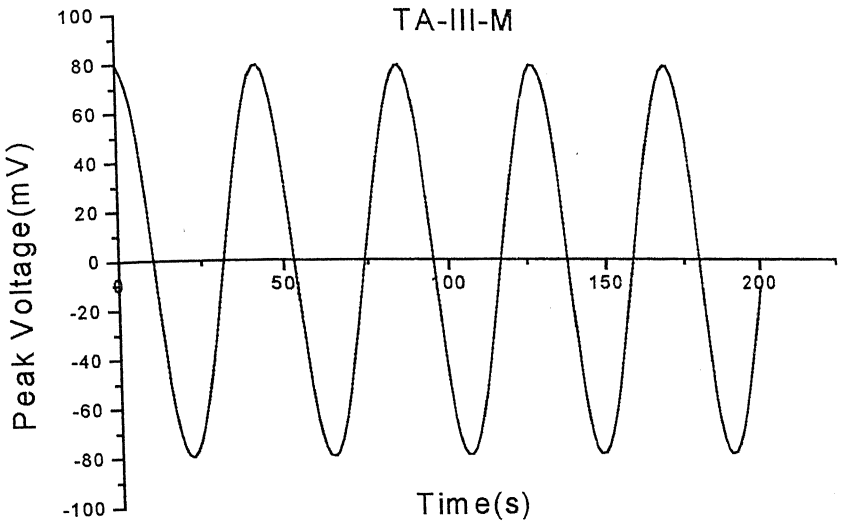

Plot. No. 4.64. This is the variation of the peak voltage induced with time, when the delamination begins at 2nd interface from top.

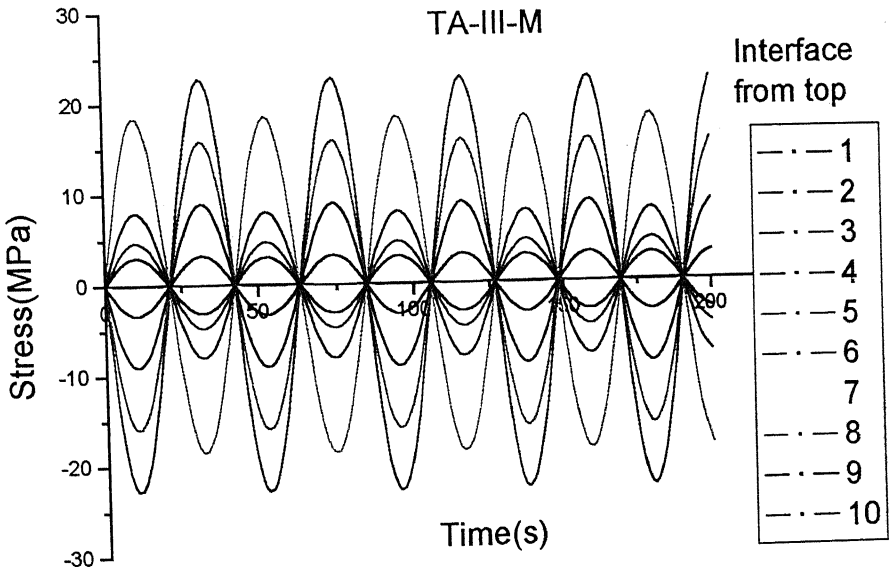

Plot No. 4.65. The above plot shows the variation of the stresses at each interface when the delamination has started at 2nd interface.

Type of Laminate: Asymmetric Laminate (TA-IV-M)

Number of Laminate above magnetostrictive Layer: 10

Ply Thickness: 0.4 mm

Stacking Sequence: $[90_{10} / m]$

Delamination Detail:

Delaminating Interface number from top: 1st

Peak Voltage: +59.155518 mV

Failure Stress: 22.589098 MPa (Tensile in nature) in the delaminating interface

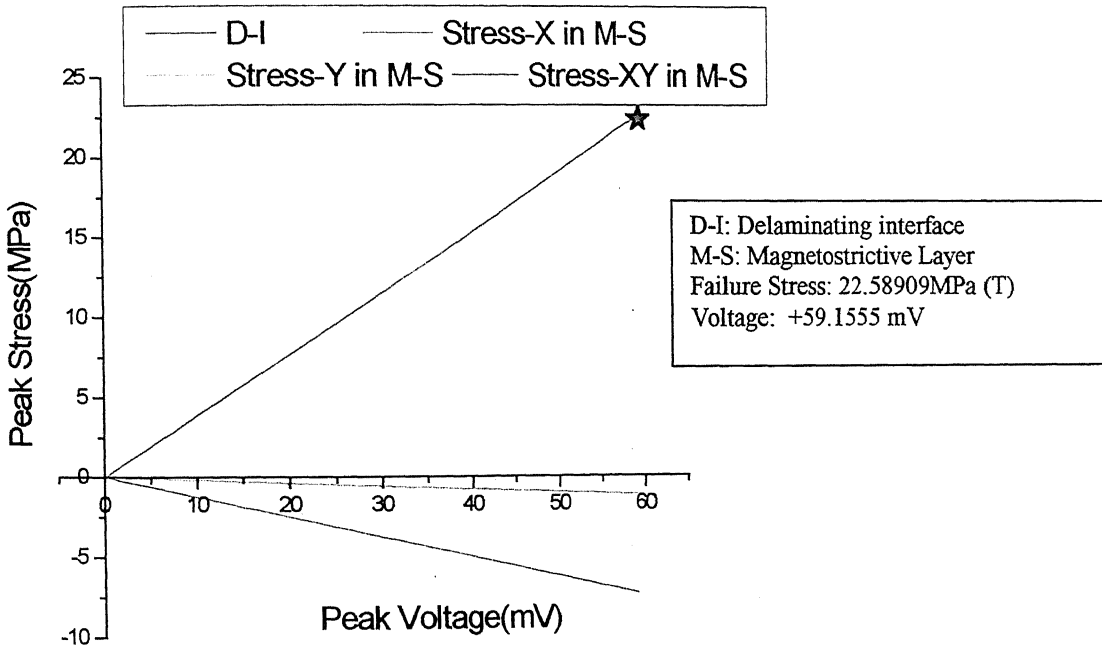

Plot No. 4.66. This plots shows the variation of the peak stress in D-I interface and M-S Layer with respect to peak voltage, and star denotes the delamination start point i.e. the 1st interface

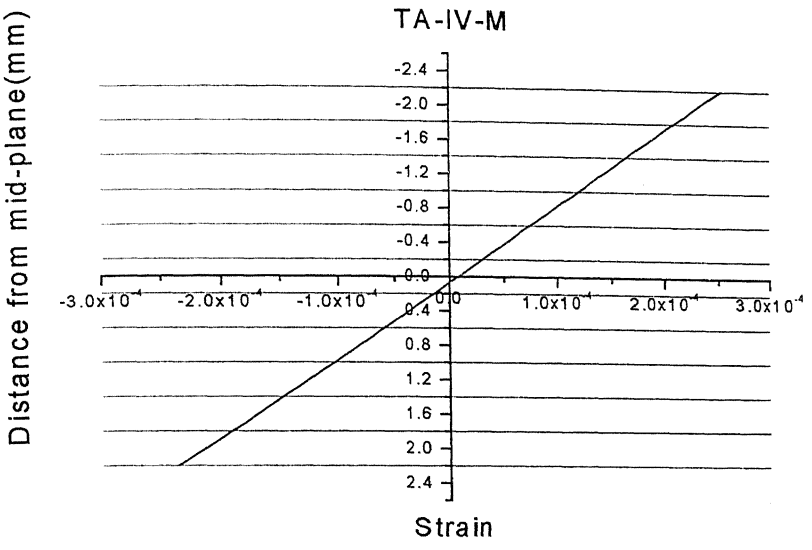

Plot. No. 4.67. This Plot shows the variation of the strain across all interfaces in the laminate when the delamination starts on 1st interface

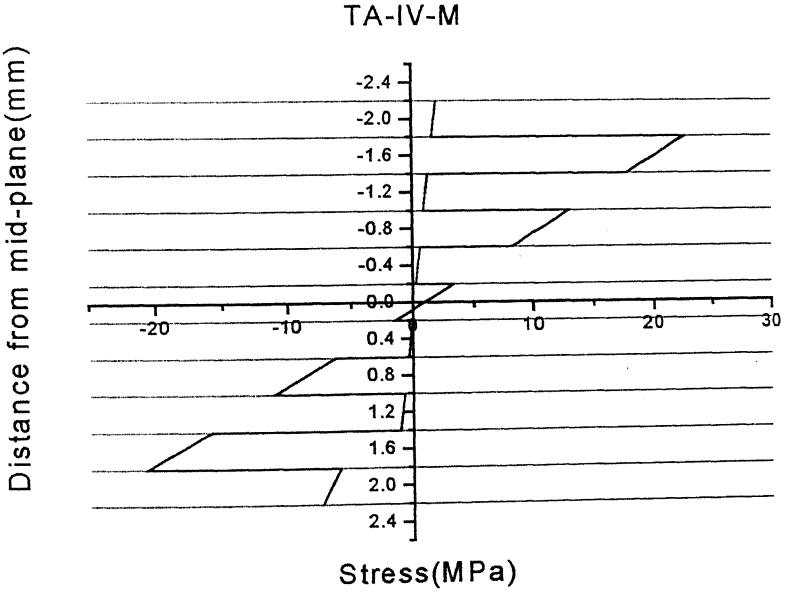

Plot. No. 4.68. This is the variation of the stresses across all interfaces in the laminate when the delamination starts on 1st interface

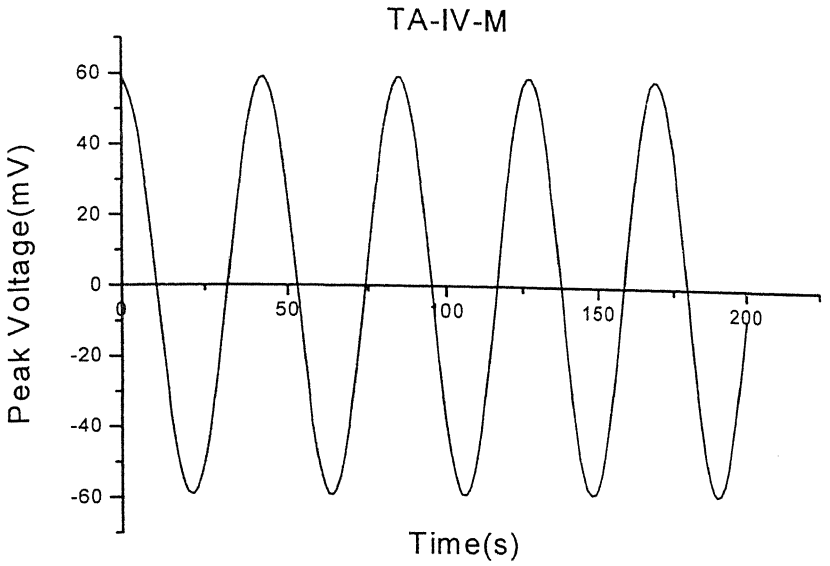

Plot. No. 4.69. This is the variation of the peak voltage induced with time, when the delamination begins at 1st interface from top.

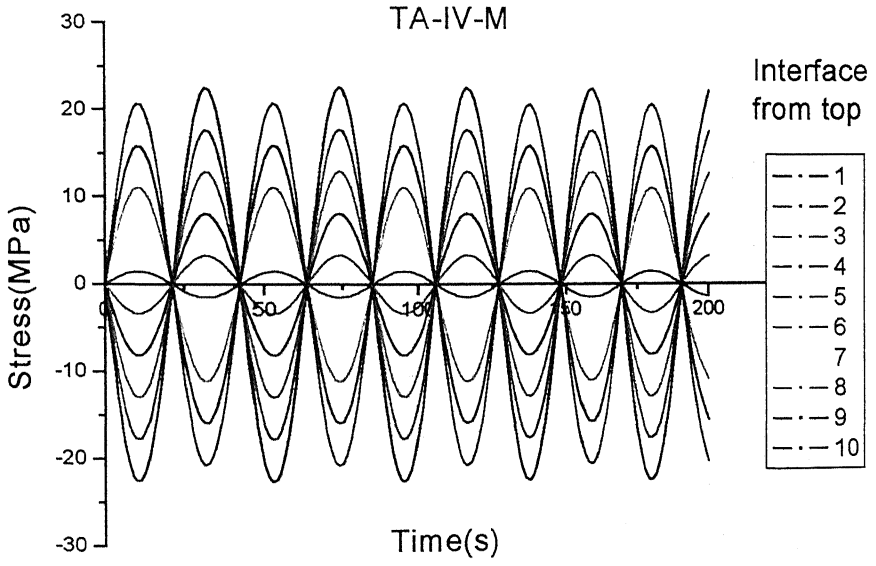

Plot No. 4.70. The above plot shows the variation of the stresses at each interface when the delamination has started at 1st interface.

Type of Laminate: Asymmetric Laminate (TA-V-M)

Number of Laminas: 11

Number of Laminate above magnetostrictive Layer: 10

Ply Thickness: 0.4 mm

Stacking Sequence: $[0_{10} / m]$

Delamination Detail:

Delaminating Interface number from top: 1st

Peak Voltage: +71.497644 mV

Peak Stress: 22.411257 MPa (Tensile in nature) in delaminating interface

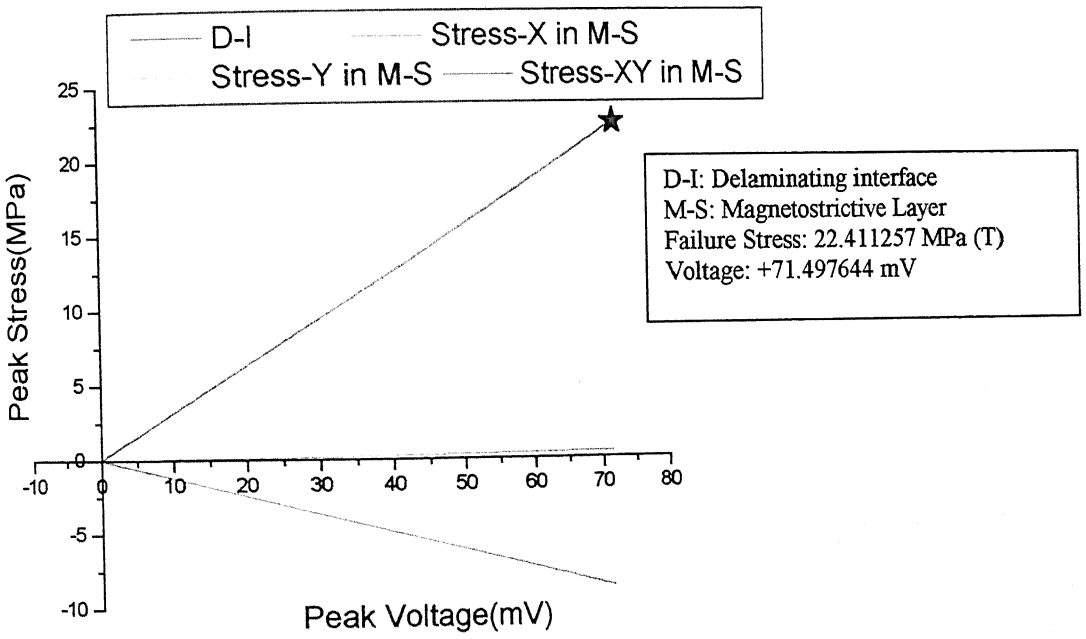

Plot No. 4.71. This plots shows the variation of the peak stress in D-I interface and M-S Layer with respect to peak voltage, and star denotes the delamination start point i.e. the 1st interface

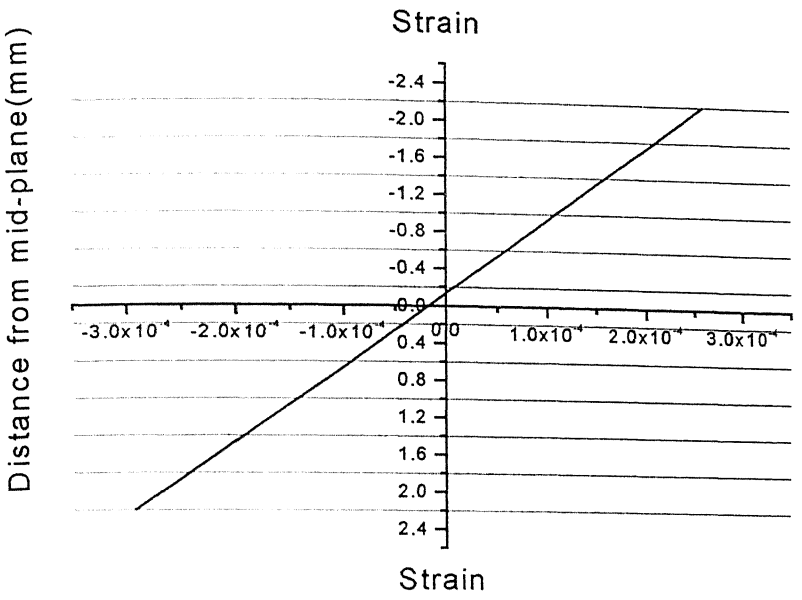

Plot. No. 4.72. This Plot shows the variation of the strain across all interfaces in the laminate when the delamination starts on 1st interface

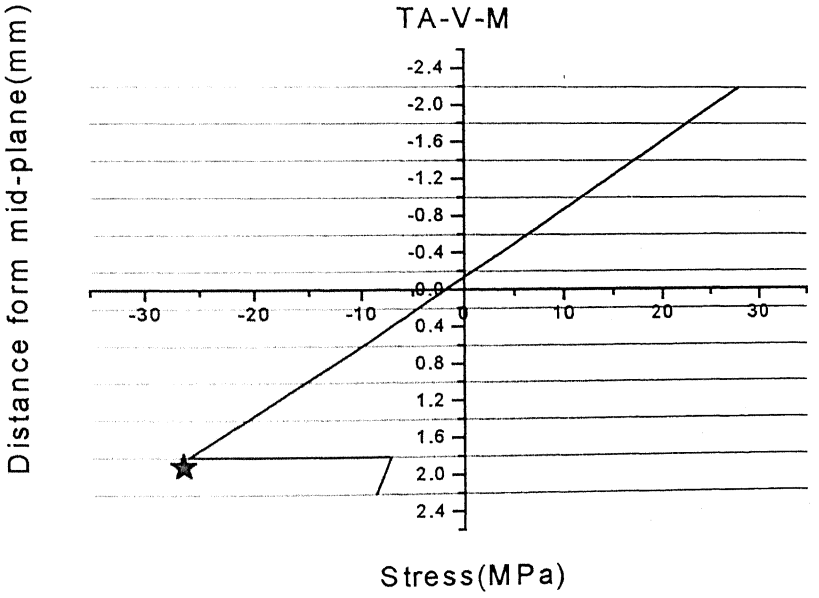

Plot. No. 4.73. This is the variation of the stresses across all interfaces in the laminate when the delamination starts on 1st interface

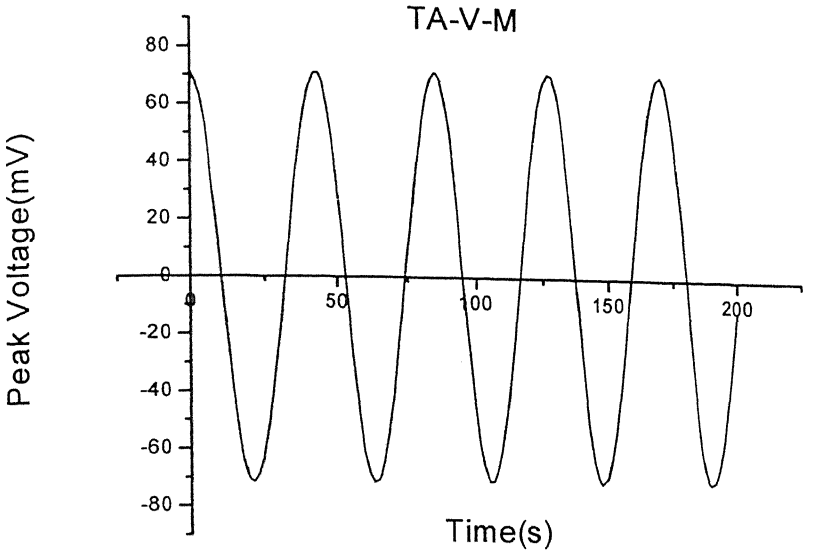

Plot. No. 4.74. This is the variation of the peak voltage induced with time, when the delamination begins at 1st interface from top.

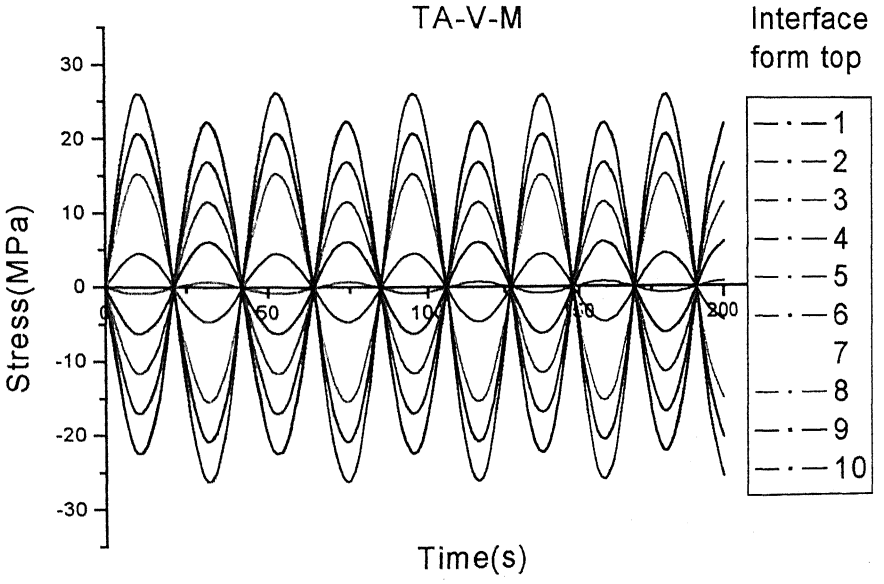

Plot No. 4.75. The above plot shows the variation of the stresses at each interface when the delamination has started at 1st interface.

Type of Laminate: Symmetric Laminate (TS-I-M)

Number of Laminas: 11

Number of Laminate above magnetostrictive Layer: 5

Ply Thickness: 0.4 mm

Stacking Sequence: $[\pm 45/0_2/90/m/90/0_2/\mp 45]$

Delamination Detail:

Delaminating Interface number from top: 2nd and 9th

Peak Voltage: $\mp$ 7.773465 mV

Peak Stress: 22.815174 (Tensile in 2nd)
-22.815174 (Compressive in 9th interface) i.e. delaminating interface

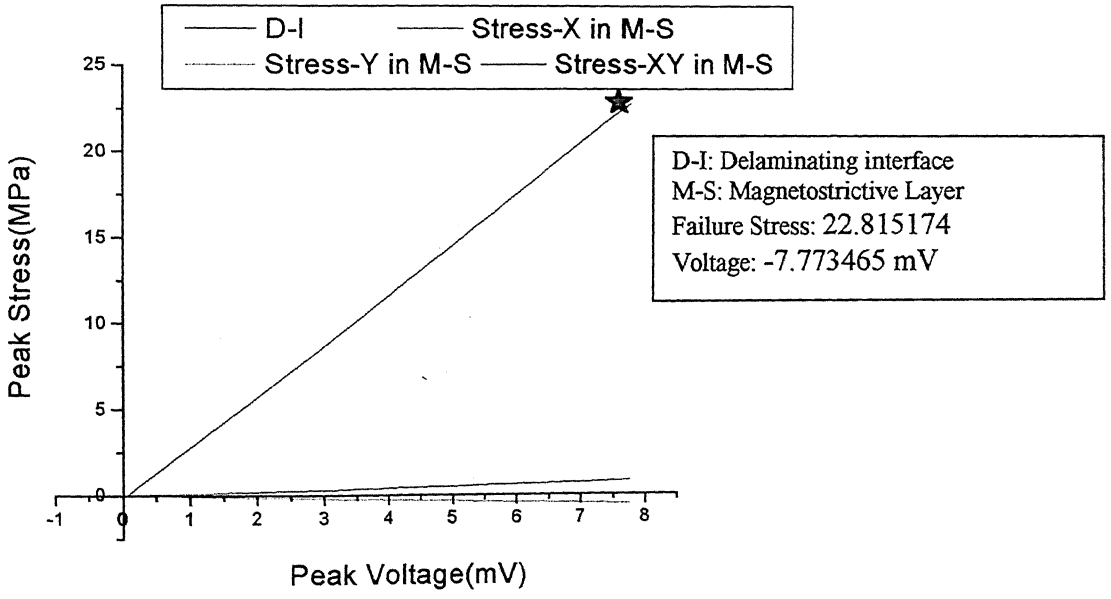

Plot No. 4.76. This plots shows the variation of the peak stress in D-I interface and M-S Layer with respect to peak voltage, and star denotes the delamination start point i.e. the 2nd and 9th interface from top.

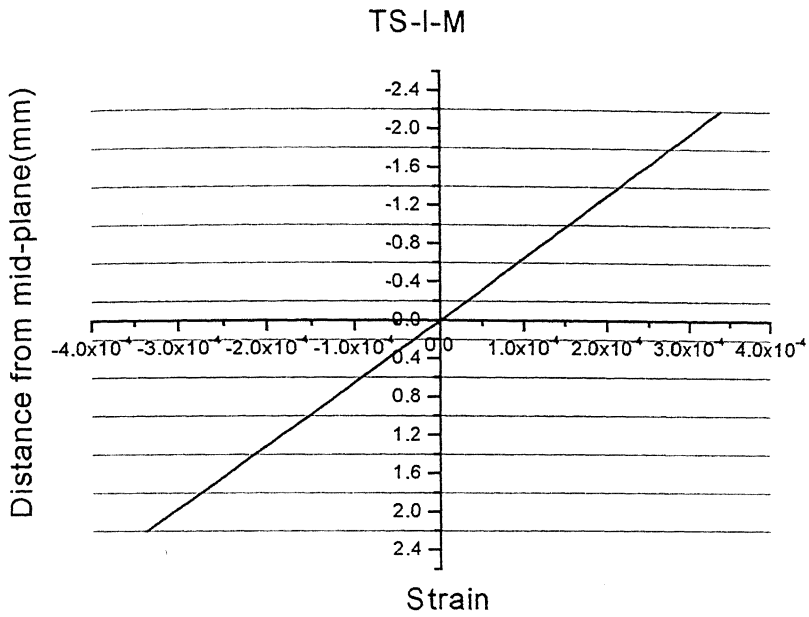

Plot. No. 4.77. This Plot shows the variation of the strain across all interfaces in the laminate when the delamination starts on 2nd and 9th interface

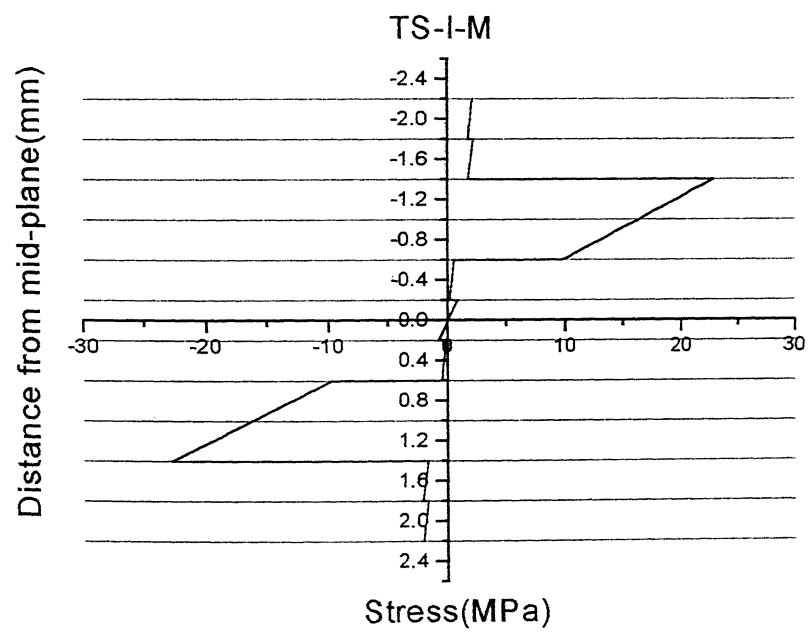

Plot. No. 4.78. This is the variation of the stresses across all interfaces in the laminate when the delamination starts on 2nd and 9th interface

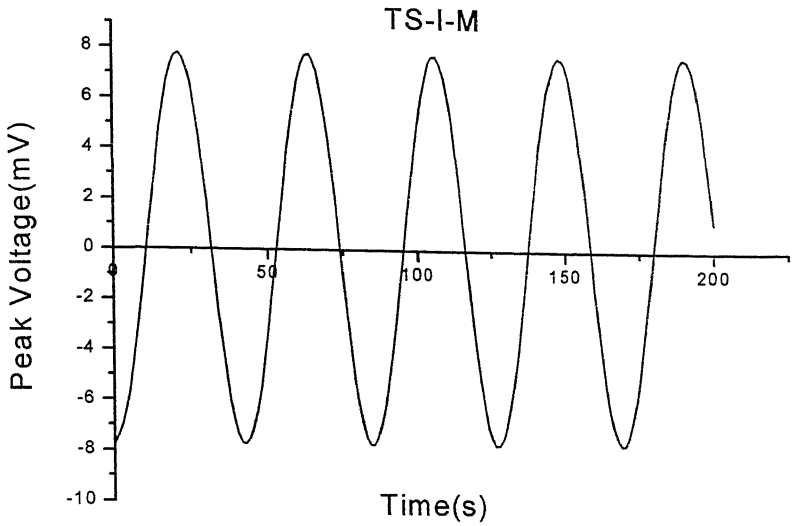

Plot. No. 4.79. This is the variation of the peak voltage induced with time, when the delamination begins at 2nd and 9th interface from top

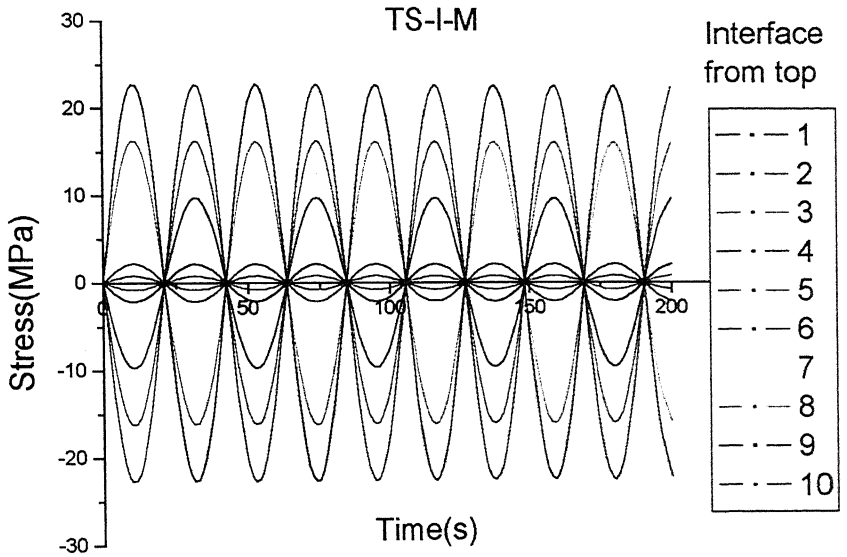

Plot No. 4.80. The above plot shows the variation of the stresses at each interface when the delamination has started at 2nd and 9th interface.

Type of Laminate: Symmetric Laminate (TS-II-M)

Number of Laminas: 11

Number of Laminate above magnetostrictive Layer: 5

Ply Thickness: 0.4 mm

Stacking Sequence: $[\mp 45/90_2/0/m/0/90_2/\pm 45]$

Delamination Detail:

Delaminating Interface number from top: 2nd and 9th

Peak Voltage: $\mp$ 19.623871 mV

Peak Stress: -22.567171 MPa (Compressive in nature) and
22.567171 MPa (Tensile in nature) i.e. in the delaminating interface

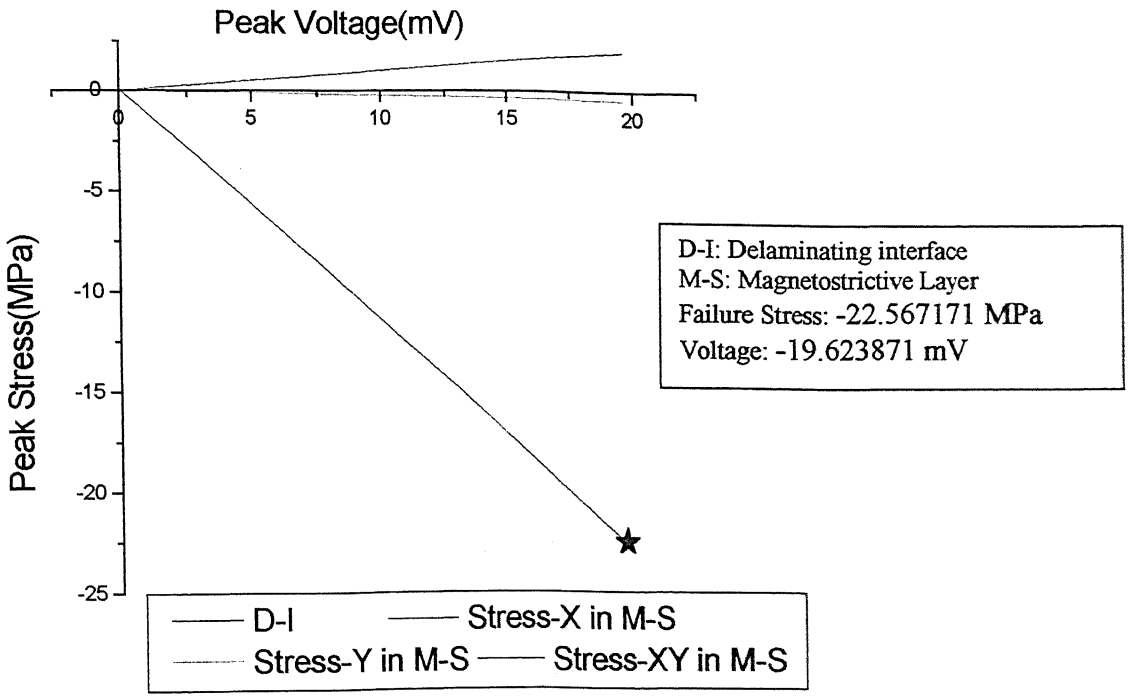

Plot No. 4.81. This plots shows the variation of the peak stress in D-I interface and M-S Layer with respect to peak voltage, and star denotes the delamination start point i.e. the 2nd and 9th interface from top.

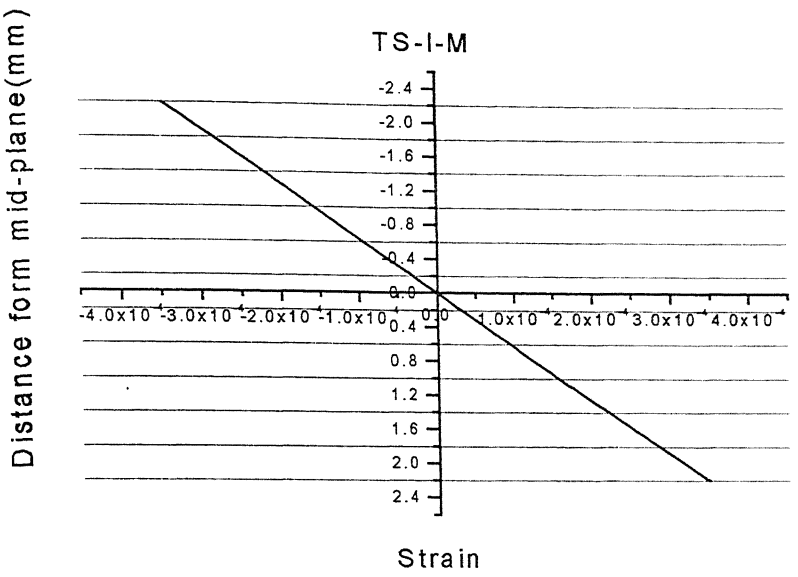

Plot. No. 4.82. This Plot shows the variation of the strain across all interfaces in the laminate when the delamination starts on 2nd and 9th interface

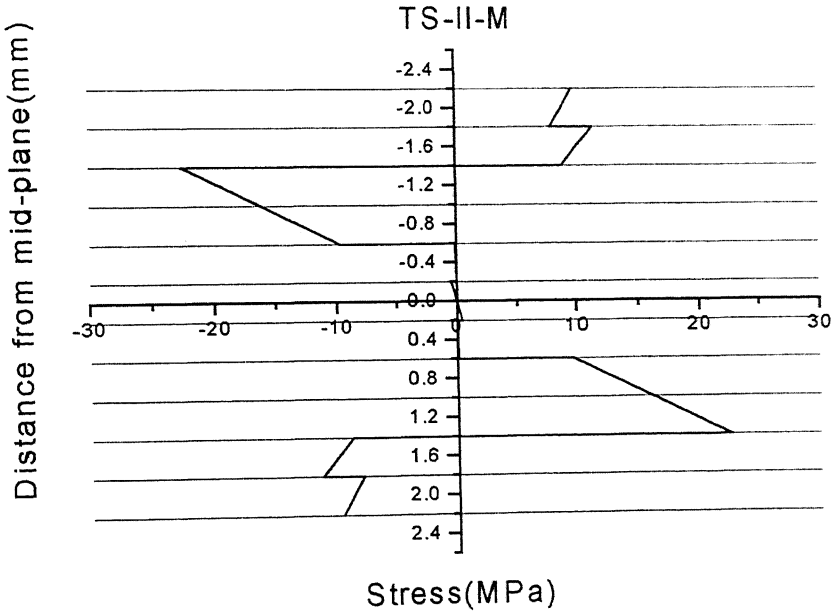

Plot. No. 4.83. This is the variation of the stresses across all interfaces in the laminate when the delamination starts on 2nd and 9th interface

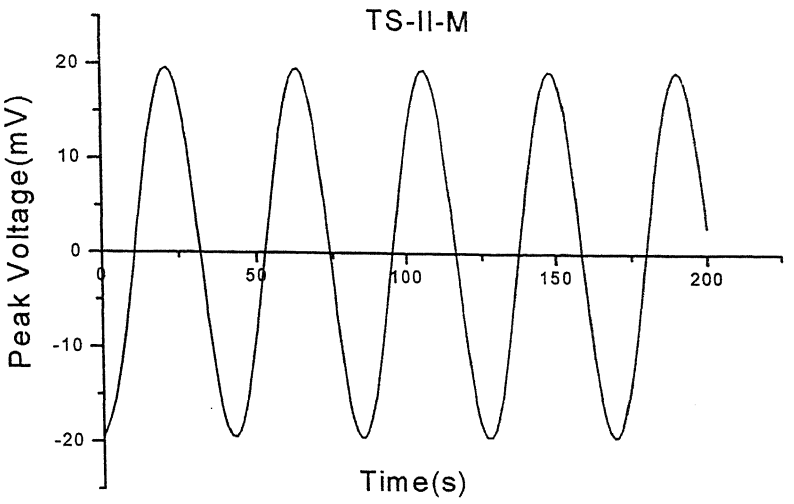

Plot. No. 4.84. This is the variation of the peak voltage induced with time, when the delamination begins at 2nd and 9th interface from top

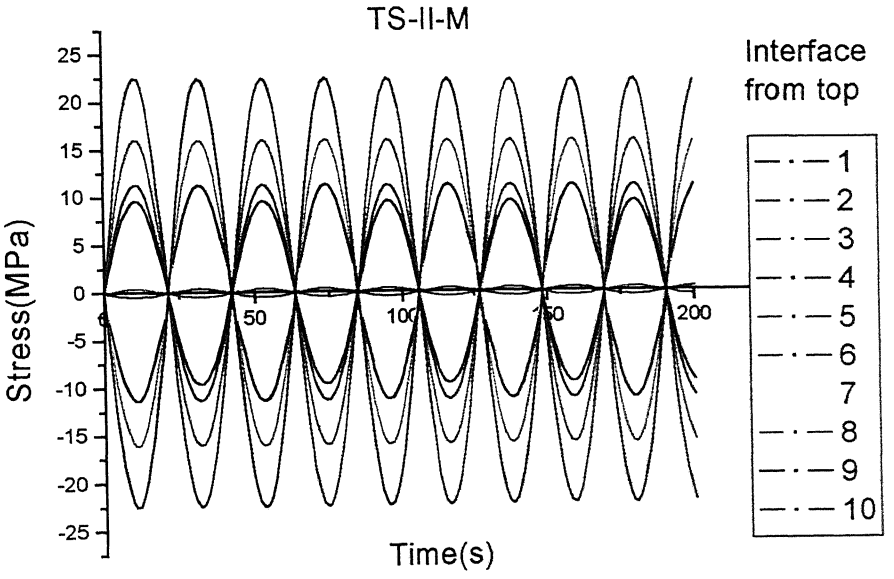

Plot No. 4.85. The above plot shows the variation of the stresses at each interface when the delamination has started at 2nd and 9th interface.

Type of Laminate: Symmetric Laminate (TS-III-M)

Number of Laminas: 11

Number of Laminate above magnetostrictive Layer: 5

Ply Thickness: 0.4 mm

Stacking Sequence: $[90_2 / 0_2 / 45 / m / 45 / 0_2 / 90_2]$

Delamination Detail:

Delaminating Interface number from top: 2nd and 9th

Peak Voltage: ∓ 9.465923 mV

Failure Stress: 22.766798 MPa (Tensile in 2nd) and

-22.766798 MPa (Compressive in 9th) interface i.e. the delaminating one.

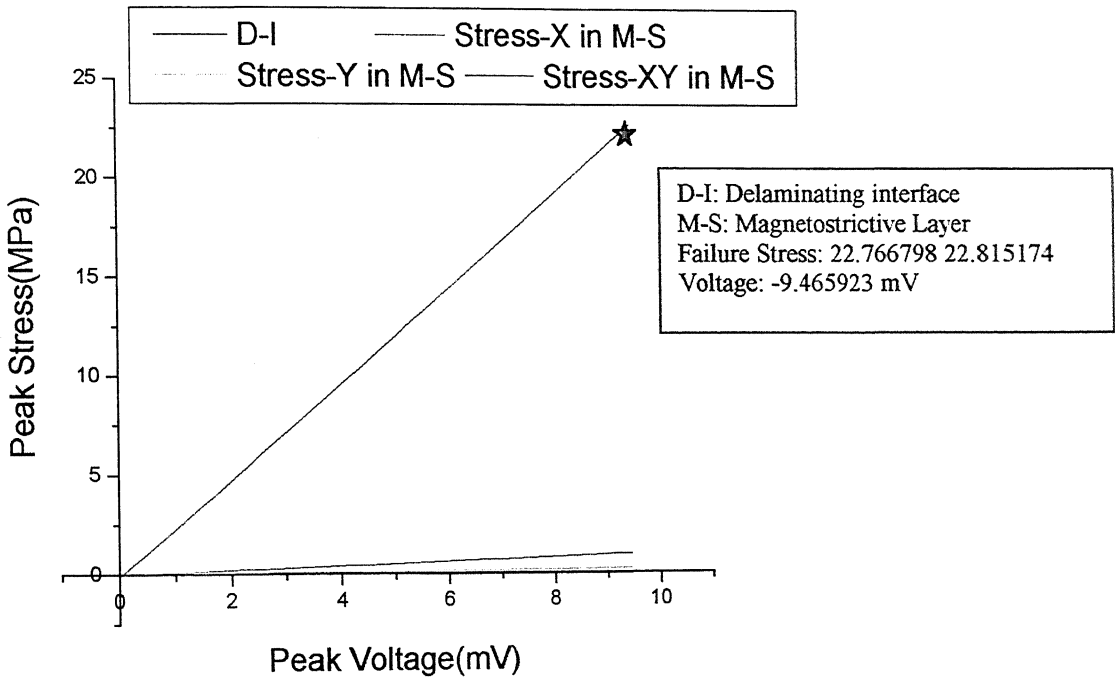

Plot No. 4.86. This plots shows the variation of the peak stress in D-I interface and M-S Layer with respect to peak voltage, and star denotes the delamination start point i.e. the 2nd and 9th interface from top.

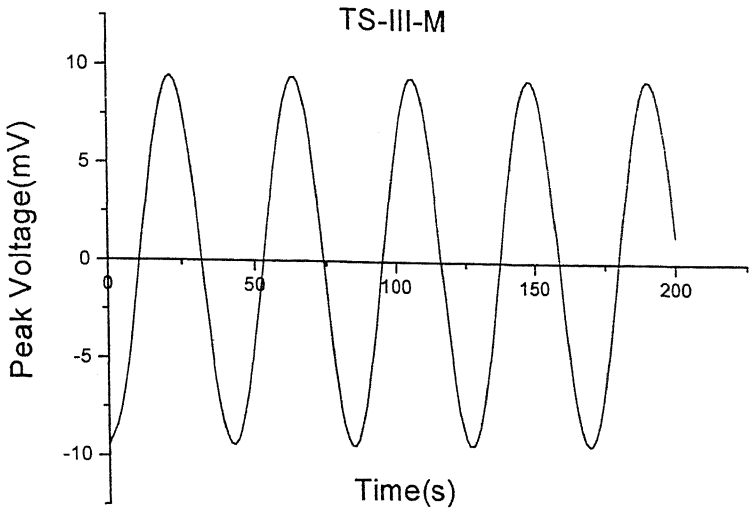

Plot. No. 4.89. This is the variation of the peak voltage induced with time, when the delamination begins at 2nd and 9th interface from top

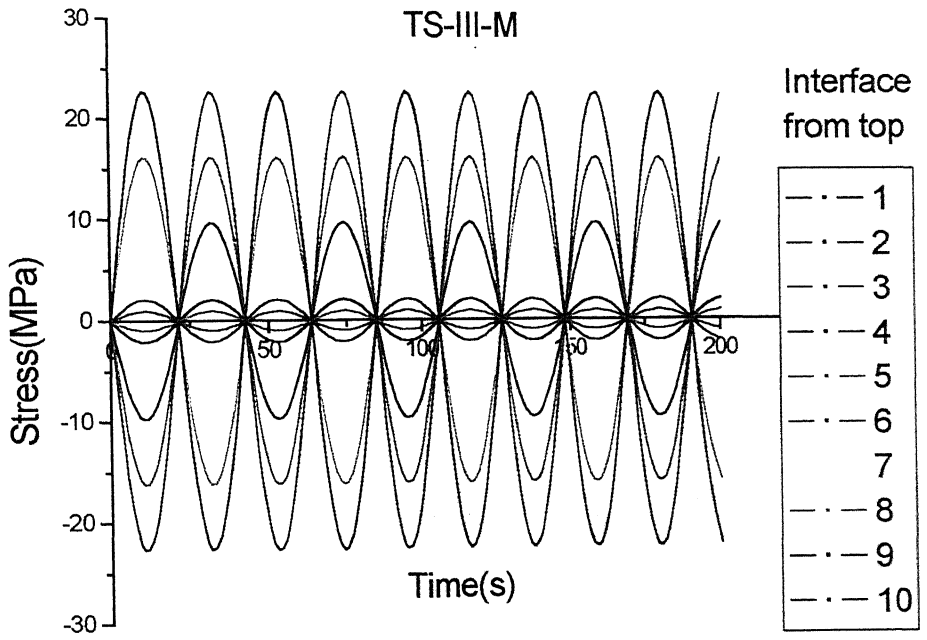

Plot No. 4.90. The above plot shows the variation of the stress at each interface when the delamination has started at 2nd and 9th interface.

Type of Laminate: Symmetric Laminate (TS-IV-M)

Number of Laminas: 11

Number of Laminate above magnetostrictive Layer: 5

Ply Thickness: 0.4 mm

Stacking Sequence: $[90_5 / m / 90_5]$

Delamination Detail:

Delaminating Interface number from top: 1^{st} ,10^{th}

Peak Voltage: ∓ 7.228642 mV

Failure Stress: 22.317943 MPa (Tensile in 1^{st} and Compressive in 10^{th} interface) i.e. the delaminating interface.

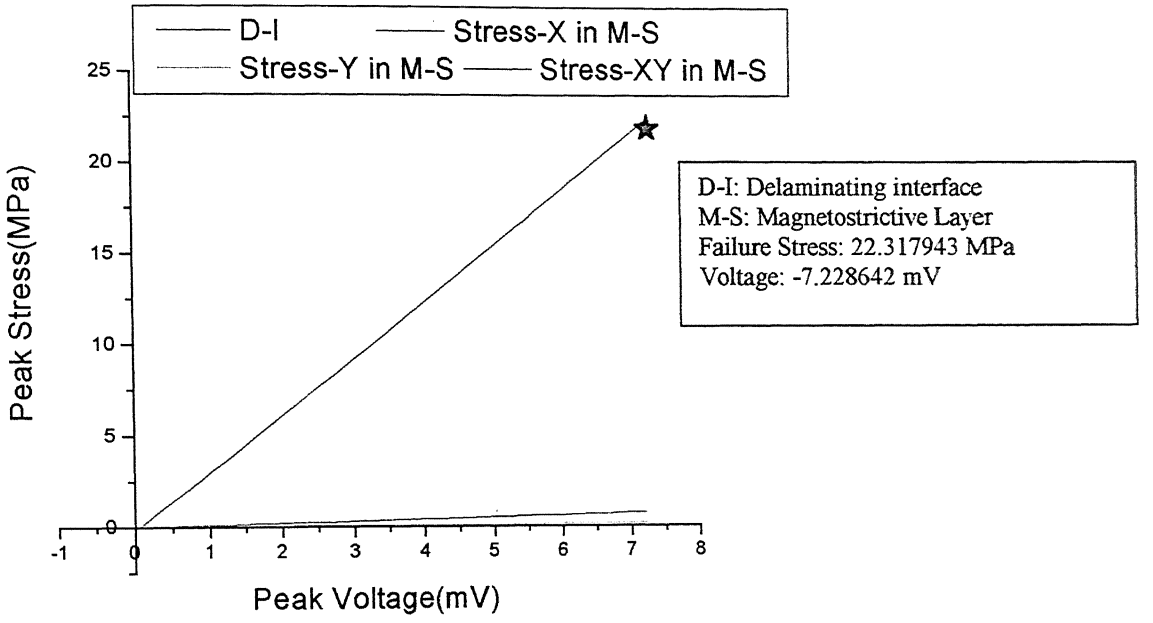

Plot No. 4.91. This plots shows the variation of the peak stress in D-I interface and M-S Layer with respect to peak voltage, and star denotes the delamination start point in 1^{st} and 10^{th} interface.

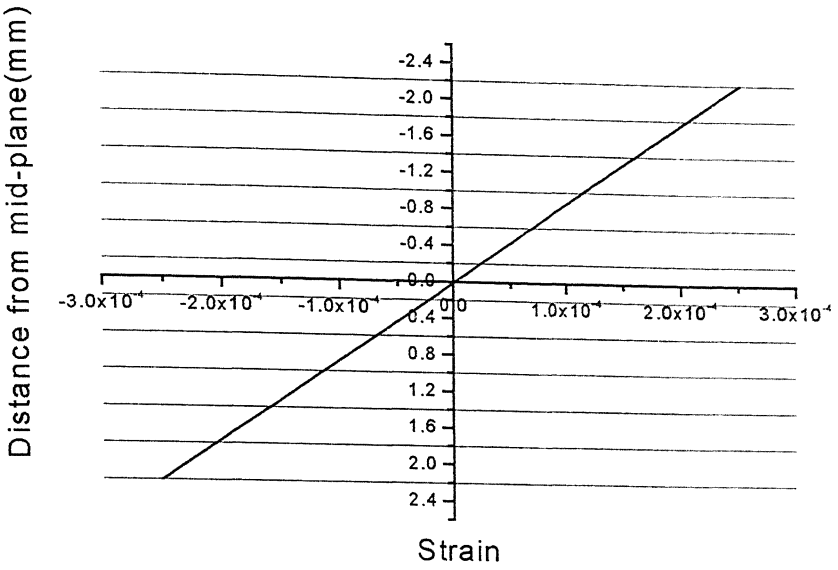

Plot. No. 4.92. This Plot shows the variation of the strain across all interfaces in the laminate when the delamination starts on 1st and 10th interface.

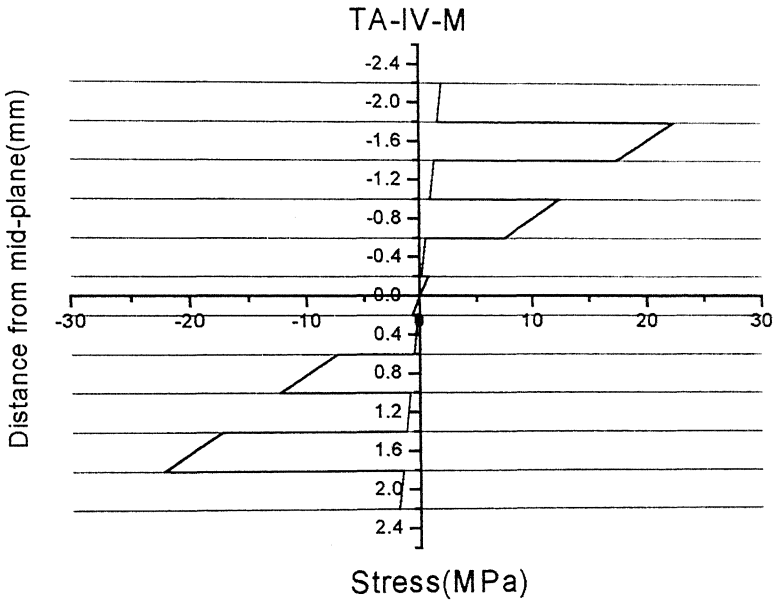

Plot. No. 4.93. This is the variation of the stresss across all interfaces in the laminate when the delamination starts on 1st and 10th interface

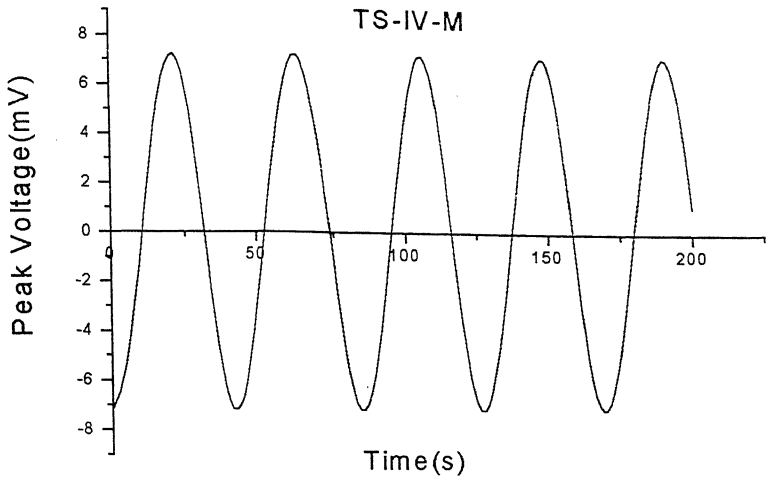

Plot. No.4.94. This is the variation of the peak voltage induced with time, when the delamination begins at 1st and 10th interface from top.

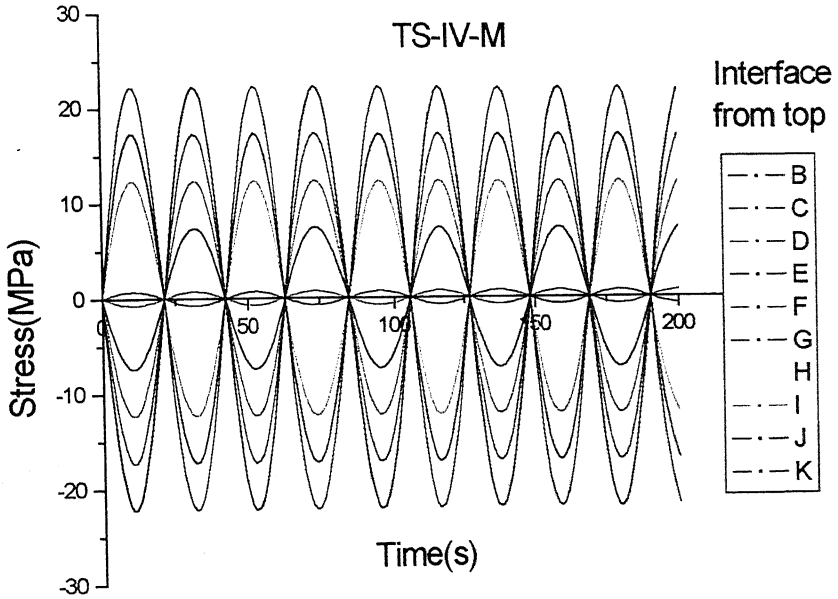

Plot No. 4.95. The above plot shows the variation of the the stresss at each interface when the delamination has started at 1st and 10th interface.

Type of Laminate: Symmetric Laminate(TS-V-M)

Number of Laminas: 11

Number of Laminate above magnetostrictive Layer: 5

Ply Thickness: 0.4 mm

Stacking Sequence: $[0_5/m/0_5]$

Delamination Detail:

Delaminating Interface number from top: 1^{st} ,10^{th}

Peak Voltage: ∓ 7.018678 mV

Failure Stress: 22.643004 MPa (Tensile in 1^{st} and Compressive in 10^{th} interface) i.e. the delaminating interface.

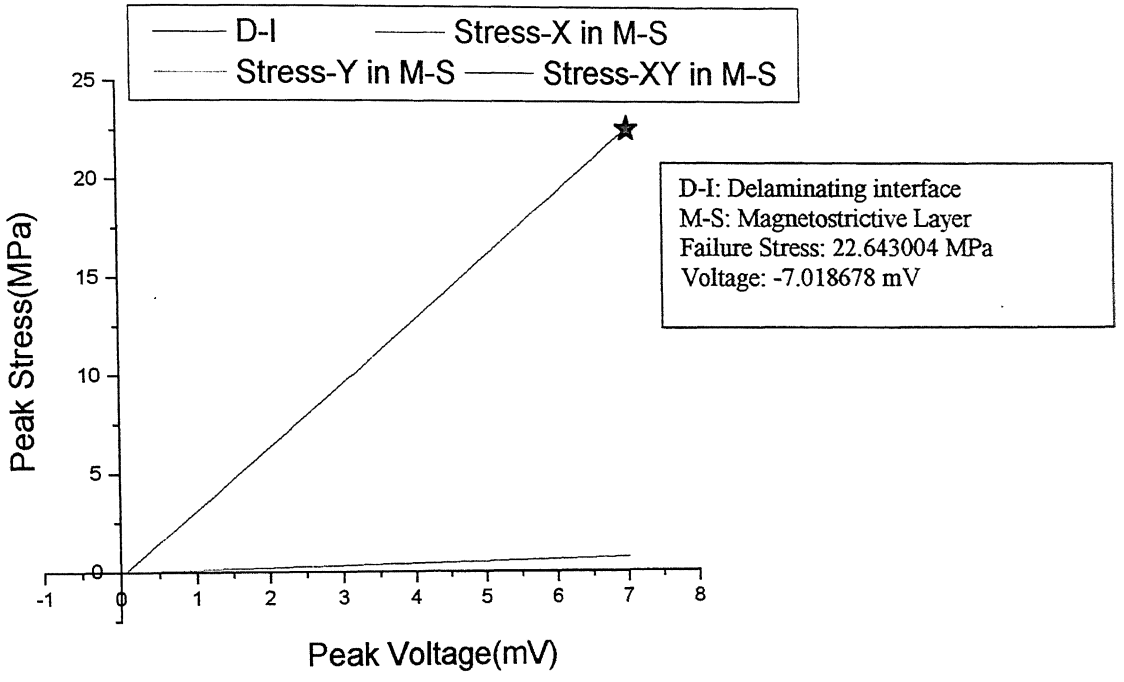

Plot No. 4.96. This plots shows the variation of the peak stress in D-I interface and M-S Layer with respect to peak voltage, and star denotes the delamination start point in 1^{st} and 10^{th} interface.

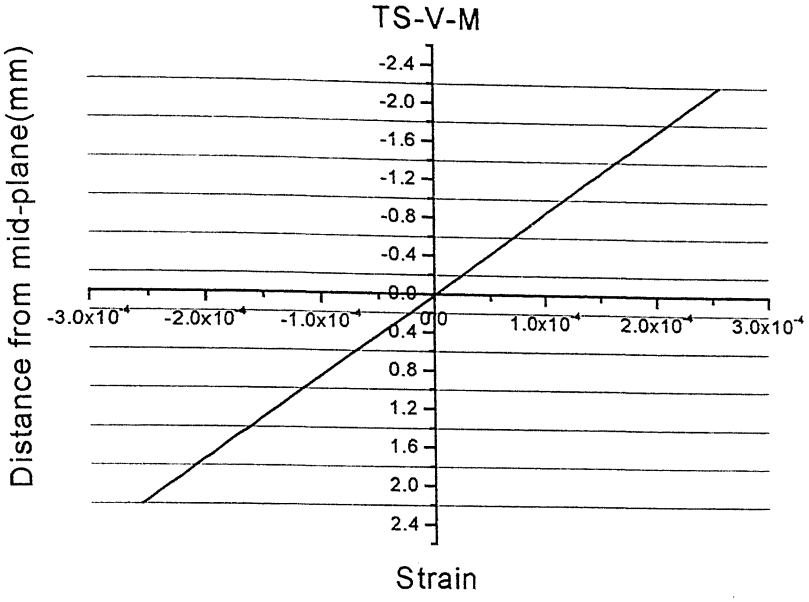

Plot. No. 4.97. This Plot shows the variation of the strain across all interfaces in the laminate when the delamination starts on 1st and 10th interface.

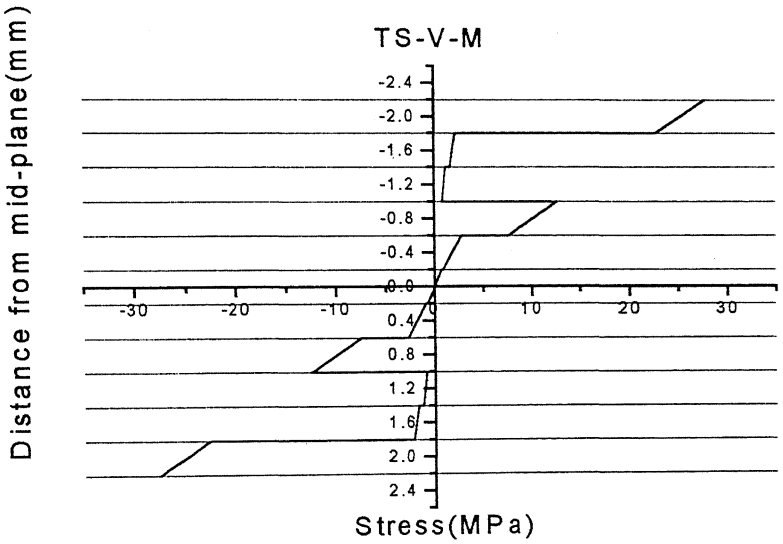

Plot. No. 4.98. This is the variation of the stresss across all interfaces in the laminate when the delamination starts on 1st and 10th interface

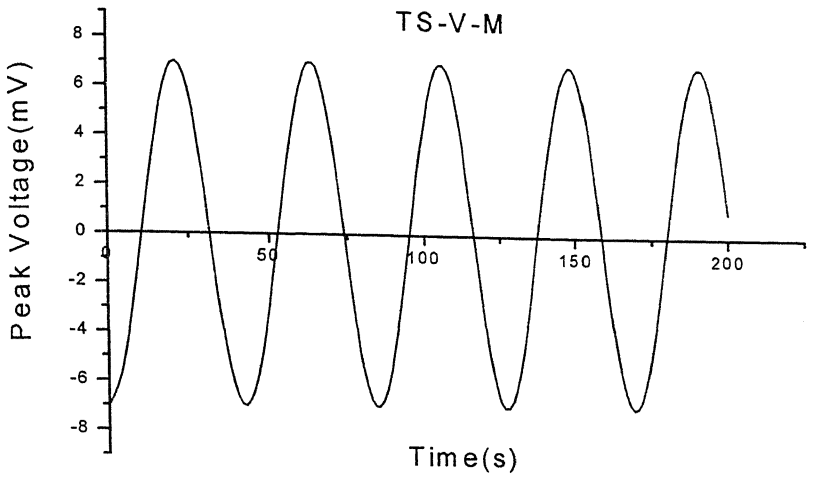

Plot. No.4.99. This is the variation of the peak voltage induced with time, when the delamination begins at 1st and 10th interface from top.

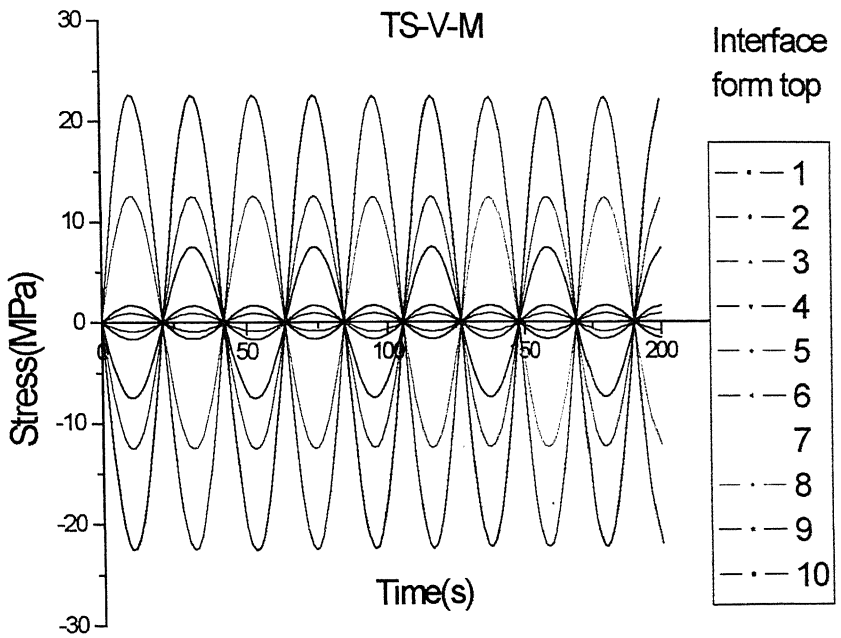

Plot No. 4.100. The above plot shows the variation of the stresss at each interface when the delamination has started at 1st and 10th interface.

4.3 Bending Effect:

Laminate Detail:

Mechanical Properties:

Elastic modulus of carbon fiber E_f = 300 GPa, Poisson's ratio ν_f =0.35

Elastic modulus of epoxy resin E_m = 80 GPa, Poisson's ratio ν_m =0.4

Magnetostrictive Material: Terfenol-D

Properties: E_L =30Gpa, E_T =30Gpa, ν_{LT} =0.25

Type of Laminate: Asymmetric Laminate (TA-I-M)

Number of Laminas: 11

Number of Laminate above magnetostrictive Layer: 8

Ply Thickness: 0.4 mm

Stacking Sequence: $[\pm 45 / 0_2 / 90_2 / 0_2 / m / \pm 45]$

Number of Turns per meter: 150

Carrier Frequency: 1000 Hz

Delamination Detail:

Delaminating Interface number from top: 2^{nd}

Peak Voltage: +38.967099 mV

Failure Stress: 22.508183 MPa (Tensile in nature) in the delaminating interface

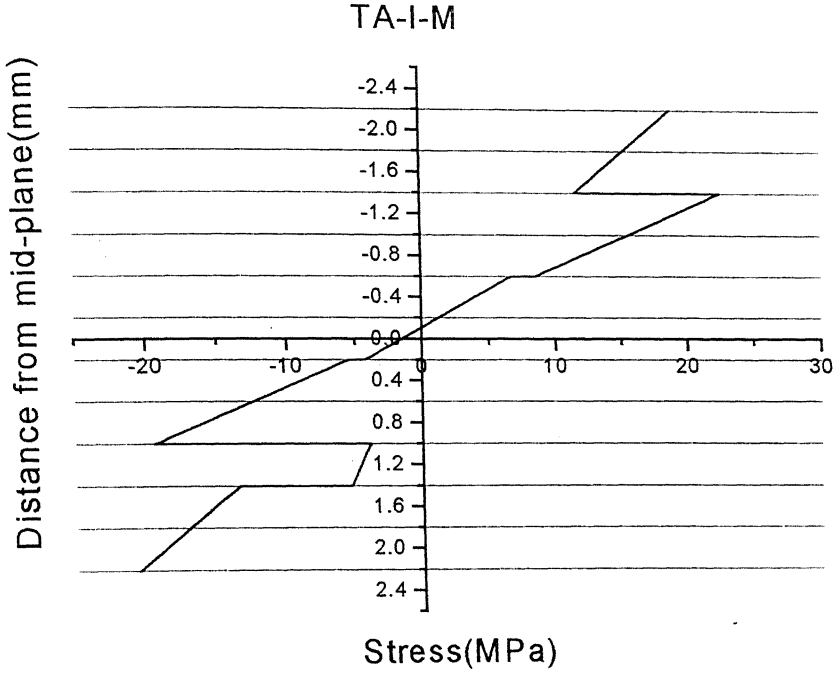

Plot. No. 4.101. This is the variation of the stresses across all interfaces in the laminate when the delamination starts on 2^{nd} interface

Type of Laminate: Symmetric Laminate (TS-I-M)

Number of Laminas: 11

Number of Laminate above magnetostrictive Layer: 5

Ply Thickness: 0.4 mm

Stacking Sequence: $[\pm 45/0_2/90/m/90/0_2/\mp 45]$

Delamination Detail:

Delaminating Interface number from top: 2nd and 9th

Peak Voltage: $\mp$ 6.514440 mV

Peak Stress: 22.584568 (Tensile in 2nd)
-22.584568 (Compressive in 9th interface) i.e. delaminating interface

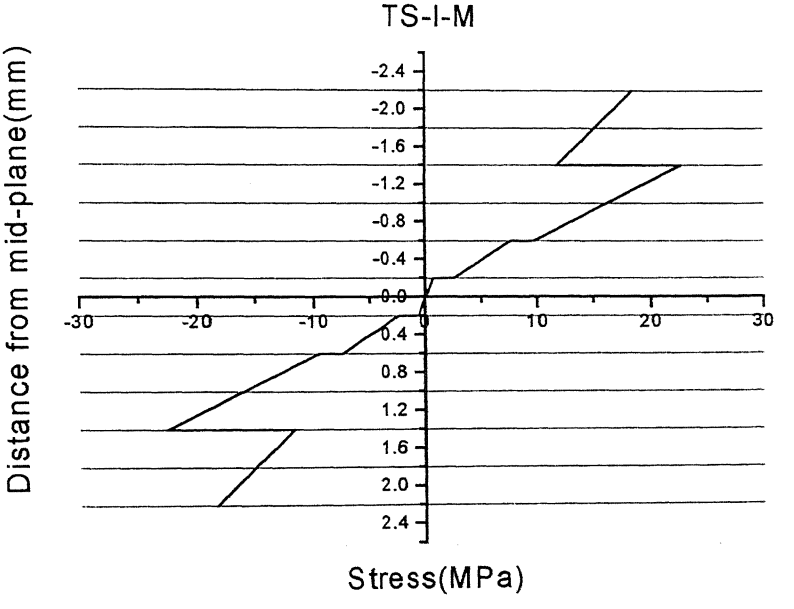

Plot. No. 4.102. This is the variation of the stresses across all interfaces in the laminate when the delamination starts on 2nd and 9th interface

4.4 Frequency Effect:

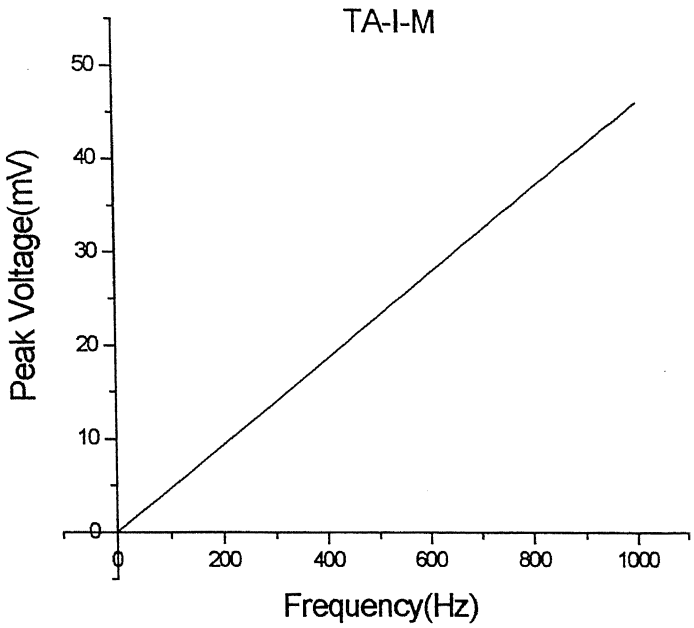

Plot No. 103. This is the variation of the peak voltage with respect to carrier frequency for the case asymmetric laminate with mechanical loading as in Plot No. 51.

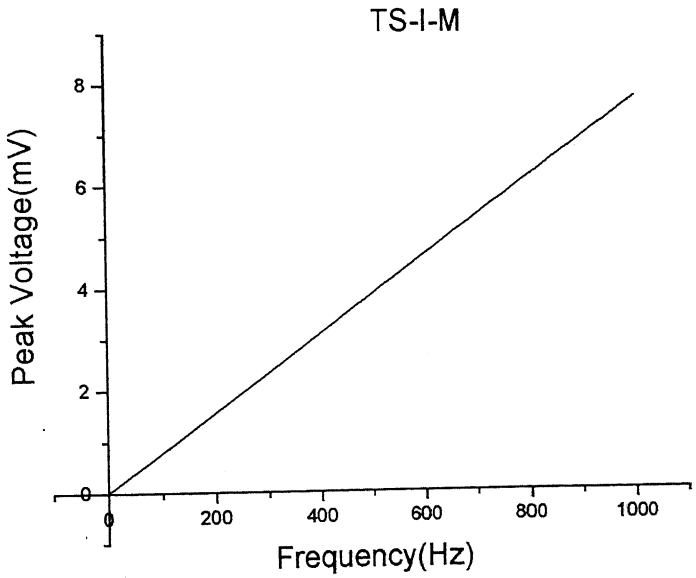

Plot No. 104. This is the variation of the peak voltage with respect to carrier frequency for the case symmetric laminate with mechanical loading as in Plot No. 76.

CHAPTER-5

5.1. Conclusion:

Detailed study is carried out on smart materials and especially on the magnetostrictive Terfenol-D, composite stress analysis. Use of magnetostrictive material in a composite beam for sensing the delamination in any of the interfaces is studied for a number of symmetric and asymmetric laminate. It is found that a reasonable voltage output could be generated for all the case and thus the magnetostrictive layer could be initially used as a sensor. In the case of only electrical loading one can expect higher value of absolute peak voltage in symmetric laminate as compared to the asymmetric laminate. In the case of symmetric laminate with electrical loading the application of current induces stress in the magnetostrictive layer, which is transmitted equally in upper and lower side of the smart layer. In the case of asymmetric beam however the distribution of stress is also affected by the bending effect. Interestingly the inverse is happening in the case of combined loading where the mechanical load is varied while the electrical loading is kept constant. The stress in the magnetostrictive layer will be lowest in the symmetric case, which leads to lowest absolute voltage response.

The dependency of stress distribution on Elastic properties of fiber and matrix is also predominant. If the ratio is too much high say about 100 as in our case then the effect of orientation will have greater effect as compared to the bending effect. Bending Effect becomes evident by decreasing the modulus ratio of E_f/E_m.

5.2 Scope for Future work:

The present work could be extended further in the following areas: -

- Study of the fracture toughness of the magnetostrictive laminate corresponding to different particulate composites.
- Study of the significance of carrier current on the magnetic flux distribution across the laminated composite.
- Extending the study from simple composite beams to more complex structure like thin-walled beams and plates.
- This work can also be extended to the different modes of failure of composite interfaces.

REFERENCES

[1] Shah D K, Chan W S and Joshi S P 1994 Delamination detection and suppression in a composite laminate using piezoceramic layer. Smart Material and Structure. Vol. 3, pp. 293-301.

[2] Rybicki E F, Schmueser D W and Fox J 1977 An energy release rate approach for stable crack growth in the free edge delamination problem. Journal of Composite Material. Vol.11, pp. 470-487

[3] David A M and Dimitris C L 2000 Thermomechanical characterization of NiTiCu and NiTi SMA actuator: influence of plastic strains. Smart Material and structure, Vol 9, pp. 640-652.

[4] Alan, J. Alan, B. Calm, M. M Ray, M. and Richard, E. http://www.physics.hull.ac.uk/magnetic/Research/Facilities/Magnetostriction/magnetostriction.html

[5] Calkins F.T., Dapino M.J., and Flatau A.B., "Effect of Prestress on the Dynamic Performance of a Terfenol-D Transducer", SPIE 1997, Proceedings on Smart Structures and Materials, paper No. 3041-23, 3/97.

[6] Smith R C 1998 Well-Posedness Issue Concerning a Magnetostrictive Actuator Model ESAIM Proceeding, Vol. 4, pp. 269-283.

[7] D.L. Hall and A.B. Flatau, 1993 Nonlinearities, Harmonics and Trends in Dynamic Applications of Terfenol-D," Proceedings of the SPIE Conference on Smart Structures and Intelligent Materials, Vol. 1917, Part 2, pp. 929-939.

[8] H Janocha, Adaptronics and Smart Structure 1999 Basic, Material, design, and applications, Springer.

[9] R M Bozarth, 1951 Ferromagnetism 2nd ed., Ed Van Nastrand, NY, pp. 980.

[10] E D Lacheisserie, 1993 Magnetostriction: Theory and application. Ed. CRC press, USA, pp.410.

[11] F Claeyssen, 1989 Deign and Building of low frequency sonar transducer based on Rare Earth Iron magnetostrictive alloys. Doct. Thesis, Ed. Defence Research Information Center. Ed. HSMO, MoD, London, also Conception et realization de transducteurs sonar basse frequence a base d'alliages magnetostrictifs Terres Rares-Fer, These INSA Lyon, p.414

[12] Kumar M. and Krishna Murthy A V 1998 Sensing of delamination in smart composite laminates. Journal of Aerospace Society of India. Vol. 51, No. 1, pp. 7-9.

[13] Agrawal B D and Broutman L J Analysis and performance of fiber composites.

[14] Engdhal G, 1996 Loss Simulation in Magnetostriction Actuator, journal of Applied Physics, Vol. 79, (8).

[15] Body C., 1996 Non linear finite element modeling of magneto-mechanical phenomenon in giant magnetostrictive thin films, Proceedings of CEFC.